Report No.474

epa Research

# STEP_WISE: Spatiotemporal Epidemiology of Primary Waterborne Infections – *Cryptosporidium* and VTEC

Authors: Authors: Paul Hynds, Jean O'Dwyer and Martin Boudou

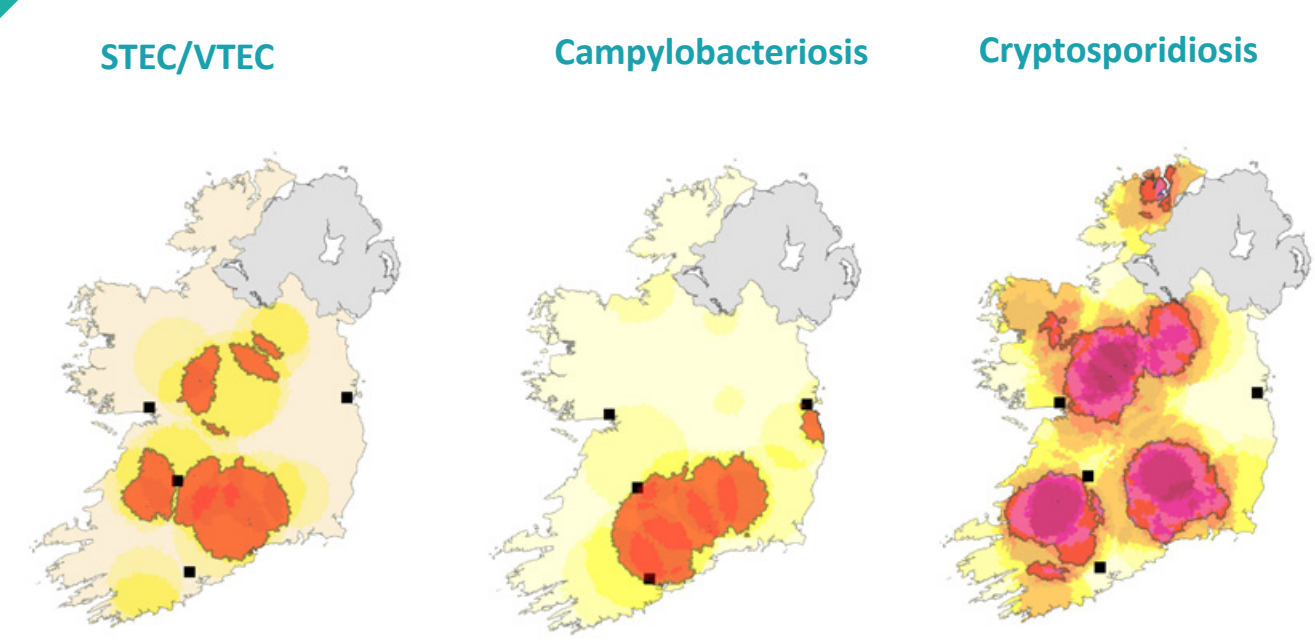


Models focusing on high risk areas

www.epa.ie

Rialtas na hÉireann
Government of Ireland

# Environmental Protection Agency

The EPA is responsible for protecting and improving the environment as a valuable asset for the people of Ireland. We are committed to protecting people and the environment from the harmful effects of radiation and pollution.

## The work of the EPA can be divided into three main areas:

**Regulation:** Implementing regulation and environmental compliance systems to deliver good environmental outcomes and target those who don't comply.

**Knowledge:** Providing high quality, targeted and timely environmental data, information and assessment to inform decision making.

**Advocacy:** Working with others to advocate for a clean, productive and well protected environment and for sustainable environmental practices.

## Our Responsibilities Include:

### Licensing

- Large-scale industrial, waste and petrol storage activities;
- Urban waste water discharges;
- The contained use and controlled release of Genetically Modified Organisms;
- Sources of ionising radiation;
- Greenhouse gas emissions from industry and aviation through the EU Emissions Trading Scheme.

### National Environmental Enforcement

- Audit and inspection of EPA licensed facilities;
- Drive the implementation of best practice in regulated activities and facilities;
- Oversee local authority responsibilities for environmental protection;
- Regulate the quality of public drinking water and enforce urban waste water discharge authorisations;
- Assess and report on public and private drinking water quality;
- Coordinate a network of public service organisations to support action against environmental crime;
- Prosecute those who flout environmental law and damage the environment.

### Waste Management and Chemicals in the Environment

- Implement and enforce waste regulations including national enforcement issues;
- Prepare and publish national waste statistics and the National Hazardous Waste Management Plan;
- Develop and implement the National Waste Prevention Programme;
- Implement and report on legislation on the control of chemicals in the environment.

### Water Management

- Engage with national and regional governance and operational structures to implement the Water Framework Directive;
- Monitor, assess and report on the quality of rivers, lakes, transitional and coastal waters, bathing waters and groundwaters, and measurement of water levels and river flows.

### Climate Science & Climate Change

- Publish Ireland's greenhouse gas emission inventories and projections;
- Provide the Secretariat to the Climate Change Advisory Council and support to the National Dialogue on Climate Action;
- Support National, EU and UN Climate Science and Policy development activities.

### Environmental Monitoring & Assessment

- Design and implement national environmental monitoring systems: technology, data management, analysis and forecasting;
- Produce the State of Ireland's Environment and Indicator Reports;
- Monitor air quality and implement the EU Clean Air for Europe Directive, the Convention on Long Range Transboundary Air Pollution, and the National Emissions Ceiling Directive;
- Oversee the implementation of the Environmental Noise Directive;
- Assess the impact of proposed plans and programmes on the Irish environment.

### Environmental Research and Development

- Coordinate and fund national environmental research activity to identify pressures, inform policy and provide solutions;
- Collaborate with national and EU environmental research activity.

### Radiological Protection

- Monitoring radiation levels and assess public exposure to ionising radiation and electromagnetic fields;
- Assist in developing national plans for emergencies arising from nuclear accidents;
- Monitor developments abroad relating to nuclear installations and radiological safety;
- Provide, or oversee the provision of, specialist radiation protection services.

### Guidance, Awareness Raising, and Accessible Information

- Provide independent evidence-based reporting, advice and guidance to Government, industry and the public on environmental and radiological protection topics;
- Promote the link between health and wellbeing, the economy and a clean environment;
- Promote environmental awareness including supporting behaviours for resource efficiency and climate transition;
- Promote radon testing in homes and workplaces and encourage remediation where necessary.

### Partnership and Networking

- Work with international and national agencies, regional and local authorities, non-governmental organisations, representative bodies and government departments to deliver environmental and radiological protection, research coordination and science-based decision making.

## Management and Structure of the EPA

The EPA is managed by a full time Board, consisting of a Director General and five Directors. The work is carried out across five Offices:

1. Office of Environmental Sustainability
2. Office of Environmental Enforcement
3. Office of Evidence and Assessment
4. Office of Radiation Protection and Environmental Monitoring
5. Office of Communications and Corporate Services

The EPA is assisted by advisory committees who meet regularly to discuss issues of concern and provide advice to the Board.

# STEP_WISE: Spatiotemporal Epidemiology of Primary Waterborne Infections – *Cryptosporidium* and VTEC

Authors: Paul Hynds, Jean O'Dwyer and Martin Boudou

Lead organisations: Technological University Dublin and University College Cork

## Identifying pressures

Ireland regularly reports the highest annual crude incidence of verotoxin-producing Escherichia coli (VTEC) enteritis and cryptosporidiosis in Europe, with notified crude incidence rates typically 5–10 times the European average. Short-term hydrometeorological conditions, elevated levels of pastoral agriculture and high reliance on septic tanks and private domestic groundwater sources have long been acknowledged as drivers of the transmission of infectious waterborne diseases. In addition, extreme weather events, including flooding, have been identified as the source of numerous outbreaks. Recent forecasts indicate that Ireland is particularly likely to experience significant hydrometeorological pattern changes due to global warming, with a 2–3°C increase in average temperature expected by 2100, in concurrence with higher winter rainfall, significantly drier summers and an increased frequency of extreme weather events. These changes are likely to increase the incidence of environmentally acquired, and particularly waterborne, infections across the country. However, to date, no study has sought to investigate the concurrent influence of shifting socioeconomic, environmental, meteorological and infrastructural profiles on these infections in Ireland. The STEP_WISE project seeks to address this knowledge gap by increasing current scientific understanding of the spatiotemporal mechanisms associated with waterborne VTEC enteritis and cryptosporidiosis in Ireland, and translate findings into enhanced environmental, infrastructural and healthcare policies.

## Informing policy

Recent estimates suggest the annual cost of gastroenteric infection in Ireland surpasses €150 million, with VTEC infection and cryptosporidiosis the most frequently reported bacterial and protozoan infections, respectively. Transmission sources, pathways and source–pathway interactions associated with both infections in Ireland are multifaceted, resulting in a complex exposure profile. Sporadic cases of infection are inherently difficult to attribute to specific risk factors for reasons that include the absence of accurate date-of-onset data, underreporting, misdiagnosis, myriad potential exposures and surveillance limitations. The high proportion of sporadic infections relative to total annual cases in Ireland, and their association with environmental exposures, has made the spatiotemporal occurrence of VTEC and cryptosporidiosis particularly important in public health. Moreover, a notable urban–rural divide exists with respect to the prevalence, frequency and severity of both infections, with the burden of disease disproportionately borne by rural communities, placing a significant strain on public health infrastructure in Ireland. Similarly, the burden of both infections is markedly more prevalent among young children (< 5 years) and older people (> 65 years), leading to reduced productivity and increased economic burden among caregivers and the Health Service Executive.

National, regional and local planning and investment decisions pertaining to healthcare, infrastructure and climate resilience must be based on robust scientific evidence, and must account for the characteristic spatiotemporal diversity of Ireland.

## Developing solutions

The STEP_WISE project investigated spatiotemporal patterns of laboratory-confirmed primary cases of VTEC enteritis and cryptosporidiosis in Ireland using, and subsequently developing, multiple statistical tools. Three analytical approaches were employed, as follows:

1. Focusing on "event based" meteorological impacts on infection, the STEP_WISE project focused on a 6-week period in November and December 2015, when a series of Atlantic storms caused widespread pluvial and fluvial flooding. An ensemble of statistical and time-series analyses were used to quantify the influence of flood hydrometeorology on the incidence of confirmed infections. Excess cases of VTEC enteritis were geographically associated with the midlands, while cryptosporidiosis clusters were widespread. Models showed a clear association between rainfall, surface water discharge, groundwater levels and infection incidence, with lagged associations from 16 to 20 weeks particularly strong. All three hydrometeorological variables were associated with the increase in cryptosporidiosis during April 2016, while only surface water discharge was associated with VTEC enteritis.

2. Random forest classification was used to identify associations between individual components of a national deprivation index and spatially aggregated cases of VTEC enteritis and cryptosporidiosis. VTEC incidence was (negatively) associated with mean number of persons per room and percentage of local authority housing in both urban and rural areas, in addition to lower levels of educational attainment in rural areas, while lower unemployment rates were associated with both infections, irrespective of settlement type. Lower levels of third-level education were associated with cryptosporidiosis in rural areas only.

3. Entirely novel "space–time cluster recurrence" indices and a decompositional clustering approach were developed for the study of waterborne infections, with recurrent clusters of both infections identified in three distinct geographical regions in the west and mid-west, all primarily rural, and characterised by high reliance on private groundwater sources and on-site domestic wastewater treatment systems.

**EPA RESEARCH PROGRAMME 2014–2020**

# STEP_WISE: Spatiotemporal Epidemiology of Primary Waterborne Infections – *Cryptosporidium* and VTEC

# (2018-W-MS-33)

# EPA Research Report

Prepared for the Environmental Protection Agency

by

Technological University Dublin and University College Cork

**Authors:**

**Paul Hynds, Jean O'Dwyer and Martin Boudou**

**ENVIRONMENTAL PROTECTION AGENCY**
An Ghníomhaireacht um Chaomhnú Comhshaoil
PO Box 3000, Johnstown Castle, Co. Wexford, Ireland

Telephone: +353 53 916 0600 Fax: +353 53 916 0699
Email: info@epa.ie Website: www.epa.ie

## ACKNOWLEDGEMENTS

This report is published as part of the EPA Research Programme 2014–2020. The EPA Research Programme is a Government of Ireland initiative funded by the Department of the Environment, Climate and Communications. It is administered by the Environmental Protection Agency, which has the statutory function of co-ordinating and promoting environmental research.

The authors would like to acknowledge the members of the project steering committee, namely Iain Lake (University of East Anglia, UK), Stephen McCarthy (EPA), Anthony Mannix (EPA), Mary Lenahan (Food Safety Authority of Ireland), Ray Parle (Health Service Executive), Bernard Harris (Department of Agriculture, Food and the Marine), Clare Casey (Department of Agriculture, Food and the Marine), Aoife Loughnane (EPA), Cormac Mac Gearailt (EPA) and Noeleen McDonald (Department of Agriculture, Food and the Marine), and Hannah Linehan and Georgia Bayliss-Brown, who co-ordinated the steering committee. The authors would also like to acknowledge the project's co-applicants, Coilín Óh Aiseadha, Patricia Garvey and Paul McKeown (Health Service Executive).

## DISCLAIMER



**EPA RESEARCH PROGRAMME 2014–2020**
Published by the Environmental Protection Agency, Ireland

ISBN: 978-1-80009-247-1 January 2025

Price: Free Online version

# Project Partners

**Dr Paul Hynds**
Environmental Sustainability and Health Institute (ESHI)
Technological University Dublin
Park House
191 N Circular Rd
Cabra East
Grangegorman
Co. Dublin
D07 EWV4
Ireland
Email: paul.hynds@tudublin.ie

**Dr Jean O'Dwyer**
School of Biological, Earth and Environmental Sciences
University College Cork
North Mall Campus
Co. Cork
Ireland

**Dr Martin Boudou**
Environmental Sustainability and Health Institute (ESHI)
Technological University Dublin
Park House
191 N Circular Rd
Cabra East
Grangegorman
Co. Dublin
D07 EWV4
Ireland

# Contents

# List of Figures

# List of Tables

# Executive Summary

Ireland regularly reports the highest annual crude incidence of verotoxin-producing *Escherichia coli* (VTEC) enteritis and cryptosporidiosis in the European Union. The STEP_WISE project investigated spatiotemporal patterns of laboratory-confirmed primary cases of VTEC enteritis and cryptosporidiosis in Ireland using multiple statistical tools. As regards VTEC enteritis, 2755 cases of infection over the period January 2013 to December 2017 were georeferenced to census small areas (SAs); overall, more than one case was notified in 2340 (12.6%) of 18,641 SAs. The highest case numbers were encountered in the 0–5 years age group ($n = 1101$, 39.6%) and were associated with serogroups O26 ($n = 800$, 29%) and O157 ($n = 638$, 23.2%). Overall, 17 space–time clusters were identified, ranging from two (in 2014) to five (in 2017) clusters of sporadic infection per year; recurrent clusters were identified in three distinct geographical regions in the west and mid-west, all primarily rural.

Between January 2008 and December 2017, 4509 cases of cryptosporidiosis infection were georeferenced to a census SA, with an ensemble of geostatistical approaches, including seasonal decomposition, Anselin Local Moran's *I* and space–time scanning, used to elucidate spatiotemporal patterns of infection. One or more confirmed cases were notified in 3413 of 18,641 census SAs (18.3%), with the highest case numbers occurring in the 0–5 years age range ($n = 2672$, 59.3%). Sporadic cases were more likely to occur in male patients [odds ratio (OR) 1.4] and in rural areas (OR 2.4), whereas outbreak-related cases were more likely to occur in female patients (OR 1.4) and in urban areas (OR 1.5). Altogether, 55 space–time clusters (≥ 10 confirmed cases) of sporadic cryptosporidiosis infection were detected, with three "high-recurrence" regions identified; no large urban conurbations were present within recurrent clusters.

Focusing on "event-based" meteorological impacts on infection, the STEP_WISE project focused on a 6-week period in November and December 2015, when a series of Atlantic storms swept across the country, causing widespread pluvial and fluvial flooding. Flooding was particularly severe in the west and midlands, with rainfall up to 200% above normal in many regions, making it the wettest winter ever recorded. While the infrastructural damage and subsequent costs associated with flood events have received, and continue to receive, widespread attention, far less coverage is given to the associated adverse human health effects. Accordingly, weekly spatially referenced infection incidence data from July 2015 to June 2016 were mapped and temporally linked to weekly time series of cumulative antecedent rainfall, surface water discharge, groundwater level and high-resolution flood risk mapping.

An ensemble of statistical and time-series analyses were used to quantify the influence of flood hydrometeorology on the incidence of confirmed infections. Seasonal decomposition (excluding seasonal patterns and long-term trends) identified a high residual infection peak during April 2016, with space–time scanning used to identify the location, size and temporal extent of clustering. Excess cases of VTEC enteritis were geographically associated with the midlands, while cryptosporidiosis clusters were widespread. Generalised linear modelling of infection locations showed that areas with a surface water body exhibited significantly higher incidence of both VTEC (OR 1.225; $p < 0.001$) and cryptosporidiosis (OR 1.363; $p < 0.001$). ARIMA models show a clear association between rainfall, surface water discharge, groundwater levels and infection incidence, with lagged associations from 16 to 20 weeks being particularly strong, thus indicating a link between infection peaks (April 2016) and the flood event that began approximately 18 weeks earlier. All three hydrometeorological variables were associated with the increase in cryptosporidiosis during April 2016, while only surface water discharge was associated with VTEC enteritis.

Spatiotemporal analysis represents an important indicator of infection patterns, enabling targeted epidemiological intervention and surveillance. The results presented may also be used to further understand the sources, pathways and receptors, and thus mechanisms, of cryptosporidiosis and VTEC enteritis in Ireland. Study findings may be employed

for improved risk communication, risk management and surveillance to safeguard public health after large hydrometeorological events.

Overall, the STEP_WISE project achieved the following research goals:

- synthesis of current and emerging sources, pathways and receptors of environmentally acquired enteric infection, including identification of existing and required national datasets for comprehensive elucidation;
- development of a unique geolinked spatiotemporal dataset comprising “gold standard” laboratory-confirmed enteric infection data and associated drivers and pressures;
- development of calibrated and validated geostatistical models elucidating the sources, pathways and receptors, and thus mechanisms, of environmentally acquired enteric infection in Ireland over a 10-year period;
- creation of spatial “hotspot” maps of infection risk in Ireland, including scenario analyses of temporally variable drivers and pressures, such as meteorology, flooding and land use changes;
- development of robust evidence-based recommendations for effective environmental and healthcare policy, legislative compliance, and spatiotemporally focused environmental monitoring in Ireland.

# 1 Introduction

Two of the principal goals of Healthy Ireland 2013–2025 are reducing the prevalence of health inequalities (goal 2) and protecting the public from threats to health and wellbeing (goal 3) through ensuring that Ireland possesses effective strategies and interventions to protect the public from existing and emerging threats (Department of Health, 2013). The health of any population is inextricably linked to a healthy environment, including the availability of clean water. This is particularly true in Ireland, which currently reports the third highest annual freshwater abstraction rate per inhabitant (141 $m^3$) in the European Union (EU) (Stavenhagen *et al.*, 2018). For this reason, environment-associated infectious diseases, including those driven by climate change, represent a critical challenge for public health in Ireland, as their source and transmission are frequently sporadic and associated mechanisms are not well understood (Portier *et al*., 2013; Wu *et al.*, 2016; Murphy *et al*., 2017).

Over the past decade, Ireland has persistently reported the highest incidence of symptomatic verotoxin-producing *Escherichia coli* (VTEC) infection in the EU (Hynds *et al.*, 2014a; Garvey *et al.*, 2016a), with national incidence significantly increasing over the same period. Confirmed VTEC cases increased from 65 cases in 2004 to 839 in 2016; 82% of cases were associated with rural exposure, 38% (313 cases) led to hospitalisation and six people died due to infection sequelae (Garvey *et al.*, 2016a). A quantitative risk analysis by Hynds *et al.* (2014a) estimated that the incidence of acute gastrointestinal infection in Ireland is approximately 4.4 times higher among rural dwellers than among their urban counterparts, thus highlighting a significant current health inequality. Waterborne transmission of VTEC through untreated (and unlegislated) private water wells has been documented as a likely infection pathway in rural regions of Europe, North America and Africa, with both cattle and on-site domestic wastewater treatment systems (OSWTSs) identified as likely sources of VTEC contamination (O'Sullivan *et al.*, 2008; ÓhAiseadha *et al.*, 2017).

Similarly, a study in Ireland has presented evidence of the widespread presence of bacterial (*E. coli*) resistance to a panel of both human (≈20%) and veterinary (> 90%) antimicrobial medications in private groundwater sources in the rural mid-west region (O'Dwyer *et al.*, 2018). Thus, it may be concluded that both OSWTSs and agricultural effluents contribute (oftentimes concurrently) to contamination of drinking water sources in Ireland by faecal bacteria, with the presence of antimicrobial resistance representing a particular concern with respect to human health in rural Ireland. Likewise, a recent systematic review of groundwater contamination in North America found that OSWTSs and public wastewater treatment plants (WWTPs) have been the most frequently reported confirmed or probable source of subsurface pathogens over the past three decades (Hynds *et al.*, 2014b). However, the relative contribution of these sources and pathways to VTEC infection and their temporal significance remains unknown.

The crude incidence of confirmed cryptosporidiosis infection has remained relatively consistent over the past decade in Ireland, ranging from 11.0/100,000 in 2004 to 13.2/100,000 in 2018 (HPSC, 2019a). However, the Galway *Cryptosporidium hominis* outbreak of 2007, attributed to insufficient wastewater treatment and subsequent surface ingress, serves as a stark reminder of the potential disruption to both health and prosperity resulting from cryptosporidiosis outbreaks. The Galway outbreak comprised > 242 confirmed laboratory cases, costing the state an estimated €19 million, with an extended boil water notice (158 days) affecting approximately 120,000 people (Chyzheuskaya *et al.*, 2017). To date, numerous studies have examined the routes of environmental exposure to *Cryptosporidium* spp., and have identified farmyards, WWTP effluents and septic tank effluents as likely sources (Efstratiou *et al.*, 2017; Toledo *et al.*, 2017), and both surface water (Dreelin *et al.*, 2014) and groundwater (Daniels *et al.*, 2018) as probable transmission routes (pathways). Recent work has shown that insufficient (waste)water treatment or treatment failure represents a major driver

of cryptosporidiosis outbreaks in Europe, with the risk of further outbreaks in Ireland most significantly associated with treatment efficacy (Spearman's non-parametric rho ($r_S$) = 0.32), individual consumption rates ($r_S$ = 0.29) and raw water (groundwater or surface water) quality ($r_S$ = 0.19) (Cummins *et al.*, 2010). To date, no integrated epidemiological investigation of the spatiotemporal mechanisms associated with confirmed cryptosporidiosis infection has been undertaken in Ireland.

Recent climate projections indicate that the incidence, severity and timing of extreme rainfall events and flooding will increase dramatically over the next century, with Ireland the second most affected European country in terms of the mean proportion of the population residing in flood-prone areas by 2100 (Arnell and Gosling, 2016). Compounding this, recent work has shown that waterborne VTEC enteritis outbreaks are significantly associated with persistent, high-intensity antecedent rainfall in Ireland (O'Dwyer *et al.*, 2016). The government's Food Harvest 2020 Strategy envisages significant expansion of livestock-based food production in Ireland as a central part of its plan for economic growth (Kenny *et al.*, 2018), with the recent abolition of EU milk quotas predicted to result in significantly increased cattle densities in many areas, with a concomitant increase in the risk of enteric infection associated with areas under grazing and manure spreading in Ireland (Brehony *et al.*, 2018). Moreover, recent studies show that geological setting has been associated with the presence of (micro)pollutants in groundwater systems, particularly those associated with karstified limestone bedrock (Hynds *et al.*, 2012; Morasch, 2013), representing a significant pressure in Ireland owing to the preponderance of karstic systems, which underlie approximately 50% of the country.

Presently, the relative importance of waterborne and other environmental routes of enteric pathogen exposure is not precisely understood in Ireland. The ubiquity of environmental sources and pathways, including OSWTSs, private groundwater supplies and animal-based agriculture, in rural Ireland makes monitoring and evaluation an extremely difficult task, particularly regarding diffuse contamination sources and unregulated private water supplies (Atherholt *et al.*, 2015). Recent Irish studies report that just 40% of wells undergo regular water testing, while 65% of well users exhibit very low levels of risk perception about potential contamination events (Hynds *et al.*, 2013; Mooney *et al*., 2021). Furthermore, where testing does take place, "one-off" sampling may be misleading and falsely reassuring, as current microbiological testing (monitoring or investigation) methods are associated with myriad inherent limitations. Owing to the combined effects of high reliance on private groundwater sources, the ubiquity of OSWTSs and pastoral agriculture, a temperate maritime climate, unique rural and peri-urban settlement patterns, and diverse bedrock and Quaternary geology, the Ireland aquatic environment may be considered the "perfect storm" with respect to the occurrence and transport of waterborne pathogens and subsequent endemic infection.

In 2015, the second Lancet Commission on Climate Change and Health noted that the threat to human health from climate change is so great that it could undermine the last 50 years of gains in development and global health (Wang and Horton, 2015). The Water Joint Programming Initiative (launched in 2018) has identified two paramount issues that warrant dedicated research efforts: water quantity and quality; and extreme events relating to water, including climate, land use, waste management production and agriculture. A panoply of economic, ecological, social and technological challenges revolve around these two issues, for which solutions are required.

Similarly, myriad Sustainable Development Goals speak to the importance of the links between environmental, ecological and human health, and the significance of "place" regarding societal equality, wellbeing and healthcare. These include Goals 3 (Good Health and Wellbeing), 6 (Clean Water and Sanitation), 10 (Reduced Inequality) and 13 (Resilience and Adaptive Capacity to Climate Events). For example, the key objective of Goal 6 is to achieve universal and equitable access to safe and affordable drinking water for all, as measurable by the proportion of the population using safely managed drinking water services. Furthermore, in 2009, the World Health Organization published detailed guidance on the implementation of the drinking water safety plan approach. The document, *Water Safety Plan Manual: Step-by-step Risk Management for Drinking Water Supplies* (Bartram, 2009), which has been adopted by the EPA, has the primary objective of protecting human health.

Under Healthy Ireland, the national framework for action to improve the health and wellbeing of people living in Ireland, compliance with environmental and water-related EU and national legislation represents a key performance indicator of a healthy Ireland. A focus on research is a critical feature of this initiative to ensure that interventions, programmes, and communication and funding strategies are based on robust evidence about the determinants of environmental and public health and the best-practice approaches in addressing them. The STEP_WISE project directly responds to the aims of multiple national and international strategies and interventions, and will inform both environmental and human health-related policy development and implementation in Ireland through reviewing practices and emerging pressures, generating robust scientific evidence, and developing models and visualisation tools for spatiotemporally focusing monitoring and compliance efforts on the most vulnerable areas/regions and susceptible subpopulations. The direct policy implications arising from this "challenge-based" project cannot be overstated, with the Water Framework Directive, river basin management plans and the EPA's *State of the Environment Report*, to name a few, all likely to be influenced by this trans- and interdisciplinary research.

The STEP_WISE project comprised six distinct work packages for completion over a 24-month time frame, with an overarching goal of using a "gold standard" outcome variable (i.e. laboratory-confirmed cases of VTEC infection and cryptosporidiosis) to improve the health and wellbeing of both the environment and the population, now and into the future. Specifically, STEP_WISE aimed to increase scientific understanding of the transmission and exposure mechanisms associated with environmentally derived infectious diseases, and translate findings into improved environmental and healthcare policies, interventions and compliance for Ireland.

# 2 Spatiotemporal Epidemiological Modelling of Cryptosporidiosis Infections in Ireland

## 2.1 Introduction

*Cryptosporidium* is an oocyst-forming protozoan parasite first identified as a causative agent of gastrointestinal infection in the mid-1970s (Nime *et al.*, 1976). Cryptosporidiosis is associated with a wide range of symptoms, including watery diarrhoea, weight loss, vomiting, abdominal pain, nausea and fever (Fayer and Ungar, 1986). In the most severe cases, infection may lead to acute dehydration and death, particularly among immunocompromised individuals, including children aged ≤5 years, the elderly (≥65) and patients with underlying health conditions (i.e. immunosuppressed) (Chalmers and Cacciò, 2016).

To date, approximately 40 genetically distinct *Cryptosporidium* species have been identified, with *C. parvum* and *C. hominis* the most frequently confirmed species among cases of human infection (Feng *et al.*, 2018). Transmission typically occurs via the faecal–oral route through consumption of contaminated water or food, in addition to direct human–animal contact and exposure to contaminated environments, including recreational water (Chappell *et al.*, 2006; Putignani and Menichella, 2010; Chique *et al.*, 2020). A previous experimental study in healthy adult volunteers found that ingestion of 30 oocysts is sufficient to initiate infection, with a significantly lower threshold dose (≈10 oocysts) associated with specific *C. hominis* and *C. parvum* strains (Chappell *et al.*, 2006).

Cryptosporidiosis occurs in both rural and urban environments, with several studies indicating that *C. hominis* is more frequent in urban areas (due to increased rates of person-to-person transmission) and that *C. parvum* predominates in rural areas (Putignani and Menichella, 2010). Environmental transmission in rural areas represents a particular concern because of the ability of oocysts to survive for prolonged periods in the natural environment (e.g. soil, water) owing to temperature buffering and high humidity (Thompson *et al.*, 2016).

Human cryptosporidiosis became a notifiable disease in Ireland on 1 January 2004, under the Infectious Diseases (Amendment) (No. 3) Regulations 2003 (S.I. No. 707 of 2003). All medical practitioners are required to notify the regional Medical Officer of Health/Director of Public Health of all confirmed cases. According to the most recent European Centre for Disease Prevention and Control (ECDC) report, Ireland consistently reports the highest crude incidence rate (CIR) of confirmed cryptosporidiosis infection in the EU (ECDC, 2019a). For example, during 2017 Ireland reported a cryptosporidiosis CIR of 12.0/100,000 residents, compared with an EU mean CIR of 3.2/100,000.

Unlike other gastroenteric infections (e.g. giardiasis), cryptosporidiosis in Ireland is primarily associated with domestic (indigenous) exposure and transmission. For example, 81% (556/629) of confirmed cases during 2018 were identified as sporadic domestic cases, 12% ($n=73$) were associated with a recognised cluster/outbreak, and travel-related cases accounted for 7% ($n=43$) of the total case number (HPSC, 2019a). While several studies have examined the likely routes of exposure to *Cryptosporidium* spp. in Ireland (e.g. Zintl *et al.*, 2009; Cummins *et al.*, 2010) few epidemiological investigations of the spatiotemporal dynamics of confirmed cryptosporidiosis infection have been undertaken. This represents a significant knowledge gap with respect to understanding pathogen sources and pathways, particularly in the light of the endemic nature of cryptosporidiosis in Ireland. An improved mechanistic understanding of infection occurrence would enable earlier detection, enhanced surveillance, and more focused public health and healthcare policies.

The current study sought to explore the temporal and spatial patterns of domestically acquired (sporadic and outbreak-related) cases of cryptosporidiosis in Ireland via identification of infection clustering. To accurately describe the epidemiological patterns of this important zoonotic parasite, the study integrated several modelling approaches, including seasonal

decomposition, spatial autocorrelation (Anselin Local Moran's *I*), hotspot analysis (Getis-Ord Gi*) and space–time scanning with a large georeferenced dataset of confirmed cryptosporidiosis cases ($n = 4509$) over a 10-year period (2008–2017). To the authors' knowledge, this represents the first spatiotemporal study of its kind in Ireland, which, as previously noted, exhibits the highest national cryptosporidiosis infection CIRs in the EU.

## 2.2 Methods

### *2.2.1 Data collection and processing*

Irreversibly anonymised cases of cryptosporidiosis reported by regional departments of public health between 1 January 2008 and 31 December 2017 were sourced from the national Computerised Infectious Disease Reporting (CIDR) database. Data prior to 2008 were excluded, to avoid potential bias being introduced by the large number of cases reported during the 2007 Galway outbreak. Data on all confirmed cases, including patient-specific data [age, gender, date of reporting, and case outcome (severity)], were geospatially linked to the geographical centroid of their associated census small area (SA) (the smallest administrative unit currently employed for census reporting in Ireland) using the Health Service Executive (HSE) Health Intelligence Unit's geocoding tools.

Sporadic, outbreak-related and travel-related (non-outbreak) cases were defined and discretised for analysis. Outbreak-related cases are defined as confirmed cases with an attached "CIDR outbreak ID", used for identifying cases associated with a recognised infection outbreak or cluster. Travel-related cases are specifically categorised for purposes of analytical exclusion or adjustment (i.e. national reporting) and defined as any patient self-reporting travel outside Ireland within the likely incubation period. Sporadic cases were subsequently delineated via exclusion of the two previous categories from the total case dataset. All case data and analyses were granted full research ethics approval by the Royal College of Physicians of Ireland Research Ethics Committee (RCPI RECSAF_84).

As cryptosporidiosis case numbers in Ireland are highest among children ≤5 years of age and in rural areas (HPSC, 2019a), specific analyses were undertaken with respect to case age (≤5 years, ≥6 years) and land use classification (rural/urban). The Central Statistics Office (CSO) censuses of 2011 and 2016 were used to extract electoral division (ED)- and SA-specific human population counts, permitting calculation of cryptosporidiosis incidence at both spatial (administrative unit) scales. The CSO's 14 urban/rural categories were used to classify each spatial unit as rural or urban. Population density and settlement size were employed to verify all classifications. For reporting purposes within the current report, Ireland has been delineated into eight distinct geographical zones (Figure 2.1). Zone NE (corresponding to Northern Ireland) is located outside Irish public health legislative jurisdiction and was not included for analyses. Pearson's $\chi^2$ test with Yates' continuity corrections and Fisher's exact test (where any cell had fewer than five cases) were used to test for association between categorical case classifications.

### *2.2.2 Seasonal decomposition*

Seasonal decomposition was carried out using seasonal and trend decomposition via the locally estimated scatterplot smoothing (LOESS) (STL) method on different subsets of the case dataset, e.g. sporadic cases, outbreak-related cases, cases in

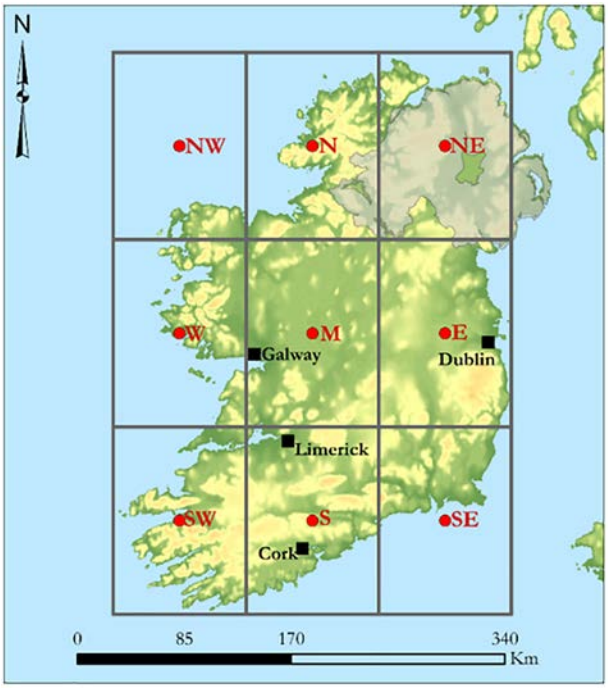


**Figure 2.1. Geographical zones of the island of Ireland.**

children ≤5 years of age, cases in people ≥6 years of age, travel-related cases and cases in urban versus rural areas. The monthly incidence of infection was calculated for each case subcategory. The STL method decomposes incidence data ($Y_v$) time series into three separate component series: seasonal variation ($S_v$), overall trend over time ($T_v$) and residuals ($R_v$), whereby the incidence data are equal to the sum of all three trends denoted by (Cleveland *et al.*, 1990):

$$Y_v = T_v + S_v + R_v$$

An additive seasonal decomposition formula was used, as opposed to a multiplicative one, to remove seasonality ($S_v$) and trend ($T_v$) from the overall time series ($Y_v$) and filter random variation from long-term trends given by the residuals ($R_v$), so that residuals ($R_v$) = time series ($Y_v$) − seasonal trend ($S_v$) − trend ($T_v$).

### *2.2.3 Spatial autocorrelation*

The total number of sporadic cryptosporidiosis cases, the number of sporadic cases among children aged ≤5 years, the number of sporadic cases among people aged ≥6 years and the number of outbreak-related cases were mapped to individual SA centroids. Age-adjusted infection rates within each subcategory were calculated at both SA and ED level, based on 2011/2016 census data. Outbreak-related infection rates were calculated as a proportion of overall cases within each SA and ED. Data aggregation and infection rate calculation were conducted in R statistical software version 3.6.0 (R Foundation for Statistical Computing, Vienna, Austria). Anselin Local Moran's *I* was employed for spatial autocorrelation.

Anselin Local Moran's *I* focuses on the relationship of individual features with nearby features and assigns clusters based on variance assigned to individual spatial units, thus negating the assumption underlying the Global Moran's *I* statistic that a single statistic appropriately accounts for clustering and dispersion of the spatial distribution of infection across the entire study area (Anselin *et al.*, 2002). The Anselin Local Moran's *I* statistic is calculated by generating a neighbour list of spatially proximal SAs or EDs and calculating spatial autocorrelation of similar infection rates as a function of distance bands, thus identifying localised clusters, which are correlated based on the variance assigned to all individual spatial units (Anselin *et al.*, 2002; Mao *et al.*, 2019). Clusters of high infection rates surrounded by high infection rates (H–H); low infection rates surrounded by low infection rates (L–L); outliers of high infection rates surrounded by low infection rates (H–L); and low infection rates surrounded by high infection rates (L–H) are subsequently identified. Local Moran's *I* values were calculated using the cluster and analysis tool in ArcGIS version 10.6 (ESRI, Redlands, CA, USA), which generates a Moran's *I* statistic, *z*-score and pseudo *p*-value for each spatial unit. A positive *I* value is indicative of spatial units with a high or low infection rate, surrounded by SAs or EDs with similarly high or low infection rates. Conversely, a negative *I* value indicates outliers of infection where an SA or ED with a high rate of infection is surrounded by SAs or EDs with low rates of infection, and vice versa (Anselin *et al.*, 2002).

### *2.2.4 Hotspot analysis (Getis-Ord GI*)*

Hotspot analysis was carried out for all sporadic cases, sporadic cases among children aged ≤5 years, sporadic cases among people ≥6 years and outbreak-related cases by calculating spatially specific Getis-Ord GI* statistics in ArcGIS. The Getis-Ord Gi* statistic is calculated for each feature (SA or ED) in the dataset, generating a unit-specific *z*-score and *p*-value, used to statistically determine significant spatial clustering of features in the dataset (Guo *et al.*, 2017). Statistically significant clusters are characterised as clusters that have high values surrounded by SAs or EDs with similarly high values, and low values surrounded by SAs or EDs with similarly low values (Varga *et al.*, 2015). Hotspots and cold spots of infection are determined based on the spatial proximity of high/low values statistically similar to neighbouring features. In contrast to Anselin Local Moran's *I* statistic, clusters based on the Getis-Ord GI* statistic are determined by comparing the sum of local features and their neighbours with the overall sum of all features. Getis-Ord GI* statistics were used to examine whether differing statistical analyses of spatial clustering of infection between spatial units yield varying results. The Getis-Ord GI* statistic is given as (Varga *et al.*, 2015):

$$G_i^* = \frac{\sum_{j=1}^{n} w_{i,j} x_j - \bar{X} \sum_{j=1}^{n} w_{i,j}}{S \sqrt{\frac{\left[ n \sum_{j=1}^{n} w_{i,j}^2 - \left( \sum_{j=1}^{n} w_{i,j} \right)^2 \right]}{n-1}}}$$

where $\chi_j$ is the attribute value for feature $j$, $w_{i,j}$ is the spatial weight between feature $i$ and $j$, $n$ is equal to the total number of features and:

$$\bar{X} = \frac{\sum_{j=1}^{n} x_j}{n}$$

$$S = \sqrt{\frac{\sum_{j=1}^{n} x_j^2}{n} - (\bar{X})^2}$$

### *2.2.5 Space–time scanning*

Space–time scanning was undertaken using SaTScan v9.6 software (Kulldorff and Information Management Services, Inc., MA, USA). SaTScan detects spatial clusters of areal units (i.e. SAs/EDs) by imposing an infinite number of overlapping circular (or elliptical) scanning windows of predetermined sizes across a defined geographical area (Kulldorff *et al.*, 2005). Temporal clusters were simultaneously assessed using the scan statistic, which includes an infinite number of overlapping cylindrical windows defined by a base (spatial scan) and height (temporal scan) statistic (Linton *et al.*, 2014). A discrete Poisson model was employed for space–time scanning to account for the high-resolution spatial scale ($n$ = 18,488 SAs), resulting in high zero/one inflation (i.e. high numbers of SAs with zero cases or one case). A case threshold of 10 cases (minimum) per cluster was selected to ensure that identified clusters were significant, i.e. to avoid single-household clusters. Similarly, a maximum population at risk (PAR) value of 10% was employed concurrently with a maximum cluster radius of 50 km to account for low case numbers within individual SAs. Data were aggregated at a monthly scale, with maximum cluster duration set to 3 months to account for the known seasonal variation in cryptosporidiosis in Ireland.

SaTScan analyses produce two primary outputs: a spatial cluster location(s) (cluster centroid and diameter) and descriptive cluster data (start/end dates, total population, number of observed and expected cases, relative risk, and $p$-value). The authors have developed a novel mapping approach for representing SaTScan results, whereby all significant clusters ($p < 0.05$) are selected and mapped in ArcGIS (ArcGIS 10.6), with binary cluster location [i.e. cluster membership (0/1)] for annual space–time scans summed at the CSO SA scale. The final mapping provides a "cluster recurrence" index ranging from 0 to 10 (i.e. annual absence/presence of cluster over the 10-year study period).

## 2.3 Results

### *2.3.1 Occurrence of cryptosporidiosis infection in Ireland (2008–2017)*

The dataset comprised 4633 confirmed cases of cryptosporidiosis from 2008 to 2017, of which 4509 cases (97%) were successfully geolinked to a distinct spatial unit (SA/ED centroid). Overall, 1964 EDs (58% of 3409), 3413 SAs (18.3% of 18,488) and all (26/26) Irish counties were associated with at least one confirmed case. Most cases were associated with children aged ≤5 years ($n$ = 2672, 59.3%) (Figure 2.2), with the reported incidence rate across all

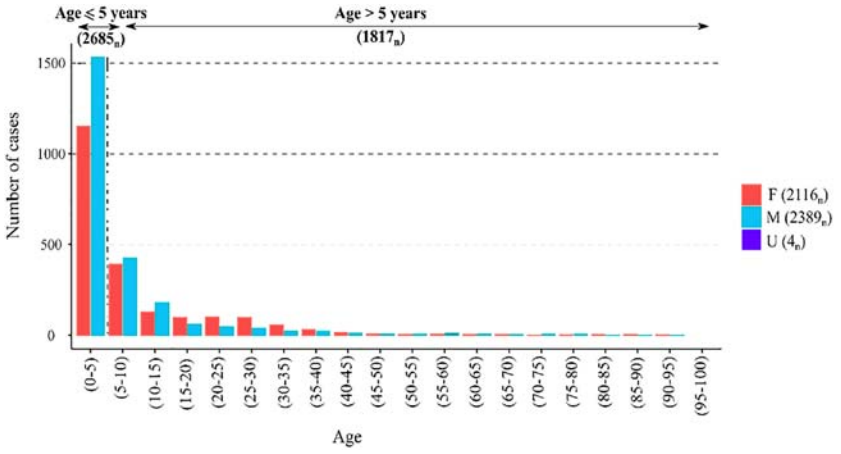


**Figure 2.2. Cryptosporidiosis cases in Ireland by age and gender (2008–2017). Note that the discrepancy between the total number of cases and total number of cases by age group and gender is a result of missing variables within acquired surveillance datasets. n, number; U, unclassified.**

case types being slightly higher among males (53%) than among females (Table 2.1).

As shown in Table 2.1, sporadic cases were statistically more likely to occur in males [odds ratio (OR) 1.4; 95% confidence interval (CI) 1.2–1.6] and children ≤5 years of age (OR 1.5; 95% CI 1.3–1.8) and in areas categorised as rural (OR 2.4; 95% CI 2–28). Conversely, outbreak-related cases were more likely to occur in females (OR 1.4; 95% CI 1.2–1.7) and in urban areas (OR 1.5; 95% CI 1.3–1.9). Travel-related cases were more likely to occur in females (OR 1.3; 95% CI 1–1.6), people >5 years of age (OR 2.4; 95% CI 1.5–3.1) and those resident in an urban conurbation (OR 3.6; 95% CI 2.8–4.6).

Temporal cumulative incidence (Figure 2.3) indicates a marked annual peak in cases in late spring ($n$=1812), with the highest incidence occurring during April ($n$=916). The lowest cumulative incidence was recorded during the winter months (November to January) ($n$=493), with the lowest incidence recorded in January ($n$=136). Case numbers peaked in 2017 ($n$=584).

### *2.3.2 Seasonal decomposition*

Seasonal decomposition of sporadic infection over the 10-year study period indicates a clear seasonal peak in mid-spring (April) annually (Figure 2.4). Residual trends show a generally consistent annual

**Table 2.1. Pearson $\chi^2$ test results for cryptosporidiosis cases in Ireland, by case type (sporadic, outbreak related, travel related), gender, age and CSO classification**

| | Sporadic | | | | Outbreak-related | | | | Travel-related | | | |
|---|---|---|---|---|---|---|---|---|---|---|---|---|
| Variable | Total cases, *n* (%) | OR | $\chi^2$ | *p*-value | Total cases, *n* (%) | OR | $\chi^2$ | *p*-value | Total cases, *n* (%) | OR | $\chi^2$ | *p*-value |
| Gender | | | | | | | | | | | | |
| Female | 1735 (45.6) | 0.72 | 15.47 | <0.001 | 224 (54.8) | 1.41 | 10.64 | 0.001 | 157 (52.5) | 1.27 | 3.71 | 0.054 |
| Male | 2066 (54.4) | 1.38 | | | 185 (45.2) | 0.71 | | | 142 (47.5) | 0.78 | | |
| Case age | | | | | | | | | | | | |
| ≤5 years | 2325 (61.2) | 1.51 | 25.50 | <0.001 | 166 (40.6) | 0.99 | 0.007 | 0.932 | 181 (60.5) | 0.41 | 53.08 | <0.001 |
| >5 years | 1476 (38.8) | 0.66 | | | 243 (59.4) | 1.01 | | | 118 (39.5) | 2.39 | | |
| CSO classification | | | | | | | | | | | | |
| Rural | 2502 (65.8) | 2.36 | 110.5 | <0.001 | 217 (53) | 0.65 | 16.83 | <0.001 | 101 (33.8) | 0.28 | 111.77 | <0.001 |
| Urban | 1299 (34.2) | 0.42 | | | 192 (47) | 1.54 | | | 198 (66.2) | 3.57 | | |

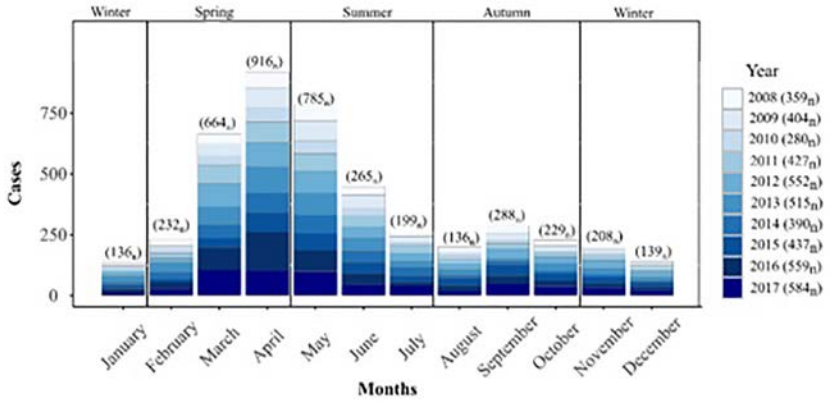


**Figure 2.3. Temporal distribution of cryptosporidiosis cases in Ireland (2008–2017). Winter, 483 cases; spring, 1812 cases; summer, 1249 cases; autumn, 653 cases.**

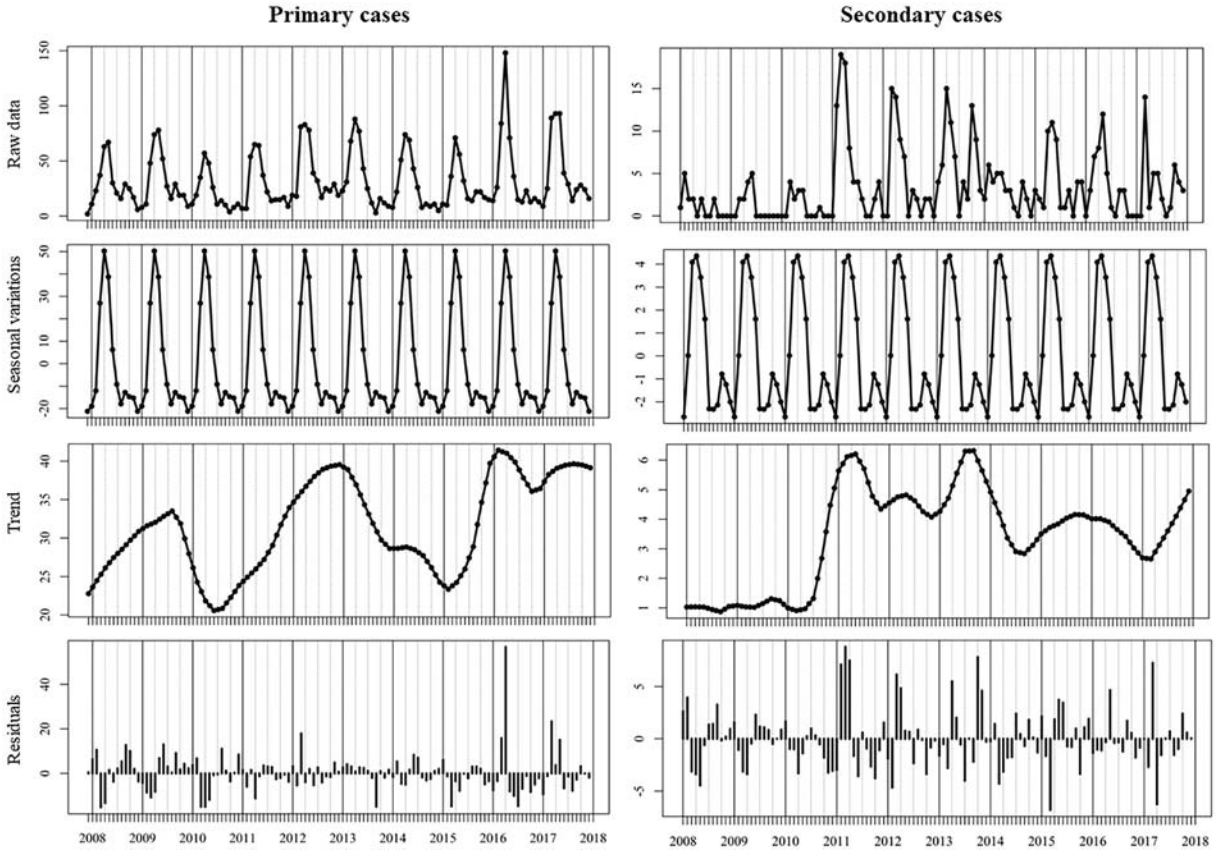


**Figure 2.4. Seasonal decomposition of sporadic (i.e. primary) (left) and outbreak-related (i.e. secondary) (right) cases of cryptosporidiosis in Ireland (2008–2017).**

and long-term trend, with a notable peak of infection in April 2016 (residual: +56). Outbreak cases exhibit a similar seasonal trend to that of sporadic cases, with annual peaks occurring in April followed by a secondary peak in September. The overall long-term trend in outbreak cases displayed a marked increase during 2011, continuing until 2014. Residuals calculated for outbreak cases point to more variation in 10-year trends, with peaks observed during the late winter/early spring months (January to March) of 2011, 2012 and 2017, while late spring/early summer peaks (April to June) were observed in 2013.

A peak in outbreak-associated cases was also observed during the winter months (October to November) of 2013. There was an increasing trend in the number/rate of travel-associated cases, with an annual peak occurring in August/September. The long-term trend exhibited a notable peak of infection during April 2016 (residual: +56). Outbreak cases exhibited a similar seasonal trend to that of sporadic cases, with the main annual peak occurring in April and a secondary peak in September. The overall long-term trend in outbreak cases displayed a marked increase during 2011, continuing until 2014. Residuals calculated for outbreak cases point to more variation in 10-year trends, with peaks observed during the late winter/early spring months (January to March) of 2011, 2012 and 2017, while late spring/early summer peaks (April to June) were observed in 2013.

A peak in outbreak-associated cases was also observed during the winter months (October to November) of 2013. The long-term trends varied significantly between delineated age categories, with considerably more variation noted among children ≤5 years of age (Figure 2.5), albeit annual peaks were observed among both age cohorts during April of each year. Residuals again point to a large transmission peak (residuals: +22, +34) within both sporadic and outbreak cohorts during April 2016. Annual decomposed patterns of infection show a peak in April of each year, followed by a significantly smaller peak during September, in both urban and rural areas (Figure 2.6). Calculated residuals point to an infection peak in April 2016 in both urban (+18) and rural

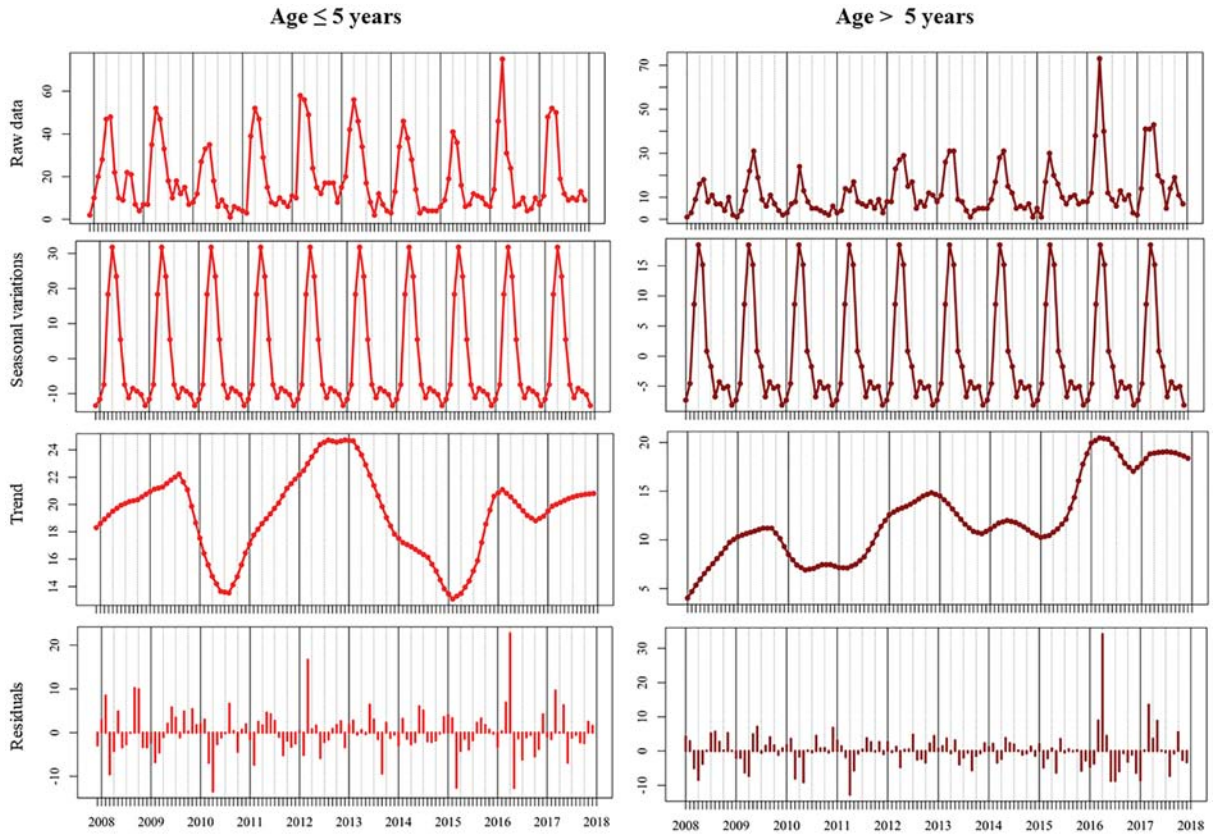


**Figure 2.5. Seasonal decomposition of cryptosporidiosis cases in Ireland among the ≤5 years (left) and >5 years (right) age groups (2008–2017).**

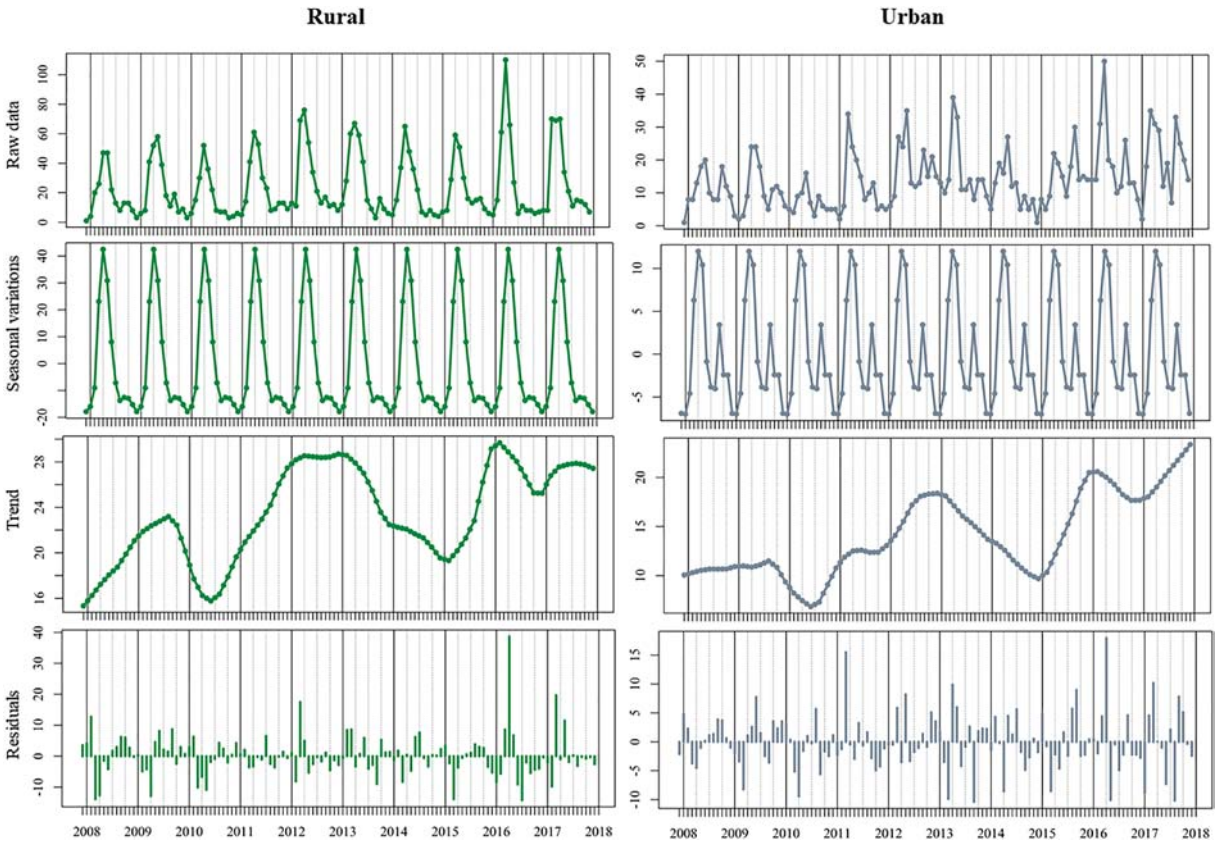


**Figure 2.6. Seasonal decomposition of cryptosporidiosis in Ireland in rural (left) and urban (right) areas (2008–2017).**

(+38) areas, consistent with trends observed among sporadic and age-delineated infection peaks.

### *2.3.3 Spatial autocorrelation*

A significant H–H cluster of sporadic cases was observed in the midlands (M) zone ('M' in Figures 2.1 and 3.1), with a large L–L cluster identified along the eastern seaboard (E), surrounding the Greater Dublin urban area and commuter belt (Figure 2.7a). L–L clusters were also observed in the south (S) and south-east (SE) regions, near the urban conurbations of Cork, Waterford and Limerick cities. Smaller H–H clusters of infection were observed in the S, SE and west (W) regions of the country, consistent with an overarching urban/rural pattern. Notable L–L outbreak-related case clusters were observed in the east of the country surrounding Dublin city and in the south surrounding Limerick city (Figure 2.7b).

Few H–H clusters were associated with outbreak-related cases; however, H–H cases identified in the M region were surrounded by L–H clusters, thus indicating potential neighbouring outliers. H–H and L–L clusters of infection in children aged ≤5 years followed a broadly similar spatial pattern to that observed within the sporadic case cohort, owing to the large proportion of cases from this cohort in the total dataset (Figure 2.7c). A large H–H cluster was observed in the M region, with smaller H–H clusters again identified in the S, SE and W regions.

L–L clusters of infection were also consistent with sporadic case clusters and typically identified around urban areas in the S and SE of the country. The spatial distribution of infection cold spots (L–L) among people aged >5 years (Figure 2.7d) followed a relatively similar pattern of infection cold spots among sporadic cases and paediatric (≤5 years) cases (Figure 2.7c). However, the spatial distribution of infection hotspots among people aged >5 years was markedly different from that of sporadic and paediatric cases, with smaller and more spatially dispersed hotspots identified, primarily in the M and SW regions.

### *2.3.4 Hotspot analysis (Getis-Ord GI*)*

Getis-Ord GI* analyses identified notable hotspots among sporadic cases in the M region, east and north-east of Galway city, with smaller hotspots also evident in the M, S and SE regions (Figure 2.8a). Again, a spatially extensive cold spot was identified in the E region, encompassing the Greater Dublin metropolitan urban area, and in the S and SE regions around Waterford, Limerick and Cork cities. Conversely, outbreak-related hotspots were centred around the border regions (e.g. Cavan, Monaghan) and northern areas within the M region (e.g. Longford) (Figure 2.8b).

The spatial distribution of hotspots and cold spots among children aged ≤5 years again followed a similar pattern to clustering of infection among all sporadic cases (Figure 2.8c). Large hotspots were observed in the M and S regions, with a previously identified sporadic infection hotspot in the W region demonstrating a significantly more pronounced occurrence among the paediatric subpopulation (north-east of Galway city). A large cold spot among children aged ≤5 years was also observed in the Greater Dublin area (E), albeit significantly reduced when compared with that observed among all sporadic infections. The spatial distribution of infection hotspots and cold spots among cases aged ≤5 years (Figure 2.8c) and cases aged >5 years (Figure 2.8d) were markedly different.

### *2.3.5 Space–time scanning*

Space–time clustering recurrence and cluster temporality for sporadic cryptosporidiosis cases are presented in Figure 2.9. Three primary hotspots were identified: south-west and east of Limerick city (SW, S, SE), and north-east of Galway city (M). Cold spots were persistent along much of the eastern seaboard, and particularly around the larger urban conurbations of Greater Dublin and Cork city, as well in several smaller areas along the western coastline.

The temporal window for space–time clusters mirrors the general seasonal distribution of cryptosporidiosis infection (section 3.2), with clusters most commonly identified during the period from March to June and peaking in April. Significantly lower levels of space–time clustering of outbreak-related cases were found (Figure 2.10), with the largest hotspots located in the western and midlands regions (M, W), and a maximum cluster recurrence of 30% (i.e. geographical area included in three identified clusters over 10 annual iterations). Two additional space–time clusters were identified, one to the north-east of Cork city (S) and one in County Donegal (N).

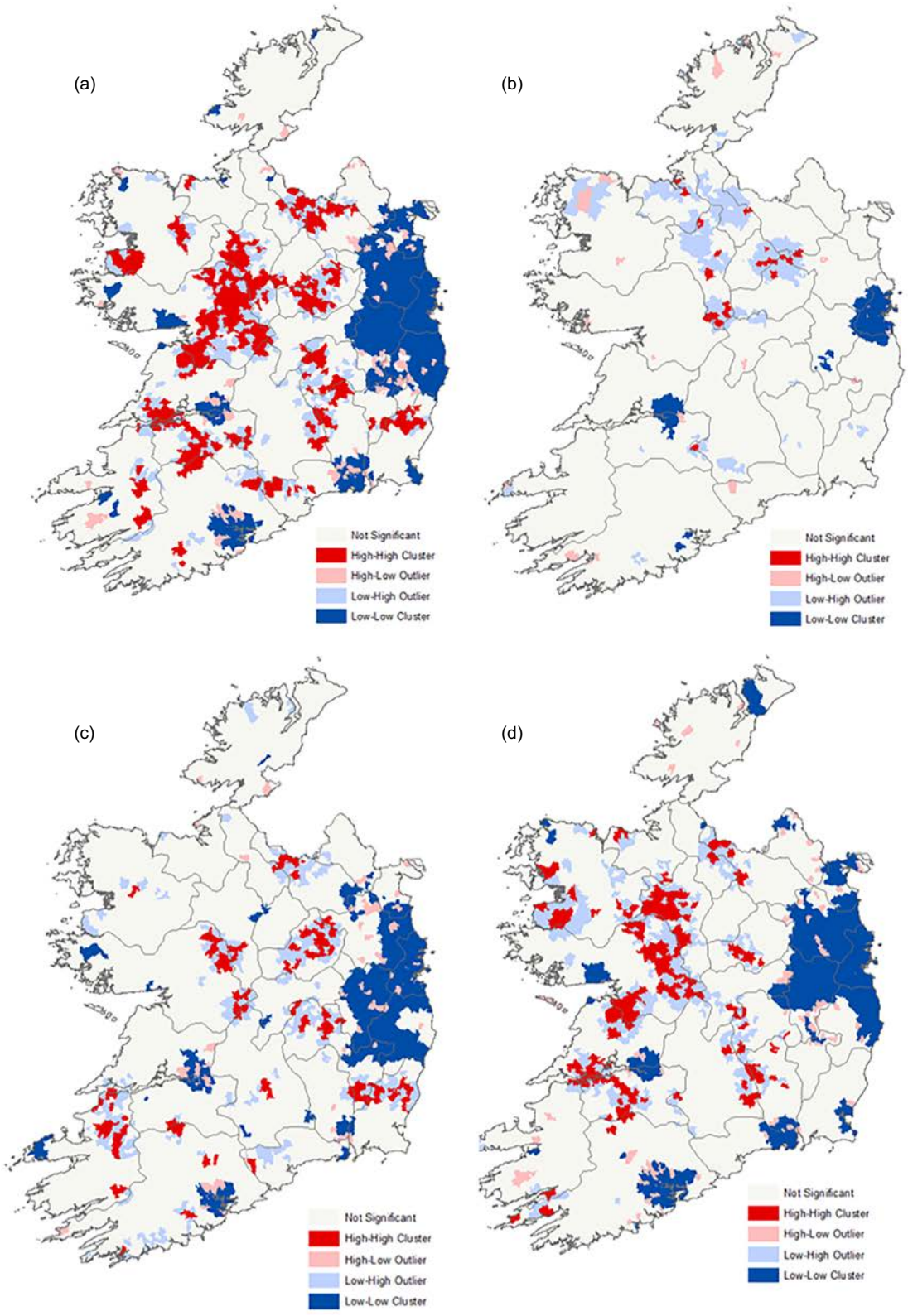


**Figure 2.7. Sporadic (a) and outbreak-related (b) cryptosporidiosis case clusters and outliers determined by Anselin Local Moran's *I* clusters. Sporadic cryptosporidiosis case clusters and outliers among children aged ≤5 years (c) and people aged >5 years (d) determined by Anselin Local Moran's *I* clusters.**

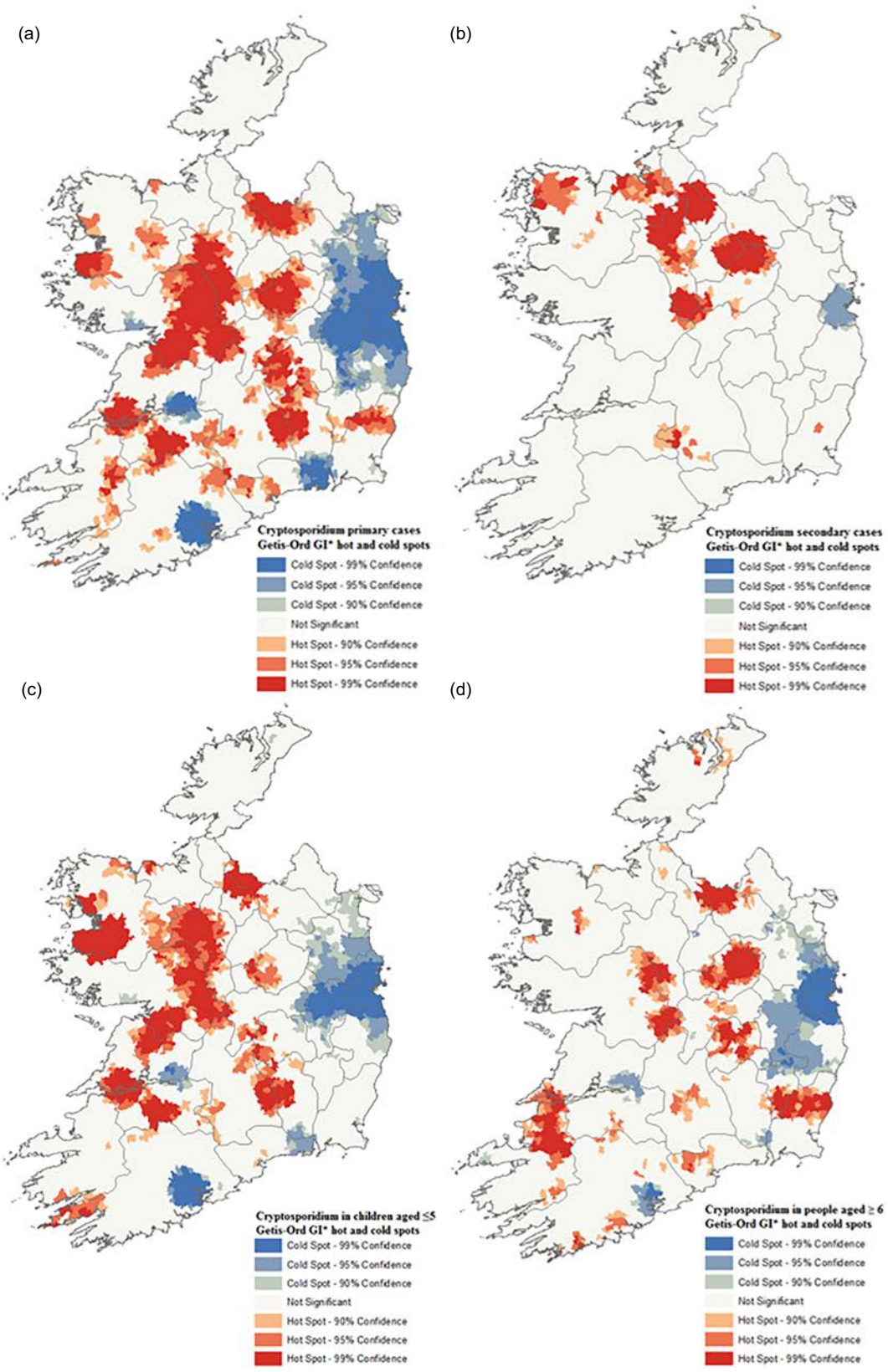


**Figure 2.8. Sporadic (a) and outbreak-related (b) cryptosporidiosis case hotspots and cold spots determined by Getis-Ord Gi* hotspot analysis. Sporadic cryptosporidiosis case hotspots and cold spots among children aged ≤5 years (c) and people aged >5 years (d) determined by Getis-Ord Gi* hotspot analysis.**

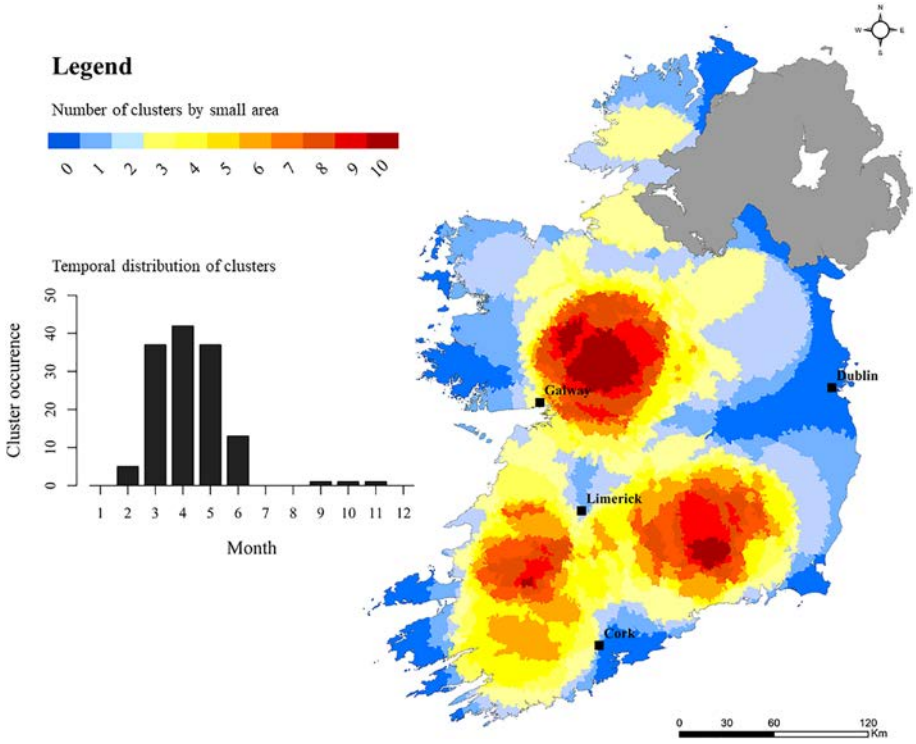


**Figure 2.9. Space–time "cluster recurrence" index (0–10) for sporadic cryptosporidiosis cases in Ireland (2008–2017).**

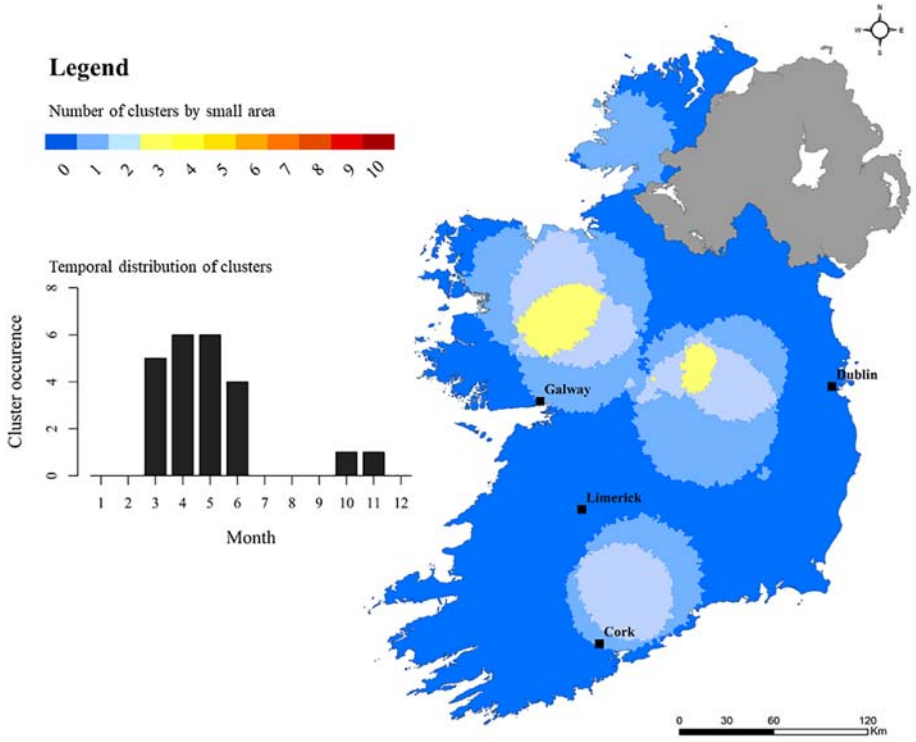


**Figure 2.10. Space–time "cluster recurrence" index (0–10) for outbreak-related cryptosporidiosis cases in Ireland (2008–2017).**

Most (8/9) outbreak-related clusters were observed from March to June, with one cluster occurring during October/November (2013). Cluster index mapping for the subpopulation aged ≤5 years mirrored that of sporadic cases, with three primary hotspots identified: one, again, occurred in a large area located north-east of Galway city (M), while two "secondary" (i.e. lower cluster recurrence indices) areas were also identified, one south-west and one south-east of Limerick city (SW, S) (Figure 2.11). The results for the subpopulation aged >5 years point to a lower level of clustering, with hotspots located south-west of Limerick city (SW), and in the M and SE regions (Figure 2.12).

## 2.4 Discussion

### *2.4.1 Occurrence of sporadic and outbreak-associated cryptosporidiosis*

The presented 10-year (2008–2017) nationwide spatiotemporal analysis of confirmed cryptosporidiosis in Ireland was undertaken to identify seasonal trends, spatial clusters and areas of repeat infection. In this study, cryptosporidiosis was shown to have a relatively wide geographical distribution in Ireland, with 58% of EDs and 17% of SAs associated with at least one confirmed case over the study period. CIRs of infection exhibited a moderately increasing trend, with these rates broadly mirroring those encountered in some other European countries, such as Sweden, Denmark and France (Stensvold *et al.*, 2015; ECDC, 2019a).

The majority (59.3%) of sporadic cases of cryptosporidiosis occurred in children aged ≤5 years, which concurs with the findings of several previous studies (Putignani and Menichella, 2010; Chalmers and Caccio, 2016; Xiao *et al.*, 2016); within this cohort, cases among boys were more frequently reported (OR 1.3873), potentially reflecting the tendency of male infants to mount weaker immune responses (Muenchhoff and Goulder, 2014) or their enhanced susceptibility to environmental exposures via gender-specific play. Conversely, girls accounted for a significantly higher proportion of outbreak-related cases of cryptosporidiosis, which may reflect higher levels of direct contact (and subsequent transmission) between female infants and parents/family members (Painter *et al.*, 2016).

A recent small-scale investigation of the regional epidemiology of cryptosporidiosis in County Cork demonstrated moderately increased infection rates

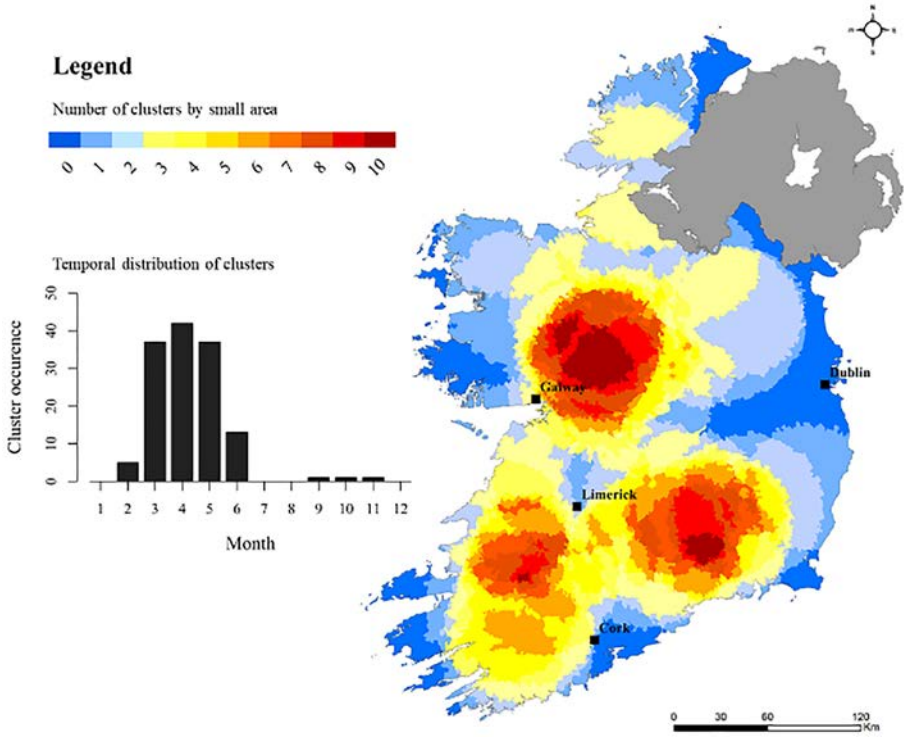


**Figure 2.11. Space–time "cluster recurrence" index (0–10) for sporadic cryptosporidiosis cases in Ireland among children aged ≤5 years (2008–2017).**

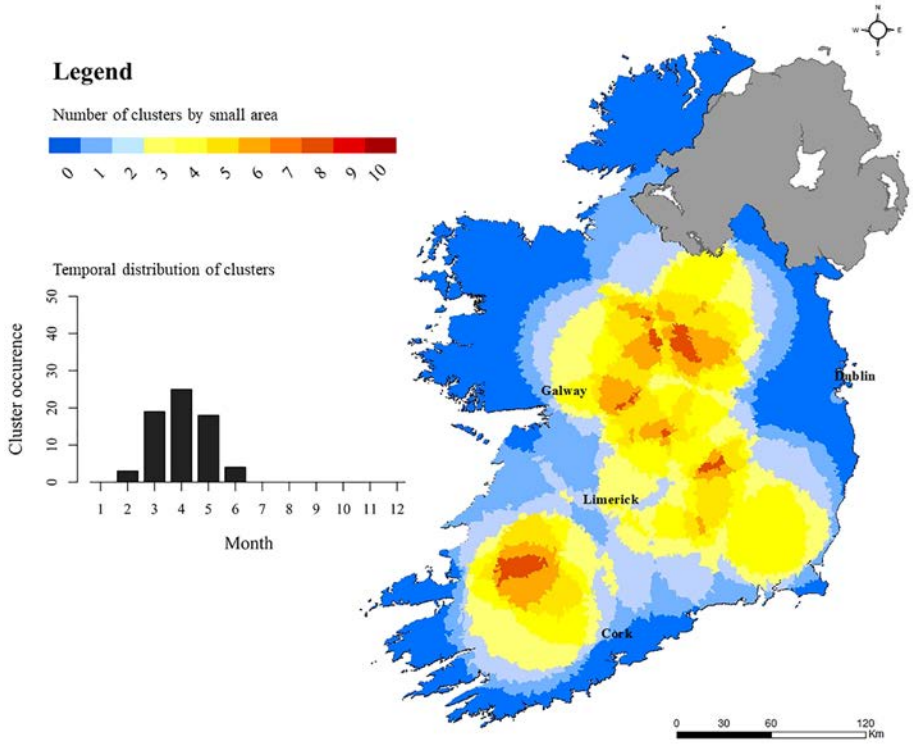


**Figure 2.12. Space–time "cluster recurrence" index (0–10) for sporadic cryptosporidiosis cases in Ireland among people aged > 5 years (2008–2017).**

among people aged 20–34 years, suggesting likely anthroponotic transmission via caregiver contact with infected children (O'Leary *et al.*, 2020). Geographically, most sporadic cases (65.8%) occurred in rural areas ($\chi^2$=110.493, $p$<0.001; Table 2.1), where approximately 37.3% of the Irish populace reside (CSO, 2018). A previous study by Pollock *et al.* (2010) in Scotland similarly found that *C. parvum* infection was associated with areas characterised by lower human population density and a higher ratio of farms to humans, both indicators of rurality.

While the current study represents the first nationwide study of the spatiotemporal epidemiology of cryptosporidiosis in Ireland, this finding was expected, and is likely to be attributable to increased exposure to sources of *Cryptosporidium* spp. oocysts in rural areas, including farmyard animals (Chalmers *et al*., 2019), direct exposure to contaminated surface water (Hamilton *et al.*, 2018) and the use of groundwater as a drinking water source (Chique *et al.*, 2020). Conversely, urban areas exhibited a significantly higher secondary (OR 1.5383) and travel-related (OR 3.5742) case occurrence, and may be representative of *C. hominis* infections as opposed to the agriculturally (rural) associated *C. parvum*; however, as data on *Crytposporidium* infections are not disaggregated by species within the Irish disease reporting system, this conclusion is somewhat speculative.

### *2.4.2 Seasonal decomposition*

Seasonal decomposition points to an overall increasing temporal trend over the 10-year study period (Figure 2.4), consistent with previously reported trends in the west of Ireland over the period 2004–2007 (Callaghan *et al.*, 2009). Specifically, the annual peak identified during April is consistent with previously reported regional peaks (March/April; Callaghan *et al.*, 2009), in addition to those reported by Pollock *et al.* (2010) in Scotland (April/May), which are likely to be associated with agricultural cycles in temperate regions, i.e. lambing/calving and manure spreading. While not reported in the current study, seasonal patterns may vary among differing *Cryptosporidium* species; for example, *C. hominis* is more prevalent during autumn in the UK and New Zealand (increased travel and school/childcare attendance), whereas *C. parvum* is more typically encountered during spring in Canada, Ireland and the Netherlands. The

secondary peak in outbreak-related cases observed during September in Ireland (Figure 2.4) is consistent with the bimodal pattern of *C. hominis* infection (with peaks in August and October) observed in Scotland (Pollock *et al.*, 2010), and may reflect the increase in national/international travel and children returning to childcare after the summer break.

Seasonal decomposition also identified several notable deviations from the overarching temporal trend (i.e. residual peaks) that merit closer investigation, particularly regarding dynamic drivers of exposure/transmission, such as extreme weather events (Jagai *et al.*, 2009; Britton, 2010; Lal *et al.*, 2012). A marked residual (i.e. minus seasonal signal) identified during April 2016 (Figure 2.4) warrants further exploration with respect to dynamic meteorological events, particularly considering severe temporally associated flooding experienced across Ireland and the UK (Barker *et al.,* 2016). Winter 2015/2016 was characterised by a succession ($n = 6$) of Atlantic storms across Ireland, resulting in exceptional and widespread flooding, with all synoptic weather stations reporting rainfall volumes significantly above their long-term average (Barker *et al.*, 2016), potentially resulting in an increase in water-associated gastrointestinal infection.

Increases in storm water and surface run-off may increase pathogen mobility in the natural environment, thus exacerbating the likelihood of human infection either directly (i.e. contaminated "raw" water and food) or indirectly through water treatment failures. Notably, the most significant outbreak of cryptosporidiosis in Ireland, that which occurred in Galway during spring 2007, resulted from direct deterioration of source water quality (Lough Corrib) coupled with inadequate water treatment (Chyzheuskaya *et al.*, 2017). Similarly, a cryptosporidiosis outbreak that occurred during August 2013 in the city of Halle, Germany, began 6 weeks after the river Saale overflowed into the floodplain and parts of the city centre (Chalmers and Caccio, 2016), thus emphasising the (lagged) impact of local meteorological conditions on the incidence of infection.

### *2.4.3 Spatial autocorrelation and hotspot analysis*

Incorporating a spatial dimension into investigations of infectious disease epidemiology is of primary importance considering the spatial variation of environmental exposure, including factors such as land use, local climate and socio-economic status (Congdon, 2016). This is particularly the case in Ireland, which has previously been described as "the perfect storm" in terms of potential gastroenteric infection risk factors (O'Dwyer *et al.*, 2018). The results of Anselin Local Moran's *I* statistics and the Getis-Ord GI* statistic provided relatively similar spatial patterns. High-incidence (H–H) clusters were identified in the midlands (M), a predominantly rural area with a high level of dependence on pastoral agriculture and "private infrastructure" (e.g. one-off housing with on-site wastewater treatment and domestic water supplies).

Several previous studies have documented strong associations between cryptosporidiosis and cattle density (e.g. Pollock *et al.*, 2010; Luffman and Tran, 2014). Similarly, Borchardt *et al.* (2003) have previously found a higher incidence of endemic diarrhoeal infections in areas characterised by elevated septic tank (OR 1.22) and private water supply (OR 6.18) densities among a population-based cohort in central Wisconsin. Low-incidence (L–L) clusters were primarily located in the vicinity of Dublin and other relatively large cities (Waterford, Cork, Limerick, Galway), thus probably highlighting the protective effect of urban living within the Irish context, where reduced environmental exposure to pathogen sources coupled with reduced pathogen transport (i.e. treated drinking water supply) may reduce the risk of exposure and subsequent infection (Lal, 2016).

Conversely, studies in other countries have shown that rates of cryptosporidiosis are typically higher in urban areas characterised by elevated human population densities; for example, Cohen *et al.* (2008) reported that higher population density and above-average household sizes were associated with increased odds of reported cases of cryptosporidiosis in Massachusetts. Likewise, Greenwood and Reid (2020) found that a majority of cryptosporidiosis clusters identified across Queensland, Australia, from 2001 to 2015 centred on major and regional cities.

Both geostatistical techniques suggest that a disparity exists between outbreak-related and sporadic case clustering over the 10-year study period (Figures 2.7a and b and 2.8a and b), with outbreak-related clusters occurring in the north midlands and "border area". This was somewhat unexpected, particularly as the aforementioned areas are traditionally characterised

as having a relatively low population density, with person-to-person transmission thus less likely within the community.

### *2.4.4 Space–time scanning and cluster recurrence*

Space–time scan statistics detect temporally specific clusters characterised by a significantly higher observed case number than expected (e.g. space–time randomness not present), based on calculated baseline incidence (Kulldorff, 1999). The approach employs a three-dimensional (cylindrical) scanning window comprising both height (time) and space (geographical area) (Kulldorff, 1999). Over the past decade, space–time scan statistics have been recognised as a powerful tool for endemic disease surveillance and early outbreak detection (Tango *et al.*, 2011); however, to the authors' knowledge, this represents the first time it has been applied to infectious disease incidence in Ireland.

A total of 69 space–time clusters (≥10 confirmed cases) were identified over the 10-year study period, of which 55 (79.7%) were clusters of sporadic infection, ranging from a minimum of four (7.3%) during 2017 to a maximum of seven (12.7%) during 2009. No statistical association was found between annual sporadic and outbreak-related cluster number during the study period; however, development of the "cluster recurrence" index permits identification of discernible spatial and temporal patterns defining the formation of clusters across the decade-long period. Three regions exhibited particularly recurrent space–time clusters of infection, with occurrences in at least 8 out of 10 years, namely south-west and east of Limerick city (SW, S, SE), and north-east of Galway city (M), with neither of these conurbations located within a highly recurrent region. The spatiotemporal frequency of space–time clusters suggests the presence of persistent reservoirs in these areas, thus maintaining community and/or transmission pathways (Greenwood and Reid, 2020).

The proximity of large urban centres to each high-recurrence region may reflect relatively narrow transitional zones between urban fabric and populated rural regions, i.e. rural commuter belts that remain unserviced with respect to municipal wastewater treatment and/or drinking supplies. Additionally, all four regions are largely underlain by karstified carboniferous limestone aquifers (Woodcock, 2009), which have previously been associated with the presence of *Cryptosporidium* spp. in private and small public drinking water supplies (Zintl *et al.*, 2009; Darnault *et al.*, 2017). Conversely, the Greater Dublin area, characterised by a large urban commuter belt, spatially extensive consolidated bedrocks and a high level of (waste)water infrastructure, did not exhibit any space–time clusters over the study period.

A significant majority of space–time clusters occurred over the 2-month period May–June, mirroring findings from the overall case cohort and further highlighting the likely association between agricultural cycles and the incidence of infection in temperate regions such as Ireland, Scotland and New Zealand (Pollock *et al.*, 2010; Khan *et al.*, 2018). Additionally, Lal *et al.* (2015) signalled a need to study the effect of spatial and temporal variations in ecological and social risk factors on the incidence of cryptosporidiosis with specific emphasis on the potential for socio-economic disadvantage to amplify disease risk within populations, e.g. in areas of low educational attainment and lower income levels, which are often associated with rural living.

From a public health surveillance perspective, identification of 55 space–time clusters of sporadic cryptosporidiosis infection over a 10-year represents a concern, while underscoring the major challenges involved in decreasing the incidence of infection via enhanced surveillance and subsequent intervention. For example, during 2008, a spatially restricted space–time cluster identified in the northern midlands was characterised by approximately 17 times more cases of infection than would be expected [relative risk (RR) 17.95] over a 3-month period (February–April), with a number of identified space–time clusters occurring over time periods as short as 4 weeks. This level of clustering may suggest the need for new surveillance and/or analytical methods to elucidate hitherto unidentified sources and pathways of infection, and identify space–time clusters while they exist, i.e. in real time, or prospective scanning.

It is important to note that a lack of species information, and particularly the inability to distinguish between C. *parvum* and C. *hominis*, the two most frequently encountered *Cryptosporidium* species in Ireland, represents a study limitation. As previously outlined, in Scotland, Pollock *et al.* (2010) found *C. parvum* infection to be associated with lower

population density and higher ratio of farms to humans – both indicators of rurality – while *C. hominis* was more likely to be found in increasingly urban areas in central Scotland. Speciation would thus make it easier to identify the socio-demographic influences on rural/urban distribution. Further investigation is required to elucidate potential sources and pathways of infection with regard to livestock densities, climate, hydrogeology and socio-economic status.

Despite surveillance of cryptosporidiosis being mandatory in Ireland owing to its communicable disease status, the disease is widely considered to remain under-reported in both Ireland and the EU. The presented study represents a significant advance in efforts to investigate the spatiotemporal epidemiology of cryptosporidiosis with a view to further elucidating pathways of infection to guide public health interventions through an improved understanding of its spatiotemporal occurrence, clustering mechanisms, levels of recurrence, and associated drivers, pathways and receptors.

# 3 Spatiotemporal Epidemiological Modelling of VTEC infections in Ireland

## 3.1 Introduction

Over the last decade, Ireland has frequently reported the highest incidence of VTEC infection in the EU (HPSC, 2019b). The reported national CIR of confirmed VTEC infections in Ireland during 2017 was 923 cases (16.6 cases/100,000 population), equating to 10 times the EU average (1.66 cases/100,000 population) (HPSC, 2019b; ECDC, 2019b). Shiga toxin-producing *E. coli* bacteria, of which there are > 100 serotypes, were first discovered in 1977; the best-known VTEC strain, *E. coli* O157:H7, was first recognised as a pathogen in 1982. The Shiga toxin-producing group of *E. coli* includes serotypes O157 and O26, and other enterohaemorrhagic *E. coli* bacteria; serotypes are typically categorised by the presence of *stx1* or *stx2* genes (Karmali *et al.*, 2010). Shiga toxin-producing *E. coli* and verotoxin-producing *E. coli* are both referred to as VTEC in this report.

VTEC enteritis is associated with a wide range of sequelae, from mild diarrhoea to haemorrhagic colitis, haematochezia (bloody diarrhoea), thrombotic thrombocytopenic purpura and haemolytic–uraemic syndrome (HUS), which causes intravascular lysis of red blood cells (Garvey *et al.*, 2016b; ECDC, 2019b). Infection is characterised by several transmission routes, including consumption of contaminated food and water, person-to-person contact or direct contact with infected animals (Garvey *et al.*, 2016b; ÓhAiseadha *et al.*, 2017). A recent study found that the incidence of confirmed sporadic (i.e. non-outbreak) VTEC O157 infection in Ireland in 2008–2013 was significantly elevated in regions characterised by high reliance on private groundwater (OR 18.727; $p < 0.001$) and high livestock densities (OR 1.001; $p = 0.07$) (ÓhAiseadha *et al.*, 2018).

Transmission sources, pathways and source–pathway interactions associated with VTEC infection in Ireland are multifaceted, resulting in a complex exposure profile (Brehony *et al.*, 2018). Sporadic cases of infection are inherently difficult to attribute to specific risk factors for reasons that include the absence of accurate date-of-onset data, under-reporting, misdiagnosis, myriad potential exposures and surveillance limitations (Hynds *et al.*, 2014b; ÓhAiseadha *et al.*, 2017; Brehony *et al.*, 2018). Of 2210 confirmed VTEC enteritis cases reported in Ireland over the period 2008–2013, a total of 1264 (57.2%) were defined as sporadic (ÓhAiseadha *et al.*, 2017). The high proportion of sporadic VTEC infections relative to total annual cases in Ireland, and their association with environmental exposures, has made analysis of the spatiotemporal occurrence of VTEC particularly important in public health. We used a suite of geostatistical approaches to explore spatiotemporal analyses of sporadic VTEC infection in Ireland, a country characterised by the highest infection CIRs in Europe.

## 3.2 Methods

### *3.2.1 Data collection and processing*

Because the primary study objective was to investigate patterns of domestic transmission, we excluded from analyses cases attributed to secondary infection (i.e. person-to-person transmission) and cases originating outside Ireland. We defined primary sporadic infection as a laboratory-confirmed case notified to the Department of Public Health during the period 1 January 2013 to 31 December 2017 that had no reported epidemiological link to another notified case, or was identified as an outbreak index case (i.e. the first documented case within a recognised cluster or outbreak). We obtained irreversibly anonymised case data from the CIDR database (http://www.hpsc.ie/CIDR), a national database of notifiable infectious disease events reported by regional departments of public health in accordance with the Infectious Diseases (Amendment) Regulations 2011 (S.I. No. 452 of 2011).

Case confirmations were determined using both clinical and laboratory criteria. Clinical confirmation was primarily based on presentation of at least one symptom (diarrhoea, abdominal pain and HUS), with

laboratory confirmation requiring more than one of the following criteria to be met: isolation of strains positive for *stx1*, *stx2* or both; direct detection of *stx1* or *stx2* nucleic acids (in the absence of strain isolation); or direct detection of Shiga toxins in faecal samples.

We geographically referenced all confirmed cases to one of 18,641 census SAs from the 2011 CSO census using the Health Atlas Ireland georeferencing tool. SAs are currently the smallest spatially defined area for census reporting in the state, and exist as subdivisions within EDs of Ireland; each covers an area of 0.001–163 $km^2$ and holds 80–120 dwellings. SAs are thus developed based on household numbers and residential population (i.e. not spatial extent or population density) and are used to report population-based statistics while ensuring personal and household anonymity. We delineated three infection subsets for additional analyses based on epidemiological and clinical significance: urban/rural classification; VTEC serogroup (O157, O26, other); and patient age (65 years).

We extracted SA-specific human population counts from the 2011 and 2016 (CSO) census datasets and used those counts to calculate SA-specific VTEC incidence. We merged the CSO's 14 urban/rural categories to classify each spatial unit as rural or urban, using population density and settlement size to verify classification. For reporting purposes, we defined eight distinct geographical zones in Ireland (Figure 3.1). Zone NE (Northern Ireland) is located outside CIDR surveillance boundaries and was not included in our analyses. The Royal College of Physicians of Ireland Research Ethics Committee granted ethics approval for the acquisition and analyses of human infection data (RCPI RECSAF_84).

### *3.2.2 Seasonal decomposition*

We analysed seasonal decomposition for monthly incidence using the STL method, which combines multiple regression with k-nearest neighbour metamodelling (Fox, 2015). The STL method decomposes a time series into trend, seasonal and residual components; we used an additive model for our study because peak values of the seasonal time series exhibit a relatively constant trend (Prema and Uma Rao, 2015). The monthly incidence ($Y_v$) is equal to the sum of the trend ($T_v$), the seasonal

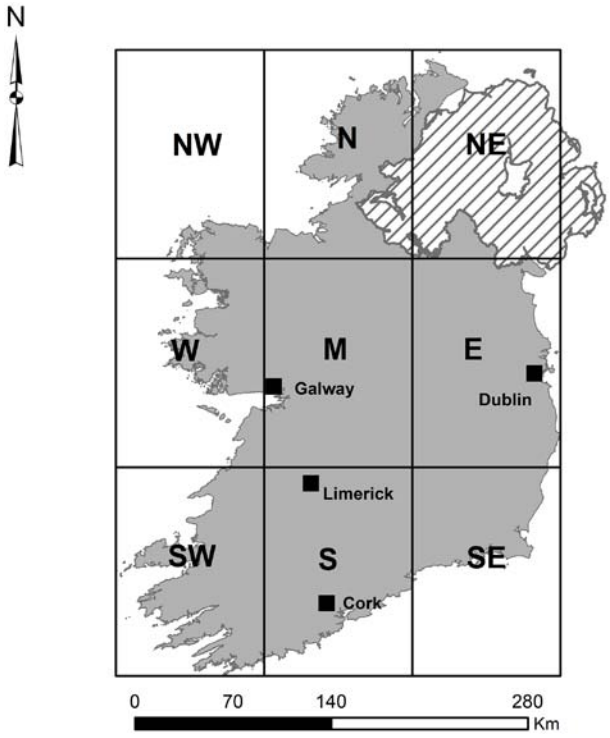


**Figure 3.1. Geographical zones of Ireland. Sections of the grid represent the eight distinct zones; zone NE, Northern Ireland, was not included in study of primary VTEC enteritis cases.**

variation ($S_v$) and the residuals ($R_v$). For the seasonal decompositions, we used the STL () function in R version 3.6.0 (R Foundation for Statistical Computing; https://www.r-project.org).

### *3.2.3 Spatial autocorrelation (Anselin Local Moran's* I*)*

We used Anselin Local Moran's *I* to examine individual features, specifically disease incidence within individual SAs, and their relationship to nearby features, returning localised clusters that may be correlated based on variance assigned to all individual spatial units (Anselin, 1995). We calculated Anselin Local Moran's *I* statistics using the cluster/outlier tool in ArcGIS software version 10.6 (ESRI; https://www.esri.com) and maps of the resultant high and low spatial clusters generated. We used cluster/outlier analysis to classify statistically significant H–H, L–L, H–L and L–H clusters. We conceptualised spatial relationships using the inverse distance and Euclidean distance methods; we set the significance at 95% based on pseudo *p*-values.

### *3.2.4 Space–time scanning*

We used SaTScan version 9.6 space–time cluster detection software (https://www.satscan.org) to identify temporally specific high- and low-risk regions. We defined the space–time scan statistic by a cylindrical window with a circular (or elliptic) geographical base (e.g. radius unit), the height of which corresponded to the time period of potential clusters (Kulldorff, 1999). The null test hypothesis presumes that geographical regions inside and outside the scanning area are characterised by an equal RR of infection during the analysed time period. We compared RR differences using the log likelihood ratio (i.e. RR within an area is expected to be proportional to population size or population-years) (Allévius, 2018). We used a discrete Poisson model owing to the high level of geographical resolution (SA, $n = 18{,}641$) in our study (i.e. high number of SAs with zero cases or one case over the modelled period). We used the total population of each SA from the 2011 national census as a control parameter; we performed multiple scans to optimise parameter selection and outcome stability. We chose a maximum geographical cluster size of 10% of the PAR to account for the low number of reported cases in many areas, in concurrence with a maximum cluster radius of 50 km. We aggregated data monthly; maximum temporal cluster duration was 3 months based on known seasonal effects. Cluster size was > 10 reported cases to ensure that identified clusters contained enough observed cases.

We used findings from annual space–time scanning to acquire a spatiotemporal picture of recurrent cluster locations via a mapped and calculated "cluster recurrence index". Several tools have been developed to detect space–time anomalies, including the spatial varying temporal trend scan, implemented in SaTScan, which is used to identify unusual spatial cluster locations that contribute to substantial increases or decreases in general trends (Kulldorf, 2021). The cluster recurrence index we describe aims to shed light on spatially specific, recurrent space–time hotspots of infection by providing an ordinal classification for all spatial units that may be amended over time and used for prospective surveillance purposes.

## 3.3 Results

### *3.3.1 Occurrence of VTEC infection in Ireland (2013–2017)*

Of 2783 confirmed sporadic cases included in the CIDR system during the period 2013–2017, we successfully geolinked 2755 (98.9%) to a distinct spatial area. The most frequently confirmed serogroups associated with notified human infection were VTEC O26 ($n = 800$, 29%) and O157 ($n = 638$, 23.2%) (Table 3.1). We classified an additional 23.5% of confirmed infections as ungroupable ($n = 391$) or not serogrouped ($n = 255$). Of the remaining confirmed infection serogroups, VTEC O145 ($n = 126$), O103 ($n = 79$) and O146 ($n = 59$) were the only serogroups associated with > 50 confirmed infections. Temporal cumulative incidence rates exhibited an annual peak during late summer and early autumn; maximum peaks typically occurred during July ($n = 366$) (Figure 3.2). We observed yearly increases in case numbers between 2013 (463 cases) and 2017 (674 cases).

We observed markedly higher case numbers among children ≤ 5 years, with older adults (> 65 years) also disproportionately affected, accounting for 462 cases (16.6%, compared with 11.7% for the national population). Females were affected slightly more often (52.5%) than males (47.2%) (Figure 3.3). We

**Table 3.1. Confirmed sporadic VTEC infections in Ireland, 2013–2017**

| Characteristic | VTEC O157 ($n = 668$) | VTEC 026 ($n = 714$) | Other serogroups ($n = 724$) | Not serotyped/ungroupable ($n = 649$) |
|---|---|---|---|---|
| Age (years) | | | | |
| ≤5 | 231 (34.6) | 431 (60.4) | 255 (35.2) | 184 (28.4) |
| 6–64 | 373 (55.8) | 232 (32.5) | 314 (43.4) | 273 (42.1) |
| ≥65 | 64 (9.6) | 51 (7.1) | 155 (21.4) | 192 (29.6) |
| | | | | |
| Setting | | | | |
| Urban | 288 (43.1) | 278 (38.9) | 329 (45.4) | 309 (47.6) |
| Rural | 380 (56.9) | 436 (61.1) | 395 (54.6) | 340 (52.4) |

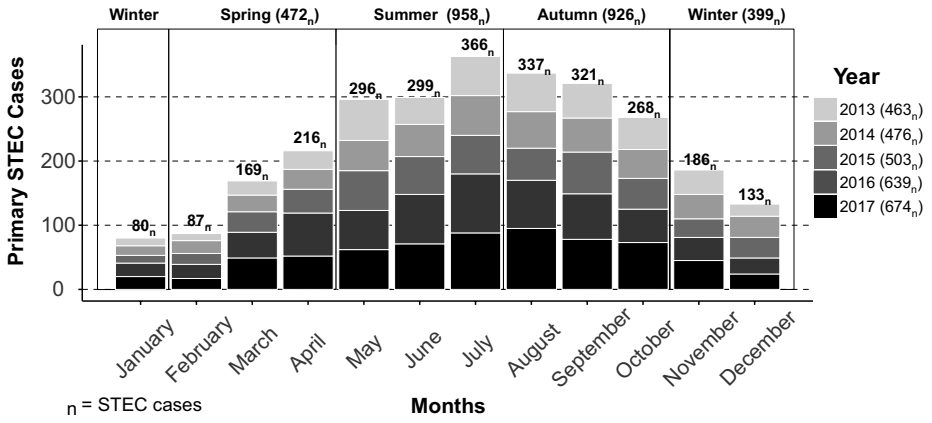


**Figure 3.2. Temporal distribution of primary VTEC enteritis cases in Ireland, 2013–2017.**

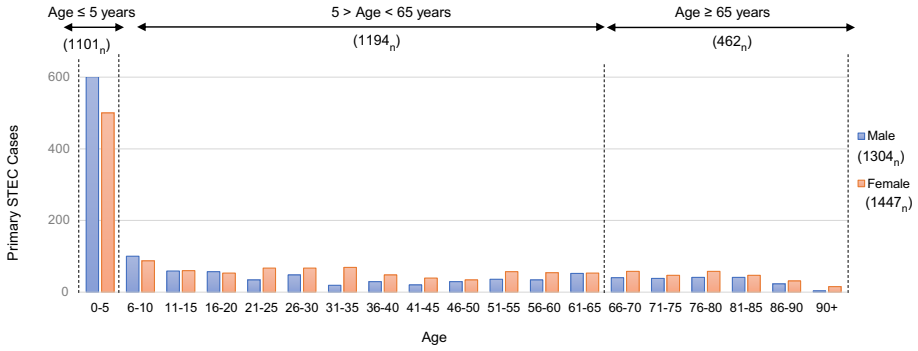


**Figure 3.3. Distribution of primary VTEC enteritis cases by age and sex in Ireland, 2013–2017. Dotted vertical lines show the main age-group divisions. STEC, Shiga toxin-producing *E. coli*.**

observed more than one case more frequently in SAs classified as rural (1252/6242, 20.1%) than in urban SAs (1086/12,246, 8.9%) (Table 3.1). Pearson $\chi^2$ tests with Yates' continuity corrections indicate a significant association between cases of VTEC O26 infection and the ≤5 years age category (OR 2.338). No statistical association was found between VTEC serogroup and urban/rural classification ($p = 0.6005$) or the incidence of age-specific cases and urban/rural classification ($p = 0.7803$).

### *3.3.2 Seasonal decomposition*

The decomposed 5-year trend indicates a monotonic increase in the occurrence of sporadic infection, with a clear annual peak occurring during late summer (July–August) (Figure 3.4). Calculated residuals point to a relatively consistent annual and longer-term trend, ranging from a maximum of +24 cases during April 2016 to −26 cases during December 2018. We found substantial variation in seasonal infection peaks (all VTEC serogroups) among delineated age categories; infections among the subpopulation aged ≤5 years peaked from May to July, whereas infections among the subpopulation aged >5 years occurred primarily in July–August, followed by a smaller secondary peak in October.

The general decomposed trend for VTEC O157 infection indicates a relatively modest overall increase over the study period, with a marked decrease during 2015 (Figure 3.5). Conversely, the incidence of VTEC O26 exhibited a greater increase from January 2013 to April 2016, followed by a consistent decrease to the end of the study period. Other (non-O157 and non-O26) VTEC serogroups exhibited a gradual monotonic increase over the study period. Seasonal signals indicate a notable difference between the two main serogroups; VTEC O157 infections exhibited the highest rates of occurrence during September–October, whereas VTEC O26 notifications peaked in July. Urban cases exhibited an annual peak from July to September, whereas rural case notifications displayed a longer but decreasing peak from May to October.

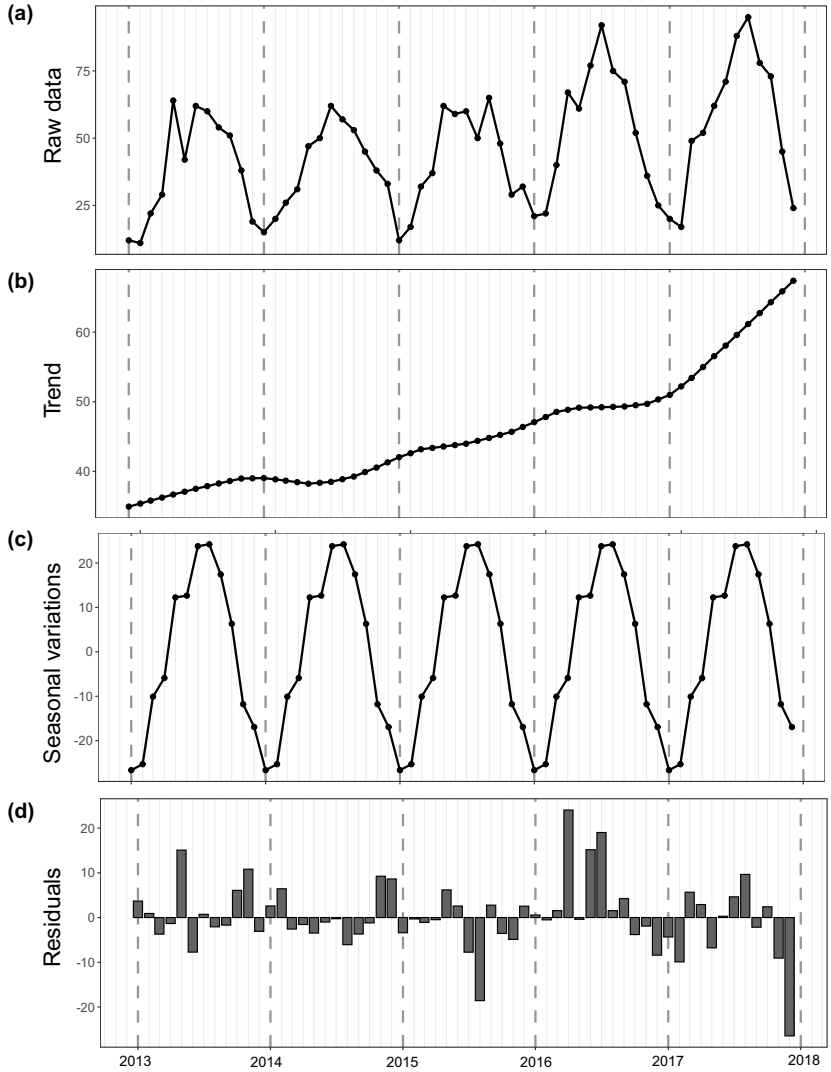


**Figure 3.4. Trends and variations in confirmed primary VTEC enteritis cases in Ireland, 2013–2017. (a) All confirmed cases; (b) decomposed 5-year trend of confirmed cases; (c) seasonal variation in confirmed cases; (d) calculated residual trend in confirmed cases.**

### *3.3.3 Spatial autocorrelation (Local Anselin Moran's* I*)*

H–H VTEC incidence clusters were predominantly situated in zones S and SE around counties Clare, Limerick and Tipperary (Figure 3.6), interspersed with smaller L–H outlier clusters. We observed infection cold spots (L–L clusters) around the greater Dublin area (zone E) and Cork city (zone S), in addition to counties Sligo (zone N) and Kerry (zone SW). VTEC O157 infection clusters were geographically sparse, with small distinct H–H clusters (hotspots) observed in zones M, E and S. We again observed large infection cold spots among the VTEC O26 serogroup and the ≤5 years age group irrespective of VTEC serogroup in the urban centres of Dublin and Cork cities (zones E and S) in addition to counties Kerry, Waterford and Sligo (SW, SE and N regions). The spatial distribution of VTEC O26 and ≤5 years age group hotspots of infection followed a similar trend to overall VTEC clustering patterns: H–H clusters were identified in zones S, M and E, in addition to one unique H–H cluster in zone NW that we did not observe for VTEC O157.

### *3.3.4 Space–time scanning*

Overall, we identified 17 distinct space–time clusters, ranging from two clusters during 2014 to five clusters during 2017 (Table 3.2 and Figure 3.7). To acquire a clearer picture of hotspots and cold spots relative to space–time cluster occurrence, we developed

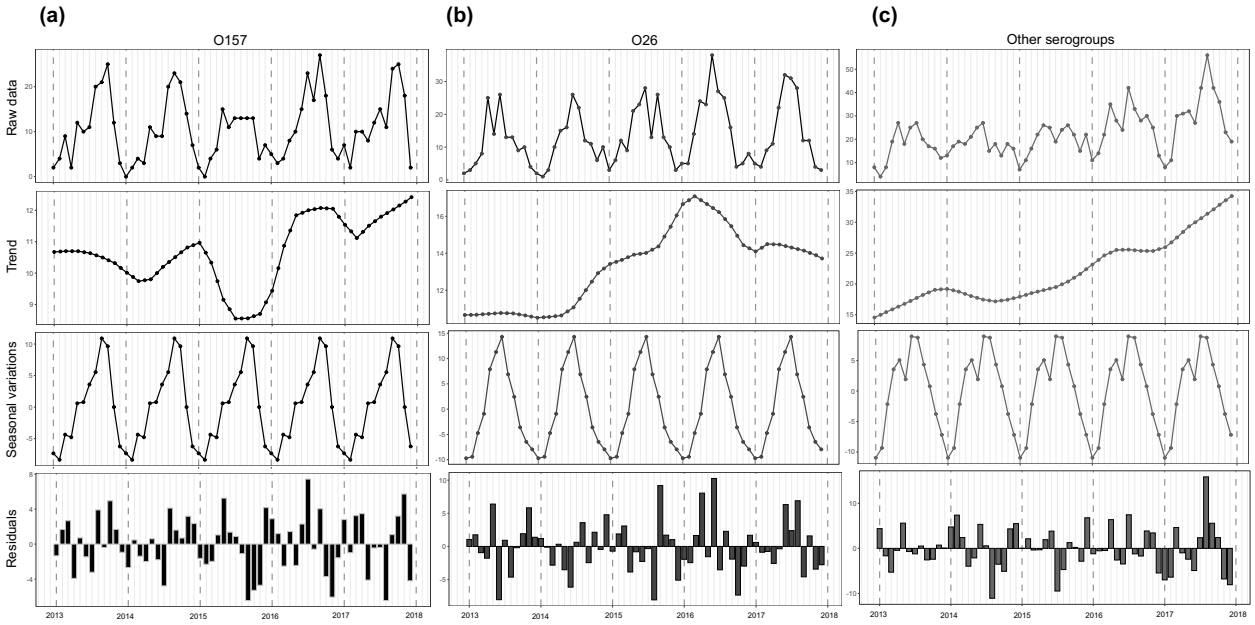


**Figure 3.5. Trends and variations in confirmed cases of primary VTEC enteritis in Ireland, 2013–2017, disaggregated by serogroup: (a) O157, (b) serogroup O26 and (c) other serogroups. Shown top to bottom are the trend for all confirmed cases, the decomposed 5-year trend, the seasonal variation in confirmed cases and the calculated residual trend in confirmed cases.**

a space–time cluster recurrence index with values ranging from 0 (SA never located within a space–time cluster) to 5 (SA situated within at least one space–time cluster over the period of the study), and generated maps of clusters (Figure 3.8). We identified two distinct areas, one situated south-east and one south-west of Limerick city (Figure 3.1, zones M and S), and one area north-east of Galway city (zone M) as VTEC infection hotspots during the study period. Notably, no major population centres other than Limerick city were located within an identified hotspot; the entire eastern seaboard was classified as an infection cold spot based on population-adjusted incidence. Space–time clusters occurred from April to September and peaked during July ($n = 11$) (Figure 3.8).

We observed much less space–time clustering (i.e. identified case clusters were spread over a greater area) for VTEC O157 infection than for VTEC O26 infection. Most VTEC O157 clustering was low (one or two clusters over the study period) in the S, SW and M regions (Figure 3.9).

The spatial distribution and recurrence index of VTEC O26 clusters mirrored those found for all confirmed VTEC infections (Figure 3.10). The temporal window of serogroup-specific space–time clusters reflected the decomposed seasonal peak for both serogroups; VTEC O157 clusters occurred more frequently in September–December, whereas VTEC O26 clusters typically occurred in June–November.

We identified much of the western seaboard as a particularly high-incidence region for the subpopulation aged ≤5 years (zones W, SW, S), with a notable temporal clustering peak (April–May) and relatively broad temporal baseline (March–September). In contrast, we noted three space–time clusters within the subpopulation aged ≥65 years (Figure 3.10); all occurred in the south of the country (zone S), with no specific temporal period associated with these clusters.

## 3.4 Discussion

The power of understanding spatial and temporal patterns of infection has long been recognised (Cameron and Jones, 1983); identifying infection hotspots and cold spots and their time periods informs targeted surveillance and control interventions, and is a precursor to increasingly complex epidemiological analyses and risk factor attribution (Lau *et al.*, 2017; Brown *et al.*, 2018; Karunaweera *et al.*, 2020). Over the past decade, space–time scanning and

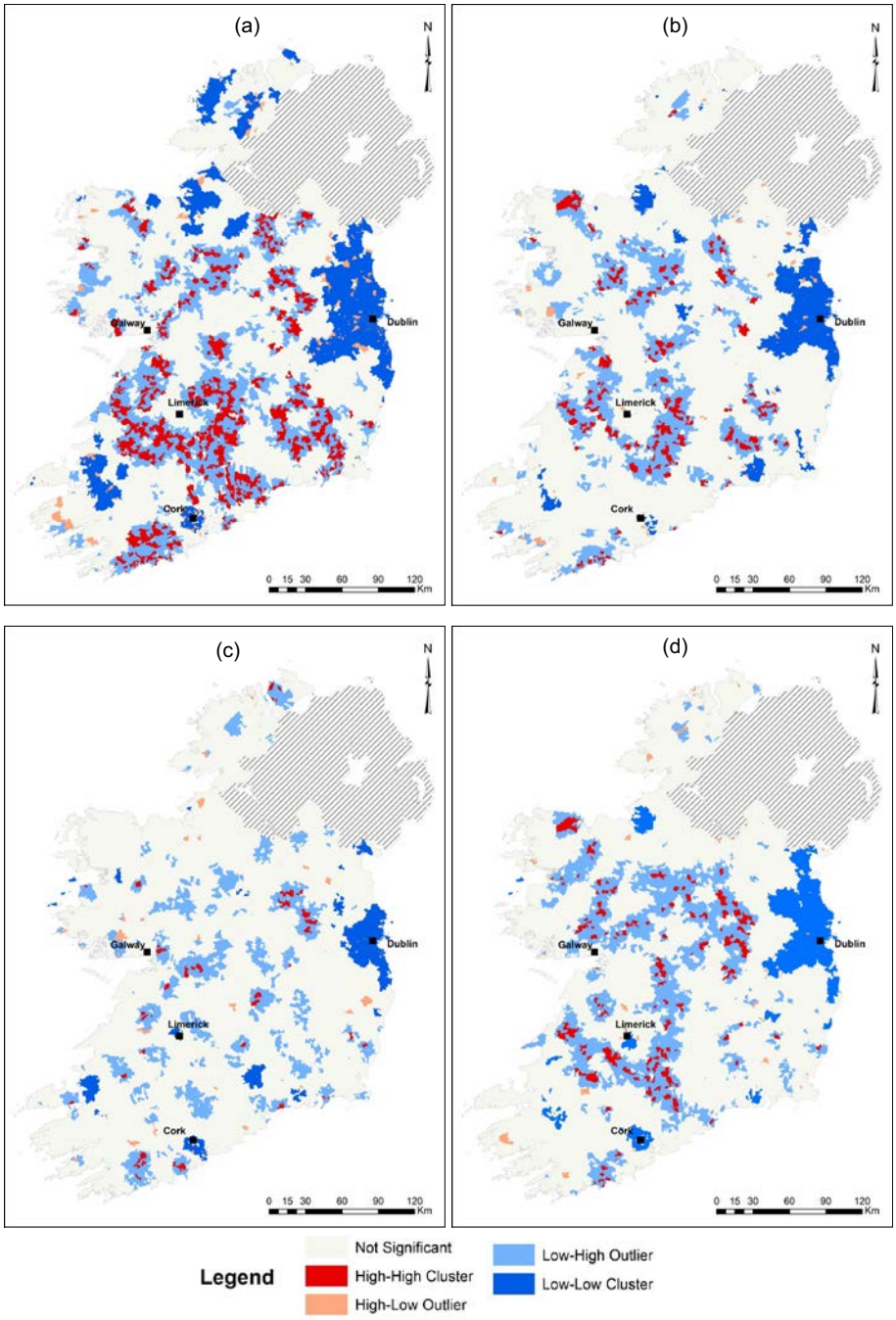


**Figure 3.6. Spatial autocorrelation clusters of VTEC enteritis in Ireland, 2013–2017. (a) All confirmed VTEC infections; (b) VTEC O157 infections; (c) VTEC O26 infections; (d) VTEC infections in children aged ≤5 years.**

geostatistical approaches have been increasingly recognised as powerful tools for endemic disease surveillance and early outbreak detection (Robertson *et al.*, 2010).

Overall, we identified 17 space–time clusters during the 5-year study period, ranging from two clusters during 2014 to five clusters during 2017. All analyses were of sporadic infections; thus, the identification of distinct space–time clusters is noteworthy and underlines the potential utility of real-time or prospective space–time scanning as part of ongoing surveillance procedures. For example, Greene *et al*. (2016) reported on the efficacy of using daily space–time statistics for 35 reportable communicable diseases in New York City, New York, during the period 2014–2015. The distribution of identified space–time clusters of sporadic VTEC enteritis reveals high

**Table 3.2. Results of year-on-year space–time scanning among all confirmed sporadic VTEC cases in Ireland, 2013–2017**

| Cluster no. | Population | No. of cases | Expected | Observed/expected | RR | Start date | End date | *p*-value |
|---|---|---|---|---|---|---|---|---|
| **2013** | | | | | | | | |
| 1 | 268,082 | 32 | 4.62 | 6.93 | 7.37 | 1 Jul | 31 Aug | 0.00000000016 |
| 2 | 140,784 | 27 | 3.60 | 7.50 | 7.90 | 1 May | 31 Jul | 0.0000000041 |
| 3 | 147,000 | 25 | 3.76 | 6.65 | 6.97 | 1 May | 31 Jul | 0.00000030 |
| 4 | 154,425 | 18 | 3.91 | 4.61 | 4.75 | 1 Apr | 30 Jun | 0.022 |
| **2014** | | | | | | | | |
| 1 | 370,743 | 40 | 9.72 | 4.11 | 4.40 | 1 Jul | 30 Sep | 0.00000022 |
| 2 | 75,467 | 14 | 1.96 | 7.15 | 7.34 | 1 Apr | 30 Jun | 0.0041 |
| **2015** | | | | | | | | |
| 1 | 165,552 | 14 | 1.50 | 9.36 | 9.60 | 1 Sep | 30 Sep | 0.00018 |
| 2 | 245,189 | 27 | 6.79 | 3.97 | 4.14 | 1 May | 31 Jul | 0.00067 |
| 3 | 59,890 | 13 | 1.66 | 7.83 | 8.02 | 1 May | 31 Jul | 0.0037 |
| **2016** | | | | | | | | |
| 1 | 299,166 | 42 | 10.59 | 3.97 | 4.18 | 31 May | 30 Aug | 0.00000033 |
| 2 | 119,941 | 21 | 4.20 | 5.00 | 5.14 | 1 May | 30 Jul | 0.0017 |
| 3 | 261,375 | 31 | 9.25 | 3.35 | 3.47 | 31 Mar | 30 Jun | 0.0044 |
| **2017** | | | | | | | | |
| 1 | 345,279 | 54 | 12.93 | 4.18 | 4.45 | 30 Jun | 29 Sep | 0.00000000006 |
| 2 | 190,947 | 27 | 7.15 | 3.78 | 3.89 | 30 Jul | 29 Oct | 0.0042 |
| 3 | 232,749 | 29 | 8.71 | 3.33 | 3.43 | 30 Jun | 29 Sep | 0.015 |
| 4 | 66,817 | 15 | 2.47 | 6.06 | 6.18 | 30 Apr | 29 Jul | 0.017 |
| 5 | 81,564 | 10 | 1.00 | 10.04 | 10.18 | 30 Sep | 29 Oct | 0.027 |

annual levels of persistence and variation in sporadic VTEC infection in Ireland. We identified three distinct regions as exhibiting particularly high space–time cluster recurrence rates, namely south-west and east of Limerick city (SW, S, SE zones), and north-east of Galway city (M zone), indicating the presence of persistent VTEC reservoirs in these areas that cause regular exposure and transmission.

Spatial autocorrelation of VTEC clusters further highlights the disparity between rural and urban living. Sporadic cases were more frequently identified in rural areas, where ≈37.3% of the populace reside (20.1% of rural SAs versus 8.9% of urban) (CSO, 2018). We identified low-incidence clusters in major cities, including Cork and the Greater Dublin area. These findings emphasise the association of rurality with VTEC transmission: increased environmental exposure to pathogen sources coupled with enhanced pathogen transport through untreated drinking water supplies, extreme weather events, etc., is likely to increase risk of exposure and subsequent infection (Andrade *et al.*, 2018).

The relative proximity of large urban centres to the three identified high-recurrence regions may also point to narrow transitional zones between urban and populated rural regions. Rural commuter belts that have inadequate municipal wastewater treatment or drinking supplies, in addition to relatively low levels of acquired immunity among children of young families residing within commuter belt regions, may contribute to this high spatial risk of transmission. National census statistics predict the strongest population growth in peri-urban/commuter belt areas in Ireland (CSO, 2018), which are potentially at high risk of VTEC infection.

All three high-recurrence regions are predominantly underlain by karstified carboniferous limestone aquifers (Woodcock and Strachan, 2009), which have previously been associated with the presence of VTEC in private and small public drinking water

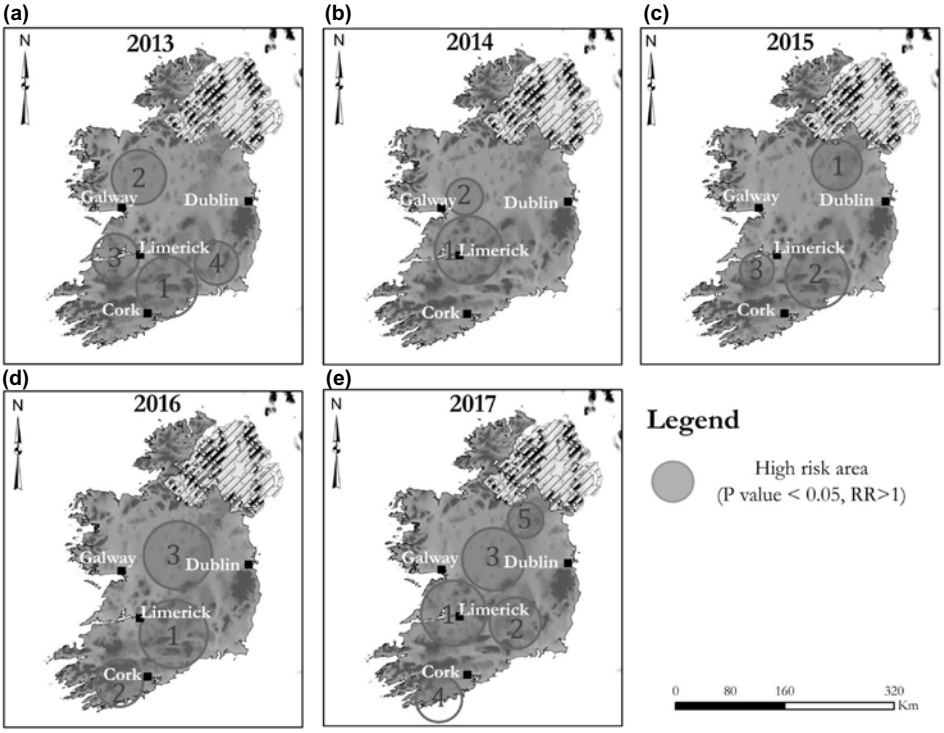


**Figure 3.7. Annual space–time scanning of all confirmed primary VTEC enteritis cases in Ireland in (a) 2013, (b) 2014, (c) 2015, (d) 2016 and (e) 2017. Circles indicate clusters and numbers indicate the order in which they were identified during the study period. Clusters shown on the map have >10 confirmed cases (RR >1, *p*<0.05).**

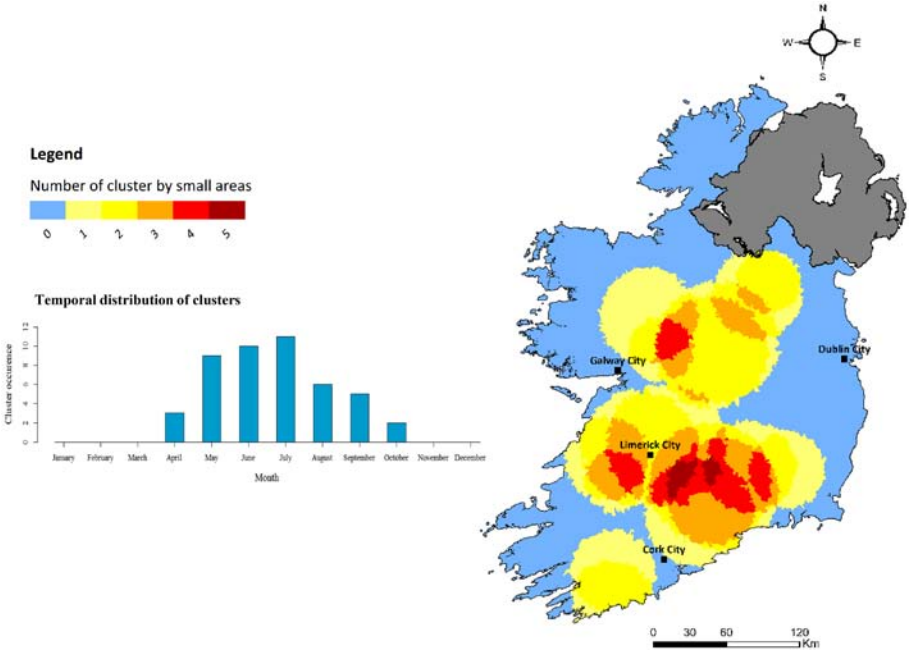


**Figure 3.8. Monthly distribution of space–time clusters (left) and cluster recurrence index (0–5) within census SAs (right) for all confirmed primary VTEC enteritis cases in Ireland, 2013–2017.**

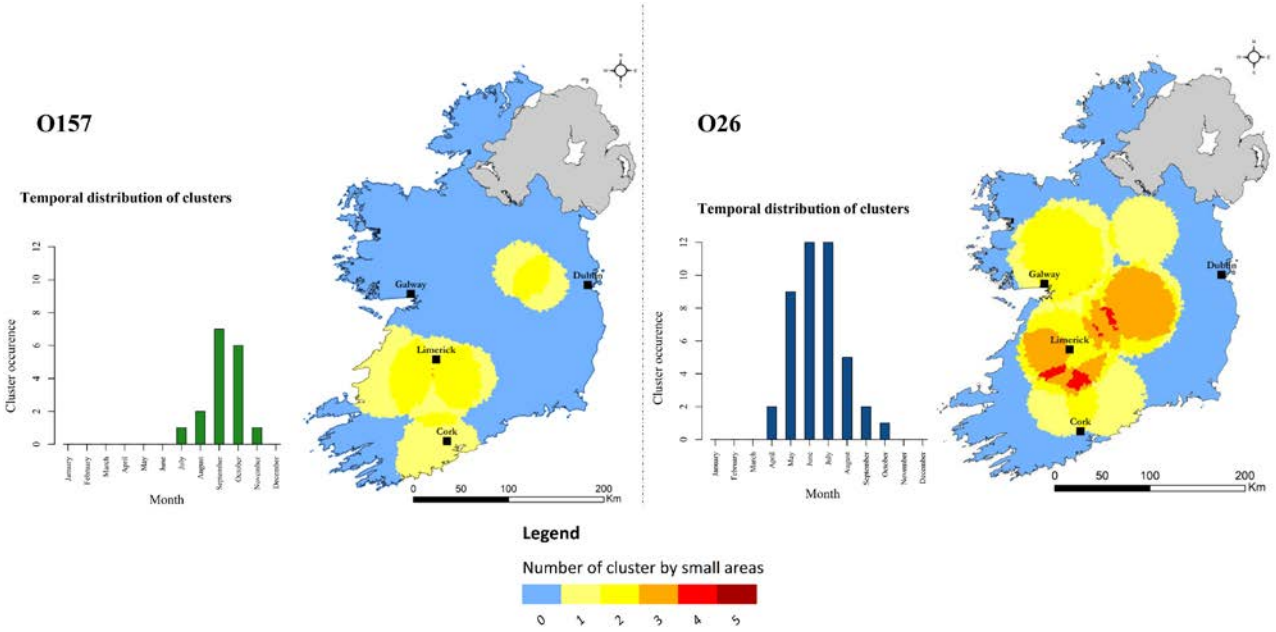


**Figure 3.9. Case clusters of VTEC O157 (left) and O26 (right).**

supplies (Hynds *et al.*, 2014b). The lack of space–time clustering found within the Greater Dublin area, which houses ≈39% of the national population (1.9 million people) and is characterised by a spatially extensive urban commuter belt, consolidated bedrock, and a high level of water and wastewater infrastructure, seems to validate our hypothesis. Boudou *et al.* (2021) report that rates of space–time cluster recurrence of cryptosporidiosis from 2008 to 2017 followed similar patterns in the same three geographically distinct regions we identified; co-occurrence of VTEC enteritis and cryptosporidiosis in Ireland requires further study (Boudou *et al.*, 2021).

Cumulative incidence rates of VTEC infection exhibit a marked seasonal distribution; we identified peaks during late summer and early autumn, reflecting previously noted patterns of VTEC shedding from zoonotic reservoirs and subsequent influx to the environment (Dewsbury *et al.*, 2015). Our findings, however, indicate a geographical and temporal disparity between the two primary serogroups, VTEC O157 and VTEC O26, with high-incidence geographical clusters of VTEC O157 occurring more frequently in the east and in the south. Previous work has identified associations between VTEC O157 infection and residence in areas characterised by a higher density of cattle, private well usage and domestic wastewater treatment systems (ÓhAiseadha *et al.*, 2018), all of which are relatively ubiquitous within spatial locations identified as H–H clusters (Hynds *et al.*, 2012).

The ≤5 years age category has been associated with cases of VTEC O26 infection, which has been characterised by an earlier annual infection peak in Ireland (HPSC, 2019b), implying age-specific peaks of infection. Garvey *et al.* (2016a) reported a 2-month phase difference between VTEC O26 (July) and VTEC O157 (September) infections in Ireland; the difference was reported as significant both when considering all (outbreak and sporadic) confirmed VTEC infections ($p<0.0001$) and when considering sporadic cases only ($p<0.0001$), and is possibly attributed to seasonal variation in infection exposure such as contact with primary animal reservoirs of infection (Brehony *et al.*, 2018). Significantly higher incidence was noted in children aged ≤5 years; previous studies attributed this pattern to an increased risk of direct contact with environmental sources of faecal matter (Rechel *et al.*, 2011) and lower standards of hygiene (Tam *et al.*, 2012) in this subpopulation.

Cumulatively, young children (≤5 years) and the older subpopulation (≥65 years) accounted for 56.7% ($n=1563$) of confirmed sporadic infections. Both of these subpopulations are known to be immunologically vulnerable and exhibit higher incidence of infection and severe sequelae (Chaisri *et al.*, 2001; Adams *et al.*, 2019). Younger cohorts especially are at increased risk of infection caused by frequent contact

with other children of a similar age, and also pose a risk as a source of infection associated with increased contact with adults, particularly among the group aged 30–39 years (Xiao *et al.*, 2016; Hoang *et al.*, 2019). Prominent clustering of infection identified among the groups aged ≤5 and ≥65 years, and the relative spatial heterogeneity of infection clusters, underscore the need for enhanced targeted surveillance measures, particularly in geographical areas characterised by a higher proportion of younger and older populations (Bhunia *et al.*, 2016).

# 4 Case Study: Flood Hydrometeorology and Gastroenteric Infection: the Winter 2015–2016 Flood Event in Ireland

## 4.1 Introduction

Recent climate change projections predict an increase in both the frequency and the severity of major flood events across Europe (Arnell and Gosling, 2016); over the past six decades, north-west Europe, and particularly the UK and Ireland, have experienced significant increases in rainfall and soil moisture, resulting in significantly elevated flood discharges (Blöschl *et al.*, 2019). For example, what was considered a 100-year flood event in this region during the 1960s is now described as a 50- to 80-year event (Blöschl *et al.*, 2019).

While the economic burden associated with current and projected flooding has been extensively explored within the scientific literature, there remain significant knowledge gaps regarding the adverse effects of increasingly frequent and severe flooding on human health, particularly in high-income regions (Cann *et al.*, 2013; Andrade *et al.*, 2018). This is partly due to the often unclear temporality related to the human health impacts of flood events, with effects frequently indirect, complex, spatially variable over small regions and delayed for days, weeks or months after the flood event (Penning-Rowsell *et al.*, 2005).

Notwithstanding this, previous studies have highlighted the link between increasing flood occurrence due to climate change and both direct and indirect human health impacts (Hajat *et al.*, 2003; Smith *et al.*, 2014; Andrade *et al.*, 2018). Apart from directly attributable human fatalities associated with these events (Jonkman *et al.*, 2008; Boudou *et al.*, 2016), indirect health impacts and, more specifically, the incidence of sporadic cases of waterborne enteric infections are likely to increase in concurrence with flood frequency and severity (Brown and Murray, 2013; Andrade *et al.*, 2018). Inundation of anthropogenic infrastructure (e.g. wastewater treatment, roads, farmyards) may lead to mobilisation of enteric pathogens and subsequent contamination of rivers, lakes, groundwater wells and aquifers, subsequently triggering waterborne infections (Semenza, 2020).

Recent work indicates that Ireland will be the second most affected European country in terms of the mean population proportion residing in flood-prone areas by 2100 (Arnell and Gosling, 2016; Forzieri *et al.*, 2017), and is thus particularly susceptible to flooding. Compounding this, notification rates of VTEC enteritis and cryptosporidiosis in Ireland, two enteric infections with historically high rates of waterborne transmission (Hunter and Thompson, 2005; Karmali *et al.*, 2010), are the highest in the EU (ECDC, 2019a,b). VTEC is a zoonotic bacterial pathogen causing gastrointestinal illness in humans, with the spectrum of symptoms ranging from mild diarrhoea to haemorrhagic colitis and HUS, a severe sequela potentially causing renal failure or death (Karch *et al.*, 2005; Karmali *et al.*, 2010). Cryptosporidiosis is caused by *Cryptosporidium* spp., an oocyst-forming protozoan parasite (Fayer and Ungar, 1986); also characterised by a wide range of symptoms (diarrhoea, weight loss, vomiting, abdominal pain, nausea and fever), it can result in acute dehydration and death in very severe cases. In Ireland, a high proportion of primary cases of both infections have been linked with the consumption of or exposure to contaminated water (Cummins *et al.*, 2010; Hynds *et al.*, 2014a).

Winter 2015–2016 was characterised by extremely wet conditions following a series of Atlantic storms, resulting in unprecedented, widespread flooding across Ireland and the UK. Along with the primary, readily observable impacts of the event (e.g. flooding of households and businesses, interruption of transport networks), a significant number (>200) of incidents were reported pertaining to Irish drinking water and wastewater services. From December 2015, several boil water notices were issued, affecting approximately 23,000 people, because of specific concerns around drinking water quality and its potential impact on public health (NDFEM and DHPCLG, 2016). Despite these warnings and the potentially high-risk scenario, no confirmed or likely outbreaks of waterborne infection were officially reported to the Irish HSE during or immediately after the event. To date, no studies have

investigated the link between this particular event and the incidence of infectious disease within the population.

Here we aimed to investigate the potential relationship between the winter flood event of 2015–2016 and the incidence of confirmed VTEC and cryptosporidiosis in Ireland via a retrospective ecological study comprising an ensemble of (geo)statistical techniques. Seasonal decomposition and space–time scanning were used to detect potential irregularities in the seasonal variation and spatial distribution of infections during and after the flood period. Subsequently, generalised linear modelling (GLM) was employed to explore spatial relationships between flood risk exposures, observed flood extent and the incidence of infection at a fine geographical resolution. Finally, exemplar hydrometeorological data (surface water discharge, groundwater level and precipitation) from the Shannon River basin were used as flood indicators and modelled via time-series analyses to provide a new understanding of the timing and "behaviour" of infections within the context of a significant flood event. The presented method aims to be transferable and could be applied for assessing links between extreme weather events and infection incidence in other regions and pertaining to various human health impacts.

## 4.2 Methods

### *4.2.1 Analytical protocol*

The developed analytical protocol used in the current study for investigating the link between infections was based on three primary phases, in line with overarching research objectives, as follows:

- **Phase 1.** Seasonal decomposition was carried out in concurrence with space–time scanning to examine the space–time distribution of atypical (i.e. minus seasonal trend) infections during and after the flood period.
- **Phase 2.** GLM was used to explore spatial links between categorical flood risk based on calculated return periods, actual flood extent and presence/absence of confirmed infections.
- **Phase 3.** A time-series analysis was performed to investigate the relationship between infection incidence and three temporally lagged hydrometeorological variables delineated as indicators of the flood event (rainfall, surface water discharge and groundwater level).

Each phase was undertaken using decision-based criteria, whereby the link between the flood event and infection incidence could either be confirmed or rejected.

### *4.2.2 The 2015–2016 flood event in Ireland*

*Meteorological characterisation*

Winter 2015–2016 has become synonymous with some of the most widespread and severe flooding ever recorded across Ireland and the UK. From November 2015 to January 2016, both countries experienced a series of winter storms, resulting in exceptionally wet conditions. Following a relatively dry October, Storm Abigail impacted Ireland over the 2-day period 13/14 November 2015, triggering heavy rainfall exceeding 80 mm over 24 hours in some areas (Walsh, 2016). Two lower intensity storms subsequently occurred on 17 November (Storm Barney) and 29 November (Storm Clodagh); November 2015 has since been ranked the seventh wettest November since records began in 1850 (Walsh, 2016).

During December 2015, a new succession of Atlantic storms was recorded – Storm Desmond, Storm Eva and Storm Frank. The highest rainfall intensities were recorded during Storms Desmond (259.7 mm over 48 hours; Leenane, Co. Galway) and Frank (159.9 mm over 48 hours; Cloone Lake, Co. Kerry). December 2015 is ranked as the wettest December ever recorded in Ireland. Approximately 500 mm of monthly rainfall was registered locally at several synoptic stations (e.g. Co. Kerry, Cork and Galway), with recorded rainfall 250% above the monthly average in most parts of the country and exceeding 300% in southern regions. January and February 2016 were also particularly wet, and were ranked as the ninth wettest January and February recorded in Ireland.

*Hydrological characterisation*

Three primary flood periods have been identified during the period 12 November 2015 to 5 January 2016, corresponding with the occurrence of the three main storm events (Figure 4.1). Flood records indicate that the spatial extent of hydrological

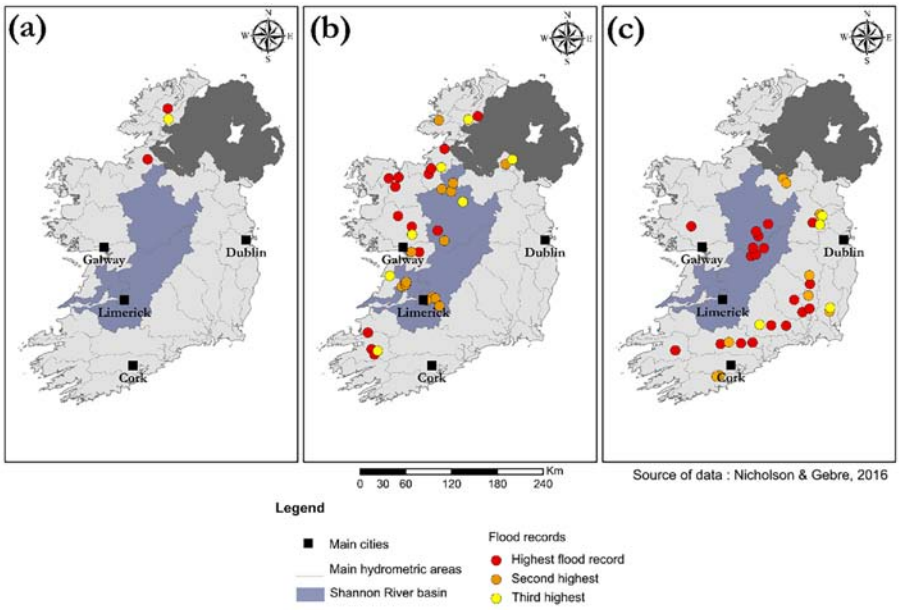


**Figure 4.1. Flood records (water levels) reached during Storms Abigail (a), Desmond (b) and Frank (c).**

impacts was widespread across the country, with 37 of 75 river gauging stations (49%) recording their highest ever discharge levels during the study period, i.e. 15 November to 5 January (Nicholson and Gebre, 2016). Owing to large uncertainties and the atypical character of the flood (succession of events), no flood periods were calculated to assess the intensity of the 2015–2016 flood events.

Flood longevity represents one of the primary characteristics underpinning the severity of the winter 2015–2016 flood event in Ireland, with flood duration far outlasting the period of maximum recorded river discharges (29 November to 5 January) (NDFEM and DHPCLG, 2016). Several secondary flood episodes associated with persistent rainfall or short-term heavy rainfall events occurring on saturated land were reported from January to April 2016. For example, on 10/11 April 2016 a 24-hour rainfall event triggered a significant increase in flood extent, increasing from 2500 hectares on 30 March to 7600 hectares on 11 April (O'Hara *et al.*, 2019).

### *4.2.3 Enteric infection data and data sources*

Datasets comprised all confirmed cases of sporadic (i.e. non-outbreak) VTEC enteritis reported by regional departments of public health between 1 January 2013 and 31 December 2017. VTEC cases prior to January 2013 were not obtained due to differences in testing and reporting protocols between areas.

The cryptosporidiosis dataset included all confirmed cases notified from 1 January 2008 to 31 December 2017; cases occurring prior to January 2008 were not integrated to avoid bias that may result from including a significant outbreak that took place in April 2007. All individual case notifications for both infections were geographically linked to the centroid of a CSO SA, the smallest administrative delineation currently employed in Ireland for national census reporting (18,488 SA in 2011). Two main periods were identified for the current study:

- The "non-flood" period corresponded to the total duration of both infection datasets: 2013–2018 for VTEC (2.7555 cases) and 2008–2017 for cryptosporidiosis (4509 cases).
- The "flood period" corresponded to the period between 1 July 2015 and 1 July 2016. A total of 577 VTEC enteritis and 607 cryptosporidiosis cases occurred during the flood period (Figures 4.2 and 4.3).

### *4.2.4 Spatiotemporal analysis of VTEC and cryptosporidiosis*

*Seasonal decomposition*

Seasonal decomposition of confirmed cases of infection was undertaken at both monthly and weekly scales using the STL method, to decompose the incidence of infection ($Y_v$) into seasonal variation ($S_v$),

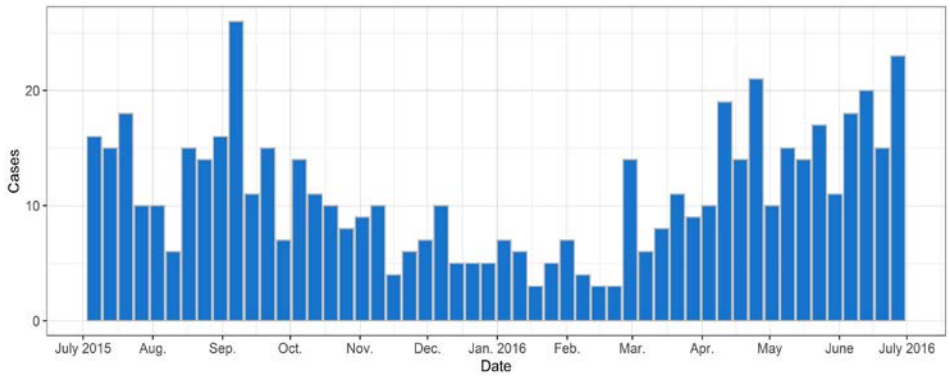


**Figure 4.2. Weekly VTEC cases in Ireland from July 2015 to July 2016.**

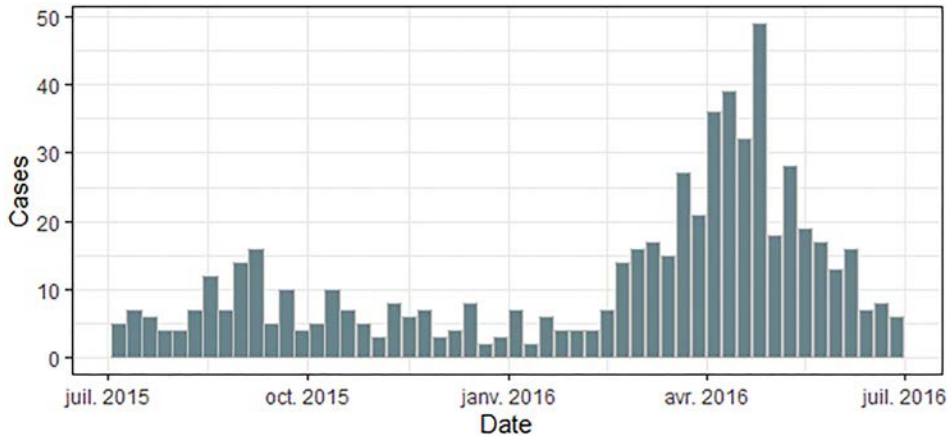


**Figure 4.3. Weekly cryptosporidiosis cases in Ireland from July 2015 to July 2016.**

overall trend over time ($T_v$) and residuals ($R_v$). An additive STL model was employed owing to the relatively constant trend associated with peak (annual/seasonal) values over time. For the purposes of the current study (i.e. examining a specific event and time period), there was a particular focus on the trend and residual series of both infections (i.e. seasonal signal extraction). Weekly decompositions were undertaken using R Studio (v 4.0) and the "forecast" package (v 3.6) on total datasets for both infections (2013–2018 for VTEC; 2008–2018 for cryptosporidiosis), and extracted for the flood period from July 2015 to July 2016.

*Space–time scanning*

Space–time scanning analyses were carried out on the entire study period (non-flood period) to detect temporally specific clusters of infection defined by significantly higher numbers of observed cases than expected within specified temporal and spatial windows. Analyses are based on the null hypothesis that cases are randomly distributed over space and time, with scanning conducted at SA scale using SaTScan v 9.6 (Kulldorff and Information Management Services, Inc., MA, USA) (Kulldorf, 1999). SaTScan requires a series of user-defined parameters. Similarly to a previous Ireland-based study (Boudou *et al.*, 2021), a discrete Poisson model was selected to account for the high spatial resolution (i.e. 18,488 SAs) and likely low case numbers per SA unit. Similarly, a maximum of 10% of the PAR was employed, with a maximum cluster radius of 50 km. A minimum threshold of 10 cases was employed to ensure that only significant infection clusters were identified (i.e. to avoid small household clusters). Data were aggregated at the monthly scale with a maximum cluster duration of 3 months, thus accounting for seasonal trends of infection.

### *4.2.5 Generalised linear modelling*

GLM was used to assess the link between dichotomised (presence/absence), spatially specific (SA level) occurrence of infection and mapped categorical flood risk/extent parameters. Analyses were undertaken using existing mapped datasets from:

- historical surface water flood maps (GWFlood Project), based on winter 2015–2016 observations and indicating the fluvial and pluvial extent of the flood event (McCormack *et al.*, 2020);
- high-resolution flood maps produced for coastal and fluvial risks, with three "risk scenarios" based on calculated return periods [low: 1000 years; medium: 100 years (fluvial) to 500 years (coastal); and high: 10 years];
- presence of permanent surface water bodies (lakes, rivers).

All mapped datasets were imported to ArcGIS 10.7, with SA identifiers (national census area centroids) used to geographically attribute anonymised spatially referenced case data, resulting in an anonymised dataset of confirmed infections linked to geographically explicit flood risk, flood extent and surface water attributes. GLM with a binary link function was applied to calculate probabilistic ORs between flood extent, fluvial/coastal flood scenarios (flood presence/absence), surface water presence and confirmed human infection (infection presence/absence). Analyses were performed using R studio (v4.0) for the flood and "non-flood" periods.

### *4.2.6 Hydrometeorological indicators*

To examine the presence of associations between flood-related hydrometeorology and incidence of infection, a national-level case study was performed using three hydrometeorological variables from the Shannon River basin: cumulative rainfall, river discharge (surface water) and groundwater level. The Shannon River basin was selected as a representative area because of its central location and geographical significance (15,695 km$^2$), covering approximatively 22% of the country. The river basin was significantly affected by flooding during the 2015–2016 event (NDFEM and DHPCLG, 2016) and is considered a "hotspot" for both VTEC enteritis and cryptosporidiosis.

A distinction was made between the Lower and Upper Shannon sub-basins to assess for potential hydrodynamic variations (Figure 4.4). For each

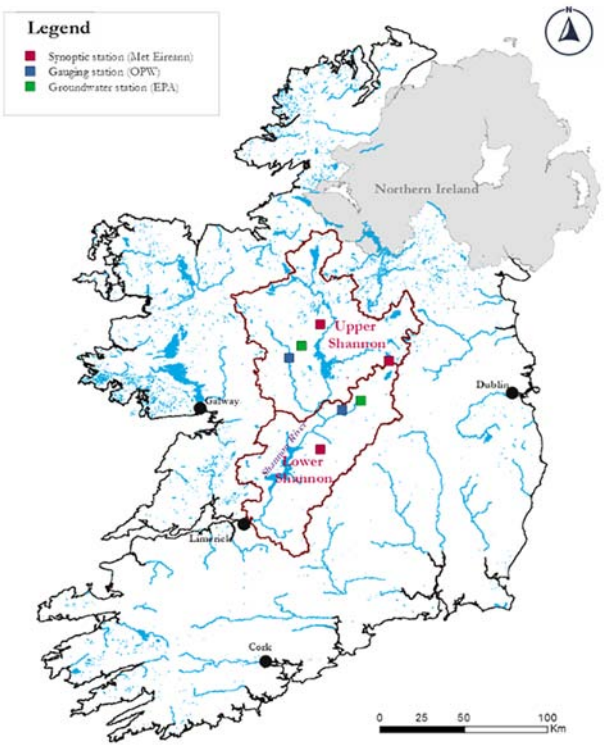


**Figure 4.4. The Shannon River basin and measurement stations selected for hydrodynamic data extraction and analyses.**

sub-basin, hydrometeorological data were extracted as follows:

- daily cumulative rainfall from Met Éireann synoptic stations;
- daily mean discharge (cubic metre per second) from Office of Public Works gauging stations;
- daily groundwater level (metres) from the EPA.

The groundwater levels extracted from the EPA stations were rescaled (0–10) to ensure homogeneity.

Measurement station/gauge selection was undertaken based on:

- dataset length and completeness;
- proximity of discharge and groundwater gauging stations to appropriately capture hydrodynamic patterns;
- selection of synoptic stations via calculation of the *k*-nearest neighbour to gauging stations (surface water and groundwater).

Two synoptic stations were used for the lower catchment, with the discharge station closer to the Gurteen station (Co. Tipperary) and the groundwater station closer to the Mullingar station (Co. Westmeath) (Figure 4.5). The mean rainfall between these two stations was used to characterise rainfall in the lower catchment.

### *4.2.7 Time-series analyses*

Based on weekly time series (29), analyses were conducted to assess levels of temporal lagged association between hydrometeorological factors and infection incidence. Analyses were carried out on the summed trend and residuals of both VTEC

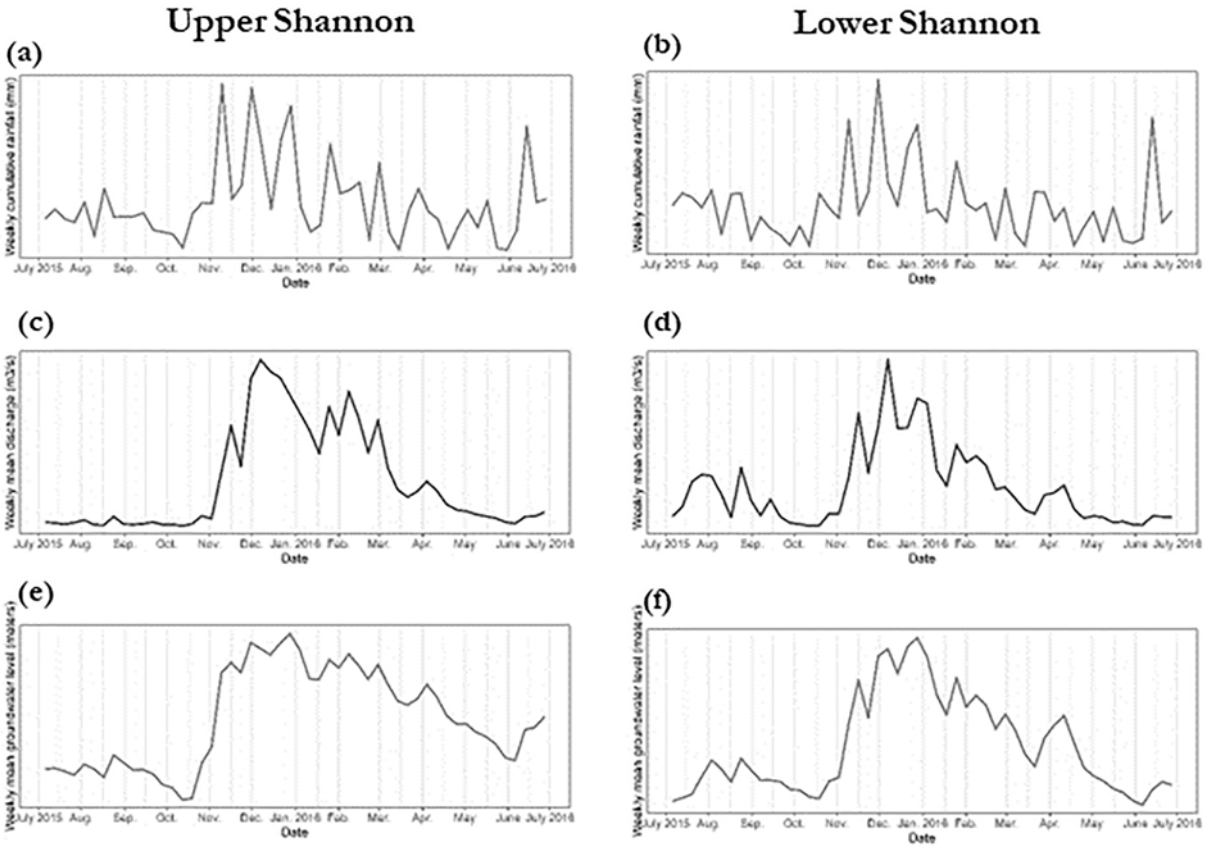


**Figure 4.5. Hydrometeorological variables recorded in the Lower and Upper Shannon for the flood period. Weekly cumulative rainfall in (a) the Lower Shannon (mean rainfall between Gurteen, Co. Tipperary and Mullingar, Co. Westmeath) and (b) the Upper Shannon (Mount Dillon station). Weekly mean discharge in (c) the Lower Shannon (Brosna River at Ferbane, Co. Offaly) and (d) the Upper Shannon (Suck River at Rookwood, Co. Galway). Weekly mean groundwater levels in (e) the Lower Shannon (Co. Offaly) and (f) the Upper Shannon (Co. Galway).**

and cryptosporidiosis obtained from seasonal decomposition, as the primary objective was to identify and elucidate atypical infection excess. Spearman's non-parametric rho was calculated for weekly hydrometeorological time series and the weekly lagged sum of infection trends and residuals in both the upper and lower sub-basins. National infection data were used, based on the hypothesis that the hydrometeorological means recorded within the Shannon catchment could be used as indicators for country-wide infection incidence. A range of 1 to 24 weeks was calculated and employed to assess minimum and maximum lag periods, with analysis carried out using R studio (v 4.0) and the GGally (v. 2.0) package. The lag range of 24 weeks was selected according to the maximum environmental survival of both pathogens, estimated to be up to 24 weeks in a 15°C environment for *Cryptosporidium* spp. (Alum *et al.*, 2014).

ARIMA modelling was used to assess the weight of weekly lagged hydrometeorological time series on infection incidence during the flood period via backcasting. Differencing (order – 1) was performed on all time series to ensure stationarity. Similarly, as ARIMA does not appropriately account for overarching trends and data seasonality (as opposed to SARIMA), environmental time series were seasonally adjusted. The final order parameters used for analysis ($p$, $d$, $q$) were ARIMA (0,1,1), obtained via optimisation diagnostics. Repeated iterations were performed on infection time series (trend and residuals from July 2015 to July 2016), using stepped lags (from 1 to 24 weeks) of the three environmental time series (rainfall, surface water, groundwater) as regressors, for both the Lower and Upper Shannon sub-basins. The Ljung–Box test, a statistical test used for examining the autocorrelation of time series, was used to indicate significance between hydrometeorological variables and infection incidence, with $p > 0.05$ used to confirm temporal association (i.e. significant autocorrelation).

## 4.3 Results

### *4.3.1 Spatiotemporal patterns of infection during 2015–2016*

*Seasonal decomposition*

Seasonal decomposition identified specific seasonal patterns (not presented) for both infections. With respect to seasonal variations, VTEC exhibited high incidence during mid/late summer (peak in July), with a second peak in September, whereas cryptosporidiosis cases were highest during spring (March to May; peak in April) (Figure 4.6). Both infections displayed

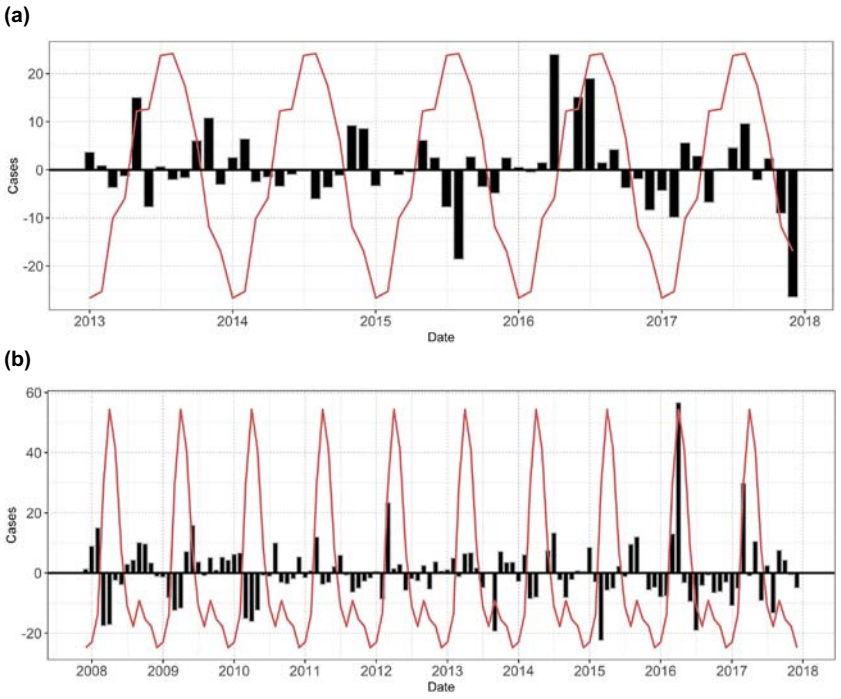


**Figure 4.6. Residuals (in black) and seasonal variations (in red) obtained from LOESS seasonal decomposition for (a) VTEC (2013–2018) and (b) cryptosporidiosis (2008–2018).**

a general (cumulative) trend increase over their study periods. Notably, both infections exhibited a marked residual (i.e. seasonal trend excluded) residual peak during April 2016, accounting for +23 observed residual cases for VTEC and +57 observed residual cases for cryptosporidiosis. Other secondary peaks were identified, particularly during June–July 2016 for VTEC enteritis.

*Space–time scanning*

The results of space–time scanning analysis from July 2015 to July 2016 are shown in Figure 4.7. Space–time scanning of VTEC cases indicated three significant (RR > 1, $p < 0.05$) clusters (83 cases in total), all of which intersected (25–35%) with the Shannon catchment area. The two primary identified clusters (40 and 29 cases) were located east and south-west of Limerick city and occurred between April and June 2016. A third cluster was observed further north (Co. Cavan) during September 2015 (14 cases).

Eight significant space–time clusters of cryptosporidiosis were identified during the flood period, accounting for 238 cases. The spatial distribution of these clusters was relatively widespread across the country, with four clusters partially located within the Shannon basin. The temporal distribution of clusters was from March to May 2016 for clusters 1, 2, 3 and 7 (south midlands and south) and from April to June 2016 for clusters 4, 5, 6 and 8 (north midlands and north).

### *4.3.2 Flood exposure and infection*

The results indicated a link between the spatial extent of the 2015–2016 flood event and the incidence of infection. Within the non-flood period, approximatively 39% of VTEC cases (OR 1.487; $p < 0.00$) and 44% of cryptosporidiosis cases (OR 1.792; $p < 0.001$) occurred within the spatial boundary of the 2015–2016 flood extent (Tables 4.1 and 4.2). Similarly, the SA units situated within the flood extent were more likely to report at least one VTEC (OR 1.355; $p < 0.001$) or cryptosporidiosis case (OR 1.574; $p < 0.001$) from July 2015 to July 2016 (Tables 4.3 and 4.4).

Generalised linear models indicated that both infections occurred significantly more frequently within areas prone to the risk of fluvial flooding. For example, from 2008 to 2018, a case of cryptosporidiosis was approximatively 13% ($p < 0.001$) more likely to occur in a SA characterised by a high probability of fluvial flood risk (10-year flood return period; Table 4.1). Similarly, during the flood period, VTEC enteritis occurred more frequently within areas classified under the medium fluvial risk scenario (100-year flood return period: OR 1.094; $p = 0.025$; Table 3.2). Results showed no

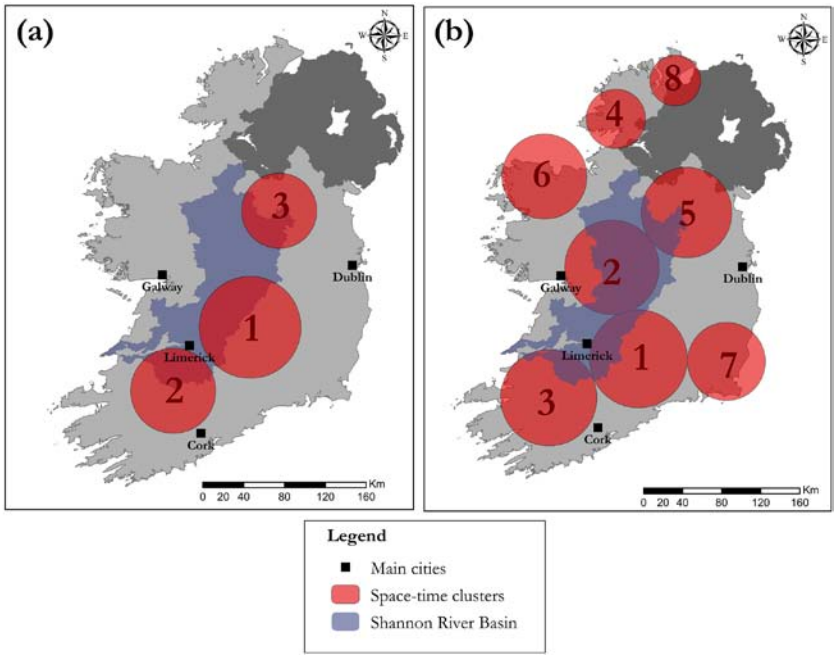


**Figure 4.7. Space–time clusters from July 2015 to July 2016 for (a) VTEC and (b) cryptosporidiosis.**

**Table 4.1. Infection cases compared to flood risk and flood extent exposure**

| Predictors | VTEC cases (2013–2018) | Crypto. cases (2008–2018) | VTEC cases (2015–2016) | Cryptosporidiosis cases (2015–2016) | Number of SAs |
|---|---|---|---|---|---|
| Flood extent 2015–2016 | 1093 (39.7%) | 1993 (44.2%) | 233 (40.4%) | 247 (40.7%) | 4585 (24.8%) |
| Fluvial – high probability | 845 (30.7%) | 1379 (30.6%) | 178 (30.8%) | 180 (29.7%) | 5012 (27.1%) |
| Fluvial – medium probability | 879 (31.9%) | 1450 (32.2%) | 194 (33.6%) | 190 (31.3%) | 5382 (29.1%) |
| Fluvial – low probability | 921 (33.4%) | 1489 (33%) | 201 (34.8%) | 194 (32%) | 5726 (31%) |
| Coastal – high probability | 234 (8.5%) | 342 (7.6%) | 46 (8.0%) | 54 (8.9%) | 1713 (9.3%) |
| Coastal – medium probability | 254 (9.2%) | 373 (8.3%) | 52 (9.0%) | 55 (9.1%) | 1874 (10.1%) |
| Coastal – low probability | 271 (9.8%) | 390 (8.6%) | 55 (9.5%) | 56 (9.2%) | 2026 (11%) |
| Lakes | 701 (25.4%) | 1393 (30.9%) | 143 (24.8%) | 178 (29.3%) | 3110 (16.8%) |

**Table 4.2. GLM results for VTEC (non-flood period: 2013–2018): flood extent of 2015–2016, fluvial and coastal risk scenarios (CFRAM mapping) and presence of surface water bodies (lakes/rivers)**

| Predictors | Estimated standard deviation | *p*-value | OR | 2.5% CI | 97.5% CI | Significance |
|---|---|---|---|---|---|---|
| Flood extent 2015–2016 | 0.397 | >0.001 | 1.487 | 1.414 | 1.564 | *** |
| Fluvial – high probability | 0.000 | >0.001 | 1.098 | 1.043 | 1.155 | *** |
| Fluvial – medium probability | 0.060 | 0.017 | 1.062 | 1.011 | 1.116 | * |
| Fluvial – low probability | 0.071 | 0.006 | 1.073 | 1.020 | 1.128 | ** |
| Coastal – high probability | –0.047 | 0.256 | 0.954 | 0.879 | 1.034 | |
| Coastal – medium probability | –0.062 | 0.110 | 0.940 | 0.871 | 1.014 | |
| Coastal – low probability | –0.053 | 0.180 | 0.948 | 0.876 | 1.024 | |
| Lakes/rivers | 0.323 | >0.001 | 1.381 | 1.304 | 1.462 | *** |

***$p<0.05$; **$p<0.01$; ***$p<0.001$.**

**Table 4.3. GLM results for VTEC (flood period: July 2015–July 2016): flood extent of 2015–2016, fluvial and coastal risk scenarios (CFRAM mapping) and presence of surface water bodies (lakes/rivers)**

| Predictors | Estimated standard deviation | *p*-value | OR | 2.5% CI | 97.5% CI | Significance |
|---|---|---|---|---|---|---|
| Flood extent 2015–2016 | 0.304 | >0.001 | 1.355 | 1.254 | 1.464 | *** |
| Fluvial – high probability | 0.073 | 0.071 | 1.076 | 0.993 | 1.165 | |
| Fluvial – medium probability | 0.090 | 0.025 | 1.094 | 1.011 | 1.182 | * |
| Fluvial – low probability | 0.076 | 0.055 | 0.998 | 1.164 | 1.164 | |
| Coastal – high probability | –0.075 | 0.262 | 0.927 | 0.810 | 1.055 | |
| Coastal – medium probability | –0.057 | 0.373 | 0.945 | 0.831 | 1.068 | |
| Coastal – low probability | 0.066 | 0.285 | 0.936 | 0.827 | 1.054 | |
| Lakes/rivers | 0.203 | >0.001 | 1.225 | 1.120 | 1.337 | *** |

***$p<0.05$; **$p<0.01$; ***$p<0.001$.**

association between coastal (surge) flood risk areas and the incidence of either infection ($p>0.05$), while a significative negative association was found with cryptosporidiosis for the flood period (Table 4.5).

A strong statistical relationship was established between infection incidence and the presence of a surface water body (lake or river); 25.4% of VTEC cases (OR 1.225; $p<0.001$) and 30.9% of cryptosporidiosis cases (OR 1.739; $p<0.001$) occurred within a SA comprising a surface water body over the non-flood period. A similarly significant association, albeit of a lower magnitude, was observed for the flood period (VTEC cases: 24.8%; OR 1.225; $p<0.001$; cryptosporidiosis cases: 29.3%; OR 1.363; $p<0.001$).

**Table 4.4. GLM results for cryptosporidiosis (non-flood period: 2007–2018): flood extent of 2015–2016, fluvial and coastal risk scenarios (CFRAM mapping) and presence of surface water bodies (lakes/rivers)**

| Predictors | Estimated standard deviation | *p*-value | OR | 2.5% CI | 97.5% CI | Significance |
|---|---|---|---|---|---|---|
| Flood extent 2015–2016 | 0.583 | >0.001 | 1.792 | 1.711 | 1.876 | *** |
| Fluvial – high probability | 0.120 | >0.001 | 1.128 | 1.077 | 1.182 | *** |
| Fluvial – medium probability | 0.103 | >0.001 | 1.109 | 1.059 | 1.160 | *** |
| Fluvial – low probability | 0.002 | 0.002 | 1.075 | 1.028 | 1.125 | ** |
| Coastal – high probability | –0.075 | 0.047 | 0.928 | 0.861 | 0.999 | * |
| Coastal – medium probability | –0.080 | 0.028 | 0.923 | 0.859 | 0.991 | * |
| Coastal – low probability | –0.106 | 0.003 | 0.900 | 0.839 | 0.964 | ** |
| Lakes/rivers | 0.553 | >0.001 | 1.739 | 1.652 | 1.831 | *** |

***p*<0.05; ****p*<0.01; *****p*<0.001.**

**Table 4.5. GLM results for cryptosporidiosis (flood period: July 2015–July 2016): flood extent of 2015–2016, fluvial and coastal risk scenarios (CFRAM mapping) and presence of surface water bodies (lakes/rivers)**

| Predictors | Estimated standard deviation | *p*-value | OR | 2.5% CI | 97.5% CI | Significance |
|---|---|---|---|---|---|---|
| Flood extent 2015–2016 | 0.317 | 0.000 | 1.574 | 1.272 | 1.482 | *** |
| Fluvial – high probability | 0.050 | 0.220 | 1.051 | 0.970 | 1.138 | |
| Fluvial – medium probability | 0.040 | 0.319 | 1.041 | 0.962 | 1.125 | |
| Fluvial – low probability | 0.015 | 0.698 | 1.015 | 0.939 | 1.097 | |
| Coastal – high probability | –0.036 | 0.582 | 0.965 | 0.847 | 1.093 | |
| Coastal – medium probability | –0.069 | 0.278 | 0.933 | 0.821 | 1.055 | |
| Coastal – low probability | –0.097 | 0.121 | 0.907 | 0.800 | 1.023 | |
| Lakes/rivers | 0.310 | 0.000 | 1.363 | 1.252 | 1.483 | *** |

***p*<0.05; ****p*<0.01; *****p*<0.001.**

### *4.3.3 Association with hydrometeorological indicators*

*Spearman's non-parametric rho*

The results indicated significant positive associations with all three hydrometeorological variables, for both the Lower and Upper Shannon sub-basins (Figure 4.8). Two primary lag periods of correlation are highlighted ($r_S$ > 0.4), namely from week 1 to week 5 and from week 18 to week 19. The highest $R_{SP}$ values calculated for each variable, thus indicating the strongest associations, were:

- rainfall: week 5 (Lower and Upper Shannon);
- surface water: week 4 (Lower and Upper Shannon);
- groundwater level: week 1 (Lower Shannon) and week 4 (Upper Shannon).

The highest $R_{SP}$ was associated with rainfall on the Lower Shannon (0.62), while associations with surface water and groundwater were stronger in the Upper Shannon (0.59).

Again, significant positive associations were found between the incidence of confirmed cryptosporidiosis and all three hydrometeorological variables (Figure 4.9), with the main positive associations ($R_{SP}$ > 0.4) occurring between weeks 15 and 19 (surface water and groundwater) and from week 16 to week 22 (rainfall). The highest $R_{SP}$ calculated for each hydrometeorological variables were:

- rainfall: week 16 (Lower Shannon) and week 19 (Upper Shannon);
- surface water: week 19 (Lower Shannon) and week 16 (Upper Shannon);
- groundwater: week 16 (Lower and Upper Shannon).

The range of highest $R_{SP}$ values was relatively similar within both sub-basins, being from 0.5 (rainfall) to 0.55 (groundwater) in the Lower Shannon and from

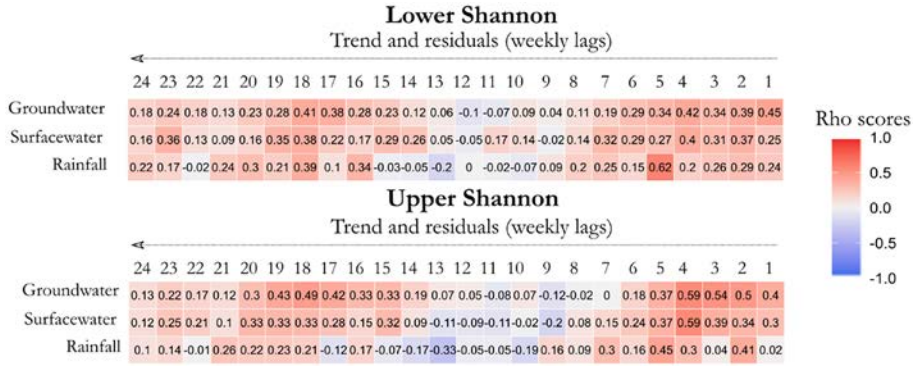


**Figure 4.8. Spearman's non-parametric rho tests for VTEC trend and residuals and hydrometeorological variables (Lower and Upper Shannon).**

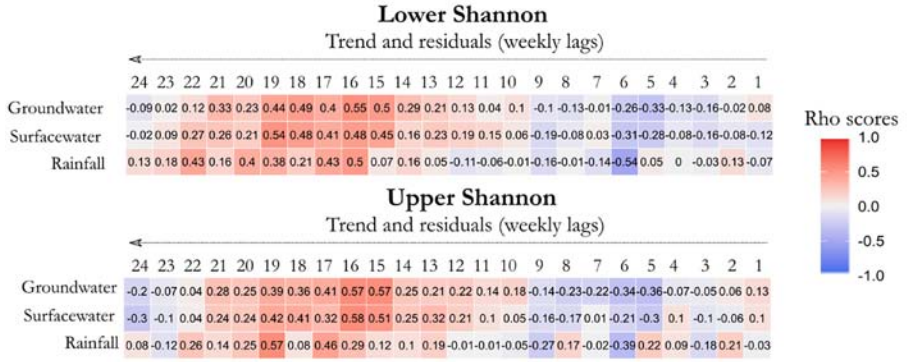


**Figure 4.9. Spearman's non-parametric rho tests for cryptosporidiosis trend and residuals and hydrometeorological variables (Lower and Upper Shannon).**

0.57 (rainfall, groundwater) to 0.58 (surface water) in the Upper Shannon.

*ARIMA modelling*

As shown in Figure 4.10, the results of optimised ARIMA modelling for VTEC indicated relatively similar responses between the two sub-basins, pointing to two significant primary associational periods ($p > 0.05$), from week 12 to week 14 and from week 17 to week 19. A slightly stronger association was observed in the Lower Shannon ($p$-values ranging from 0.01 to 0.105) than in the Upper Shannon ($p$-values from 0.013 to 0.072). Similarly, the results showed that the maximum $p$-values calculated for surface water discharge were significantly higher than the $p$-values obtained for the other two hydrometeorological variables (rainfall and groundwater level) in both sub-basins. The maximum association found for each variable was:

- rainfall: week 12 ($p = 0.062$, Upper Shannon) and week 13 ($p = 0.071$, Lower Shannon);
- surface water: week 18 ($p = 0.072$, Upper Shannon) and week 19 ($p = 0.105$, Lower Shannon);
- groundwater level: week 12 ($p = 0.061$, Upper Shannon; $p = 0.06$, Lower Shannon).

Two specific cluster periods were found to occur between lagged hydrometeorological variables and cryptosporidiosis cases, namely from week 8 to week 10 and from week 16 to week 21 (Figure 4.11). The range of $p$-values tended to be wider in the Upper Shannon (0.022 to 0.577) than in the Lower Shannon (0.029 to 0.371). The best-fit weekly lags found by calculating the $p$-values of Ljung–Box tests appear identical between both sub-basins, as follows:

- rainfall: week 19 ($p = 0.274$, Lower Shannon; $p = 0.522$, Upper Shannon);
- surface water: week 18 ($p = 0.371$, Lower Shannon; $p = 0.577$, Upper Shannon);
- groundwater level: week 18 ($p = 0.395$, Lower Shannon; $p = 0.424$, Upper Shannon).

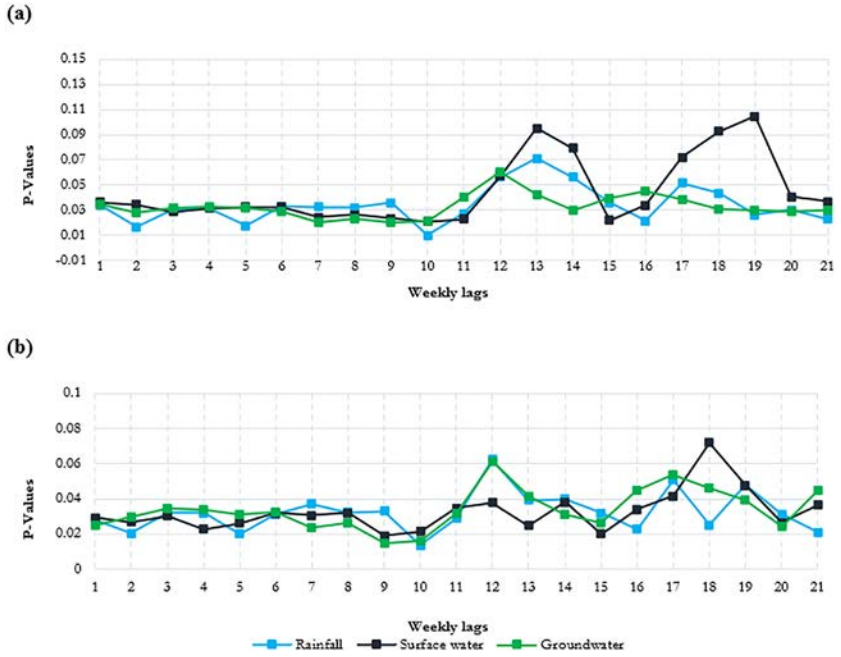


**Figure 4.10. ARIMA Ljung–Box test results for VTEC in (a) the Lower Shannon and (b) the Upper Shannon.**

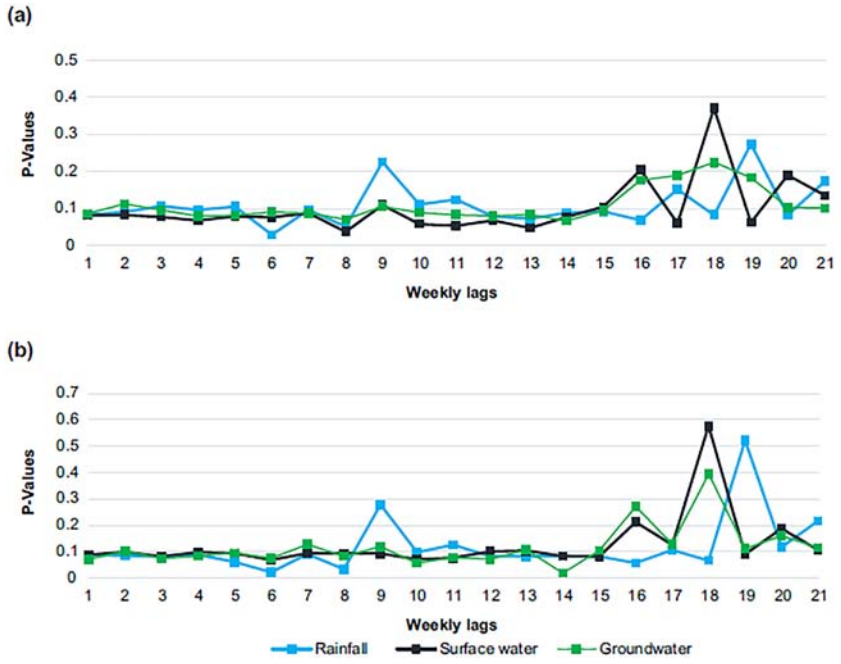


**Figure 4.11. ARIMA Ljung–Box test results for cryptosporidiosis in (a) the Lower Shannon and (b) the Upper Shannon.**

## 4.4 Discussion

### *4.4.1 Spatiotemporal distribution of VTEC and cryptosporidiosis in 2016*

The research protocol developed during the current study allowed the authors to investigate the associations between the winter 2015–2016 flood event and the incidence of confirmed cryptosporidiosis and VTEC in Ireland. Seasonal decomposition of both infections provided evidence of atypical temporal peaks (i.e. residual infections) notified during April 2016, with this month exhibiting the highest residual values over the entire duration of

both datasets. In total, +24 VTEC cases (total number of cases: 67; trend: 49; seasonal variation: –6) and +57 cryptosporidiosis cases (total number of cases: 160; trend: 49; seasonal variation: 54) were identified during that month. This finding demonstrates an unusual pattern of infection during the year 2016: VTEC and cryptosporidiosis are characterised by different seasonal patterns. The highest incidence of human cases of cryptosporidiosis usually occurs during late spring, from March to May (peak in April) in Ireland, temporally concurring with agricultural cycles (i.e. calving and lambing seasons, slurry spreading) (Callaghan *et al.*, 2009; Pollock *et al.*, 2010). In contrast, the highest incidence of VTEC typically occurs during summer and early autumn (peak in July) owing to increased consumption of meat products, livestock grazing and international travel (Lal *et al.*, 2012; ÓhAiseadha *et al.*, 2017). Accordingly, the atypical timing of the decomposed VTEC peak, in concurrence with the residual synchronicity between both infections, provides a strong indication of an impacting external factor, such as a relatively large, spatially diffuse outbreak (overlooked by standard surveillance measures), or a temporally specific societal or environmental event.

Space–time scanning identified 10 spatiotemporally distinct clusters that overlapped in April 2016, with the occurrence of an overlooked infection cluster or outbreak adjudged to be extremely unlikely. The spatial distribution of identified clusters indicates that cryptosporidiosis cases were nationally widespread, while VTEC clusters were proximal to the Shannon River basin, albeit relatively separate from each other. The Shannon River basin and, more generally, rural areas in the midlands of Ireland have previously been identified as hotspots for both infections (HPSC, 2019a,b). The susceptibility of this area may be associated with a high cattle density and reliance on private (unregulated) groundwater supplies (CSO, 2018), or the presence of karst areas, previously identified as risk factors for both infections (Money *et al.*, 2010; Garvey *et al.*, 2016b; HPSC, 2019a,b). The presence of unseasonal VTEC clusters in this area also calls into question the potential relationship between the flooded areas and the infection incidence. During the 2015–2016 flood event, a large part of the Shannon River basin, including a majority of agricultural lands, was identified as the worst-affected area of the country (O'Hara *et al.*, 2019).

#### *4.4.2 Generalised linear modelling*

The spatial extent of the 2015–2016 flood event was found to have a systematic association with both infection incidence and study duration (flood and non-flood periods; see section 3.2). This finding, in concurrence with the Spearman's results (Figures 4.8 and 4.9) exhibiting systematic significant positive associations between surface water and both infections, suggests that fluvial flooding played a role in infection incidence. Fluvial flooding has previously been identified as a potential transmission route for both infections. For example, a study from Germany (Gertler *et al.*, 2015) revealed that an unexplained outbreak in the city of Halle might have been related to the unusually high concentration of *Cryptosporidium* oocysts (*C. hominis*) in the Saale River approximatively 2 months after a major flood event. Similarly, Schwartz *et al.* (2008) showed that enterotoxigenic *E. coli* (ETEC) was a major source of acute watery diarrhoea during a flood period in Bangladesh. The flood extent association was found to be lower during the flood period. A potential explanation for this may be a change in social behaviours; a recent study (McDowell *et al.*, 2020) demonstrated that private well owners experiencing (or observing) flooding in the vicinity of their domestic water source are more likely to change their drinking source and switch to bottled water.

In comparison with VTEC, significantly higher levels of associations were found between cryptosporidiosis and:

- the 2015–2016 flood extent (flood and non-flood periods);
- presence of water bodies (flood and non-flood periods);
- fluvial flood risk scenarios (non-flood period only).

These findings suggest that human cases of cryptosporidiosis are more likely to occur in flood-prone areas and areas with surface water bodies than VTEC enteritis outside flood periods. This result may be explained by a higher concentration of *Cryptosporidium* spp. in surface water. To date, several studies have illustrated that *Cryptosporidium* oocysts can be found in various surface water sources such as lakes, rivers and drinking water supplies (Castro-Hermida *et al.*, 2009; Mons *et al.*, 2009; Hamilton *et al.*, 2018). The prevalence of *Cryptosporidium* in

water sources may be associated with the strong resistance of pathogens in the environment (Medema and Schijven, 2001). *Cryptosporidium* oocysts can survive for up to 24 weeks in fresh surface water (Alum *et al.*, 2014), while VTEC survives for approximatively 6–12 weeks (Lothigius *et al.*, 2010). Similarly, *Cryptosporidium* spp. is particularly resistant to chemical treatments, including chlorination (Dillingham *et al.*, 2002), while VTEC is typically inactivated by this process (Kaneko, 1998).

No associations were found between cryptosporidiosis and fluvial scenarios for the flood period, while a significant statistical association between VTEC and the fluvial medium probability scenario was noted (OR 1.094; $p = 0.025$). Conversely, the stronger link between VTEC and fluvial risk scenarios from 2015–2016 suggests that VTEC might be more driven by surface water during a flood period. This point was partially confirmed by ARIMA findings.

Lower levels of association were found between the fluvial flood risk probability scenario and the actual flood extent for the non-flood period. This result suggests that the low-probability fluvial flood risk scenario (based on the 1000-year flood return period or the maximum historical flood extent known) might have been underestimated, but also illustrates the exceptional intensity reached by the 2015–2016 flood event (i.e. > 1000-year flood return period).

Both infections were found to be less likely to occur in areas characterised by a coastal flooding risk, with significant negative associations found for cryptosporidiosis during the non-flood period. Living in a coastline area was also excluded as a risk factor for VTEC in England and was associated with the lack of popularity of freshwater swimming in the country (Elson *et al.*, 2018). Lower cattle and private well densities in coastal areas, triggering a lower level of pathogen concentrations on the surface, might also explain that absence of correlation. Likewise, a recent study pointed out that coastal areas of Ireland do not figure as a hotspot for cryptosporidiosis incidence (Boudou *et al.*, 2021). Moreover, this result suggests that coastal surge risk might not be considered a risk factor for infection: to date, no scientific studies have reported a groundwater contamination with enteric pathogens in relation with a coastal surge (Andrade *et al.*, 2018).

### *4.4.3 Time-series analysis*

Significative positive associations between the summed trend and residuals of both VTEC and cryptosporidiosis, and all three hydrometeorological studies, were obtained by both Spearman's correlation tests ($R_{SP} > 0$) and ARIMA modelling ($p > 0.05$). The link between hydrometeorological variables and incidence of gastroenteric infection has been shown by several studies. For example, extreme rainfall has already been identified as one of the various environmental factors associated with acute gastroenteric infections (Levy *et al.*, 2016). Tornevi *et al.* (2014) demonstrated that the occurrence of a rainfall event (> 15 mm/24 hours) contributed to an increase in the concentration of *E. coli* in a river 2 days later. Likewise, rainfall has been identified to increase transport of pathogens by overland flows or resuspension from sediments, subsequently leading to contamination of adjacent groundwater sources (Atherholt *et al.*, 1998; Latchmore *et al.*, 2020). Similarly, Gleason and Fagliano (2017) have shown that precipitation is a key factor explaining the high incidence of acute gastrointestinal illness among the younger population in areas characterised by a high reliance on untreated water systems.

With regard to the groundwater level association, the high incidence of VTEC and cryptosporidiosis has been attributed to the consumption of contaminated groundwater in Ireland (Hynds *et al.*, 2014a). To date, only a few studies have assessed the link between groundwater level and gastrointestinal infections. A case study from Canada showed that the *E. coli* concentration was higher in surface water during recharging groundwater months in winter due to the higher transport capacity of pathogens in surface and subsurface water during wet conditions (Dwivedi *et al.*, 2016).

Spearman's and ARIMA results revealed different time responses between VTEC and cryptosporidiosis. With regard to Spearman's, the strongest associations for all three hydrometeorological variables with higher $R_{SP}$ scores were obtained between weeks 1 and 5. ARIMA results obtained for VTEC indicate a longer time response, with the strongest associations (highest *p*-values) found for weeks 12 and 13 (rainfall and groundwater level) and between weeks 18 and 19 (surface water). The associations found with

surface water and VTEC are significantly higher than the ones found with rainfall and groundwater.

This result tends to confirm the finding obtained from GLM (e.g. significative association with the medium-probability fluvial flood risk scenario), indicating that VTEC might be more driven by surface water during a flood period. Moreover, considering the incubation period for VTEC, estimated to be between 1 and 9 days (1–2 weeks; Karmali *et al.*, 2010), and the timing of the flood event (16 weeks from April 2016), a link may therefore be established between the river flow measured in early 2016 and the unusual and unseasonal peak of infection in April 2016. This indirect response between stream flows and VTEC incidence might be associated with the mobilisation of faecal contaminants, present on an already saturated floor by overland flows, subsequently leading to an increase in the level of bacteria in water sources. Accordingly, Nagels *et al.* (2002) showed that the concentration of *E. coli* pathogen in a pastoral agricultural stream follows the streamflow peaks recorded during the flood event.

In contrast to surface water, the timing of the lags obtained with ARIMA between VTEC and both rainfall and groundwater (between weeks 12 and 13) does not suggest a link with the storms of 2015–2016. However, an association with the secondary VTEC incidence peaks of infections recorded in June and July 2016 might be suggested. Indeed, as mentioned previously, while the April 2016 peak association with surface water may be explained by the high soil saturation from December 2015 to January 2016 (due to the high volumes of precipitation), the secondary peaks of June and July 2016 might be explained by the relatively drier conditions. Accordingly, significantly lower levels of soil saturation occurred nationwide from February to April 2016, probably contributing to increased recharge to soils and groundwater, and increased levels of groundwater contamination. This hypothesis supports the findings from a study conducted by Carlton *et al.* (2014), who showed that heavy rainfall occurring after a dry period of 8 weeks enhanced the transfer capacity of pathogens by run-off and surface water, consequently leading to an increase in the concentration of *E. coli* pathogens in drinking water sources. In contrast, heavy rainfall occurring after an 8-week wet period would tend to dilute the concentration of pathogens, and was not directly associated with an increase in infection incidence (Carlton *et al.*, 2014).

The strongest associations obtained for cryptosporidiosis were between weeks 15 and 19 for Spearman's correlation test, and between weeks 18 (groundwater, rainfall) and 19 (surface water) for ARIMA. Both of these findings therefore indicate a significantly longer response for cryptosporidiosis than for VTEC. This may be explained by the survival capacity of both pathogens: up to 24 weeks for cryptosporidiosis (Alum *et al.*, 2014) and approximatively 6 to 12 weeks for VTEC (Lothigius *et al.*, 2010). Likewise, cryptosporidiosis pathogens were shown to be more persistent in subsurface environments than *E. coli* (Bouchier, 1998), consequently suggesting a more indirect response to weather for cryptosporidiosis.

Similarly to VTEC and surface water, the lags obtained by ARIMA suggest a potential link between the hydrometeorological variables from the flood events of 2016 and the cryptosporidiosis peak of infection of April 2016. Given the incubation period of approximatively 2 weeks for cryptosporidiosis, the association might be established between 16 to 17 weeks prior to the April peak and then associated with the hydrometeorological features from December 2015 to January 2016. In contrast to VTEC, the peak of cryptosporidiosis might therefore be associated with all three hydrometeorological variables.

The modelling step suggests that the lag between flood events and peak infection is longer than that reported in previous studies. Bimal *et al.* (2017) found that the risk of cryptosporidiosis and giardiasis for an urban population supplied by a single drinking water system was significantly higher between 4 and 6 weeks after the occurrence of a heavy rainfall event (and more particularly after a dry period). Galway *et al.* (2015) showed a link between total precipitation, mean streamflow and acute gastroenteric incidence during the same month. The specific context of the flood events might explain the longer lag periods found in the current study. For example, Gartner *et al.* (2015) established a link between a flood event and peak incidence of cryptosporidiosis almost 10 weeks after the flood event.

The Spearman's results showed no major differences between the Lower and Upper Shannon basins.

However, the ARIMA results showed a significantly higher association between VTEC and surface water discharge (and potentially associated with the 2015–2016 flood event as mentioned previously) in the Lower Shannon river basin. The space–time scanning analysis also confirmed the higher incidence of VTEC in the Lower Shannon; the two clusters occurring in April 2016 were partially located in this subcatchment. In contrast to VTEC, a slightly higher level of association was obtained for the Upper Shannon river basin. Several factors might explain this difference, such as a potential higher density of private wells or septic tanks – both key factors of infection incidence (Money *et al.*, 2010; Garvey *et al.*, 2016b) – different geological features [the presence of karst, especially limestone (predominant in Ireland), has been identified as a risk factor for both *E. coli* and *Cryptosporidium* (Luffman and Tran, 2014)], or a higher intensity of rainfall/flood events in one of the two catchments. Additional analyses based on the geological and anthropogenic characteristics of both catchment areas would be required to explain those differences.

## 4.5 Conclusions and Perspectives

The current study identified several patterns indicating a potential link between the 2015–2016 flood and an unusual peak of infections of cryptosporidiosis and VTEC in April 2016. The findings highlight concerns about the association between extreme flood events and waterborne infections in Ireland, particularly with regard to the expected increase in flood frequency and severity. Accordingly, a few recommendations can be made for public health services. First, the incidence of waterborne infections within a flood context should, as a precaution, be monitored for up to several months after the flood occurs. This is particularly the case in flood-prone areas given the high susceptibility of these areas, as highlighted by the results. Second, the use of private well supplies should be strictly regulated. A sampling campaign would be relevant within the perspective of a future flood in order to fully understand the spatiotemporal dynamics of both pathogens during a flood event.

The research protocol developed for the current study enabled a retrospective analysis of the impact of a generalised and exceptional flood event on the incidence of two gastrointestinal infections. The seasonal decomposition and space–time scanning contributed to highlighting an unusual pattern of infections during the flood year. Similarly, the time-series analysis, supported by Spearman's and ARIMA, identified a link between infections and weather variables, and provided some insights into the weight and timing of each factor. A similar method could be employed to assess the impact of future events on infectious diseases.

# 5 Conclusion and Recommendations

Despite the mandatory surveillance of cryptosporidiosis and VTEC enteritis in Ireland owing to their communicable disease status, it is widely considered that both diseases remain under-reported in Ireland and on a broader European level (ECDC, 2019a,b; HPSC, 2019a,b). The spatiotemporal epidemiology of the assessed infections reflects Ireland's diverse population and geography, although it shows a markedly higher rate of occurrence in rural areas, likely to be due to the ubiquity of disease sources (e.g. cattle) and pathways (e.g. karstic limestone bedrocks). The elevated burden among children aged ≤5 years is likely to be related to both immunological status and specific routes of exposure, and warrants further study. The STEP_WISE project represents a significant advance in efforts to investigate the spatiotemporal epidemiology of environmentally associated diseases with a view to further elucidating pathways of infection to guide public health interventions through an improved understanding of their spatiotemporal occurrence, clustering mechanisms, levels of recurrence, and associated drivers, pathways and receptors. Moreover, the STEP_WISE project has produced several recommendations for further research and to overcome limitations, as follows.

### *Spatial resolution: limitations of the small area scale*

The STEP_WISE project has shed light on the complexity of working with data at the SA resolution. SAs are the smallest administrative units existing in Ireland, and were found to be too granular for modelling. The large number of units (approximatively 18,000), along with potentially haphazard spatial delineations (non-uniform spatial zoning associated with an approximate number of dwellings), led to spatial conflicts when performing modelling techniques. Similarly, the SA scale, which changes every 5 years, is not properly adapted to static spatial modelling of complex sporadic infections characterised by multiple source attributions and pathways, such as cryptosporidiosis (low frequency of cases across the spatial units).

### *A need for data harmonisation*

Another limitation of the SA, along with ED and county, is the fact that none of these spatial units were initially designed for public health purposes. This results in difficulties and approximation when linking data provided from other public sources, themselves designed for other purposes. A future objective is the creation of a novel geographical health atlas, which would lead to the creation of a new spatial scale adapted for studying sporadic or endemic infections in Ireland. Similarly, the data of interest (socio-economic or geographical) identified and collected during the STEP_WISE project would be harmonised to this new spatial scale and made publicly accessible through a data platform to facilitate the study of infectious diseases by the stakeholders involved.

### *The benefit of space–time cluster frequency index mapping*

The first part of the STEP_WISE project aimed to identify the spatiotemporal patterns of cryptosporidiosis and VTEC in Ireland. This led to the elaboration of a space–time cluster frequency index mapping. This new tool detects and overlays yearly clusters of infections, and was specifically adapted to the study of these two sporadic infections. Accordingly, the space–time cluster frequency index resolved the spatial issues related to the scarcity of cases among Ireland by identifying hotspots and cold spots of infections for the total duration of the datasets. The cluster index mapping was extensively and successfully used to detect general spatial patterns associated with cryptosporidiosis, VTEC, and the VTEC O26 and O157 serotypes through machine learning techniques (i.e. GLM, decision trees). The STEP_WISE project recommends using and developing this tool for the purpose of better understanding sporadic infections in Ireland. This would require facilitating yearly access to cases of infection from the Health Protection Surveillance Centre, enabling the mapping to be updated. One specific objective is to make this tool available for public health scientists or stakeholders through the data platform built for the Health Index Atlas project.

### *A geographically and temporally adapted surveillance policy*

The cluster frequency index mapping identified the hotspots of infections and confirmed the rural character of both VTEC and cryptosporidiosis infections. The spatial distribution of space–time clusters also highlighted the need for a geographically adapted surveillance policy. Accordingly, the STEP_WISE project recommends the further testing of centres outside Dublin and in hotspot areas to increase the diagnosis speed and accuracy. Similarly, these hotspot areas must be seen as a priority target for risk management and communication among general practitioners and the PAR.

Along the same lines, the STEP_WISE project highlighted the urgent need to develop a temporally adjusted surveillance policy. The case–case modelling revealed once again that the seasonal signal of both infections remains the most important temporal characteristic of cryptosporidiosis and VTEC (and associated serotypes). Sampling campaigns of groundwater quality should therefore focus on time frames consistent with the highest incidence of cases (April for cryptosporidiosis; July and September for VTEC). This may improve the understanding of potential pathways of infection. Consequently, a real-time surveillance policy should be developed after the onset of extreme weather events. Accordingly, the STEP_WISE project established the relationship between the extreme winter flood event of 2015–2016 and the abnormal surge of cases reported from April to June 2016. Unfortunately, owing to the absence of groundwater contamination data and the temporal gap between the study and the onset of the extreme weather event, our understanding of the mechanisms that explain the high number of cases remains incomplete.

### *The importance of socio-economic and demographic attributes*

The modelling of spatial attributes of both infections allowed for a clearer picture of their potential drivers. The variables related to septic tanks, private wells and cattle density were surprisingly found to be not as significant as expected. This result may reflect the existence of better indicators of high-risk areas, such as geology, landscape type, flood risk areas or socio-economic attributes. Among these, socio-economic and demographic variables were found to be important to consider. All final models revealed the presence of at least one variable belonging to this subgroup. For example, the number of people per room was found to be negatively associated with the presence of cryptosporidiosis. A similar finding, along with a higher proportion of low-skilled workers, was identified among the main factors explaining the increased presence of VTEC. Along the same lines, a higher percentage of vulnerable population, i.e. aged under 18 and over 65 years, was highlighted as a factor common to both infections. These results indicate the importance of risk education in identified hotspots, especially among dwellings associated with a low level of education. The STEP_WISE project recommends establishing adapted risk communication strategies in identified hotspots.

### *The importance of a data pipeline*

The creation of a data pipeline that would improve access to the datasets of the different actors involved in the prevention of sporadic infection is one of the key recommendations of the STEP_WISE project. As mentioned previously, the cluster frequency index would need to be updated on a yearly basis to ensure continuity and detect potential spatial evolution among infection hotspots. Easier, expedited access to anonymised cases of sporadic infections, along with awareness of ongoing outbreaks, could significantly improve the knowledge of sporadic infections in Ireland.

# References


Adams, N., Byrne, L., Rose, T., Adak, B., Jenkins, C., Charlett, A., Violato, M., O'Brien, S., Whitehead, M., Barr, B. and Taylor-Robinson, D., 2019. Sociodemographic and clinical risk factors for paediatric typical haemolytic uraemic syndrome: retrospective cohort study. *BMJ Paediatrics Open* 3(1).

Allévius, B., 2018. Scanstatistics: space-time anomaly detection using scan statistics. *Journal of Open Source Software* 3: 515.

Alum, A., Absar, I.M., Asaad, H., Rubino, J.R., and Ijaz, M.K., 2014. Impact of environmental conditions on the survival of Cryptosporidium and Giardia on environmental surfaces. *Interdisciplinary Perspectives on Infectious Diseases* 2014: 210385.

Andrade, L., O'Dwyer, J., O'Neill, E. and Hynds, P., 2018. Surface water flooding, groundwater contamination, and enteric disease in developed countries: a scoping review of connections and consequences. *Environmental Pollution* 236: 540–549.

Anselin, L., 1995. Local indicators of spatial association – LISA. *Geography Annals* 27: 93–115.

Anselin, L., Syabri, I. and Smirnov, O., 2002. Visualizing multivariate spatial correlation with dynamically linked windows. *Proceedings*, *CSISS Workshop on New Tools for Spatial Data Analysis*, Santa Barbara, CA.

Arnell, N.W. and Gosling, S.N., 2016. The impacts of climate change on river flood risk at the global scale. *Climatic Change* 1343: 387–401.

Atherholt, T.B., LeChevallier, M.W., Norton, W.D. and Rosen, J.S., 1998. Effect of rainfall on Giardia and Cryptosporidium. *Journal – American Water Works Association* 909: 66–80.

Atherholt, T.B., Korn, L.R., Louis, J.B. and Procopio, N.A., 2015. Repeat sampling and coliform bacteria detection rates in New Jersey domestic wells. *Groundwater Monitoring & Remediation* 352: 70–80.

Barker, L., Hannaford, J., Muchan, K., Turner, S. and Parry, S., 2016. The winter 2015/2016 floods in the UK: a hydrological appraisal. *Weather* 71(12): 324–333.

Bartram, J., 2009. *Water Safety Plan Manual: Step-By-Step Risk Management for Drinking-Water Suppliers*. World Health Organization, Geneva.

Bhunia, G.S., Siddiqui, N.A., Shit, P.K., Chatterjee, N. and Sinha, S.K., 2016. Spatial clustering of *Plasmodium falciparum* in Bihar (India) from 2007 to 2015. *Spatial Information Research* 24(6): 639–648.

Blöschl, G., Kiss, A., Viglione, A., Barriendos, M., Böhm, O., Brázdil, R., *et al*., 2020. Current European flood-rich period exceptional compared with past 500 years. *Nature* 583(7817): 560–566.

Borchardt, M.A., Bertz, P.D., Spencer, S.K. and Battigelli, D.A., 2003. Incidence of enteric viruses in groundwater from household wells in Wisconsin. *Applied and Environmental Microbiology* 69(2): 1172–1180.

Bouchier, I., 1998. *Cryptosporidium in Water Supplies: Third Report of the Group of Experts*. Departments of Health and the Environment, London, UK.

Boudou, M., Lang, M., Vinet, F. and Coeur, D., 2016. Lessons from analysing mortality from six major flood events in France (1930–2010). In *3rd European Conference on Flood Risk Management (FLOODrisk 2016)* 7: 06005.

Boudou, M., ÓhAiseadha, C., Garvey, P., O'Dwyer, J. and Hynds, P., 2021. Flood hydrometeorology and gastroenteric infection: the winter 2015–2016 flood event in the Republic of Ireland. *Journal of Hydrology* 599: 126376.

Brehony, C., Cullinan, J., Cormican, M. and Morris, D., 2018. Shiga toxigenic *Escherichia coli* incidence is related to small area variation in cattle density in a region in Ireland. *Science of the Total Environment* 637: 865–870.

Britton, E., Hales, S., Venugopal, K. and Baker, M.G., 2010. The impact of climate variability and change on cryptosporidiosis and giardiasis rates in New Zealand. *Journal of Water & Health* 8(3): 561–571.

Brown, E.M., McTaggart, L.R., Dunn, D., Pszczolko, E., Tsui, K.G., Morris, S.K., Stephens, D., Kus, J.V. and Richardson, S.E., 2018. Epidemiology and geographic distribution of blastomycosis, histoplasmosis, and coccidioidomycosis, Ontario, Canada, 1990–2015. *Emerging Infectious Diseases* 24(7): 1257.

Brown, L. and Murray, V., 2013. Examining the relationship between infectious diseases and flooding in Europe: a systematic literature review and summary of possible public health interventions. *Disaster Health* 12: 117–127.

Callaghan, M., Cormican, M., Prendergast, M., Pelly, H., Cloughley, R., Hanahoe, B. and O'Donovan, D., 2009. Temporal and spatial distribution of human cryptosporidiosis in the west of Ireland 2004–2007. *International Journal of Health Geographics* 81: 1–9.

Cameron, D. and Jones, I.G., 1983. John Snow, the Broad Street pump and modern epidemiology. *International Journal of Epidemiology* 12(4): 393–396.

Cann, K.F., Thomas, D.R., Salmon, R.L., Wyn-Jones, A.P. and Kay, D., 2013. Extreme water-related weather events and waterborne disease. *Epidemiology & Infection* 1414: 671–686.

Carlton, E.J., Eisenberg, J.N., Goldstick, J., Cevallos, W., Trostle, J. and Levy, K., 2014. Heavy rainfall events and diarrhea incidence: the role of social and environmental factors. *American Journal of Epidemiology* 1793: 344–352.

Castro-Hermida, J.A., García-Presedo, I., Almeida, A., González-Warleta, M., Da Costa, J.M.C. and Mezo, M., 2009. Detection of Cryptosporidium spp. and Giardia duodenalis in surface water: a health risk for humans and animals. *Water Research* 4317: 4133–4142.

Chaisri, U., Nagata, M., Kurazono, H., Horie, H., Tongtawe, P., Hayashi, H., Watanabe, T., Tapchaisri, P., Chongsa-nguan, M. and Chaicumpa, W., 2001. Localization of Shiga toxins of enterohaemorrhagic Escherichia coli in kidneys of paediatric and geriatric patients with fatal haemolytic uraemic syndrome. *Microbial Pathogenesis* 31(2): 59–67.

Chalmers, R.M. and Cacciò, S., 2016. Towards a consensus on genotyping schemes for surveillance and outbreak investigations of Cryptosporidium, Berlin, June 2016. *Eurosurveillance* 2137: 30338.

Chalmers, R.M., Robinson, G., Elwin, K. and Elson, R., 2019. Analysis of the Cryptosporidium spp. and gp60 subtypes linked to human outbreaks of cryptosporidiosis in England and Wales, 2009 to 2017. *Parasites & Vectors* 12(1): 1–13.

Chappell, C.L., Okhuysen, P.C., Langer-Curry, R., Widmer, G., Akiyoshi, D.E., Tanriverdi, S. and Tzipori, S., 2006. Cryptosporidium hominis: experimental challenge of healthy adults. *The American Journal of Tropical Medicine and Hygiene* 75(5): 851–857.

Chique, C., Hynds, P.D., Andrade, L., Burke, L., Morris, D., Ryan, M.P. and O'Dwyer, J., 2020. Cryptosporidium spp. in groundwater supplies intended for human consumption – a descriptive review of global prevalence, risk factors and knowledge gaps. *Water Research* 176: 115726.

Chyzheuskaya, A., Cormican, M., Srivinas, R., O'Donovan, D., Prendergast, M., O'Donoghue, C. and Morris, D., 2017. Economic assessment of waterborne outbreak of cryptosporidiosis. *Emerging Infectious Diseases* 2310: 1650.

Cleveland, R.B., Cleveland, W.S., McRae, J.E. and Terpenning, I., 1990. STL: a seasonal-trend decomposition. *Journal of Official Statistics* 61: 3–73.

Cohen, S.A., Egorov, A.I., Jagai, J.S., Matyas, B.T., DeMaria Jr, A., Chui, K.K., Griffiths, J.K. and Naumova, E.N., 2008. The seeds of two gastrointestinal diseases: socioeconomic, environmental, and demographic factors related to cryptosporidiosis and giardiasis in Massachusetts. *Environmental Research* 108(2): 185–191.

Congdon, P., 2016. Spatiotemporal frameworks for infectious disease diffusion and epidemiology. *International Journal of Environmental Research and Public Health* 13(12): 1261.

CSO (Central Statistics Office), 2018. *Census 2016 Profile 1 – Town and Country*. Stationery Office, Dublin.

Cummins, E., Kennedy, R. and Cormican, M., 2010. Quantitative risk assessment of *Cryptosporidium* in tap water in Ireland. *Science of the Total Environment* 4084: 740–753.

Daniels, M.E., Smith, W.A. and Jenkins, M.W., 2018. Estimating Cryptosporidium and Giardia disease burdens for children drinking untreated groundwater in a rural population in India. *PLoS Neglected Tropical Diseases* 121: e0006231.

Darnault, C.J., Peng, Z., Yu, C., Li, B., Jacobson, A.R. and Baveye, P.C., 2017. Movement of Cryptosporidium parvum oocysts through soils without preferential pathways: exploratory test. *Frontiers in Environmental Science* 5: 39.

Dewsbury, D.M., Renter, D.G., Shridhar, P.B., Noll, L.W., Shi, X., Nagaraja, T.G. and Cernicchiaro, N., 2015. Summer and winter prevalence of Shiga toxin-producing *Escherichia coli* (STEC) O26, O45, O103, O111, O121, O145, and O157 in feces of feedlot cattle. *Foodborne Pathogens and Disease* 12(8): 726–732.

Dillingham, R.A., Lima, A.A. and Guerrant, R.L., 2002. Cryptosporidiosis: epidemiology and impact. *Microbes and Infection* 4(10): 1059–1066.

Department of Health. *Healthy Ireland: A Framework for Improved Health and Wellbeing 2013–2025*. Department of Health, Dublin.

Dreelin, E.A., Ives, R.L., Molloy, S. and Rose, J.B., 2014. Cryptosporidium and Giardia in surface water: a case study from Michigan, USA to inform management of rural water systems. *International Journal of Environmental Research and Public Health* 1110: 10480–10503.

Dwivedi, D., Mohanty, B.P. and Lesikar, B.J., 2016. Impact of the linked surface water–soil water–groundwater system on transport of *E. coli* in the subsurface. *Water*, *Air*, *& Soil Pollution* 2279: 351.

ECDC (European Centre for Disease Prevention and Control), 2019a. Cryptosporidiosis. In *Annual Epidemiological Report for 2017*. ECDC, Stockholm.

ECDC (European Centre for Disease Prevention and Control), 2019b. Shiga toxin-/verocytotoxin-producing Escherichia coli (VTEC/VTEC) infection. In *Annual Epidemiological Report for 2017*. ECDC, Stockholm.

Efstratiou, A., Ongerth, J.E. and Karanis, P., 2017. Waterborne transmission of protozoan parasites: review of worldwide outbreaks – an update 2011–2016. *Water Research* 114: 14–22.

Elson, R., Grace, K., Vivancos, R., Jenkins, C., Adak, G.K., O'Brien, S.J. and Lake, I. R., 2018. A spatial and temporal analysis of risk factors associated with sporadic Shiga toxin-producing *Escherichia coli* O157 infection in England between 2009 and 2015. *Epidemiology & Infection* 14615: 1928–1939.

Fayer, R. and Ungar, B.L., 1986. *Cryptosporidium* spp. and cryptosporidiosis. *Microbiological Reviews* 50(4): 458–483.

Feng, Y., Ryan, U.M. and Xiao, L., 2018. Genetic diversity and population structure of *Cryptosporidium*. *Trends in Parasitology* 34(11): 997–1011.

Forzieri, G., Bianchi, A., e Silva, F.B., Herrera, M.A.M., Leblois, A., Lavalle, C., Aerts, J.C.J.H., Feyen, L., 2018. Escalating impacts of climate extremes on critical infrastructures in Europe. *Global Environmental Change* 48: 97–107.

Fox, J., 2015. *Applied Regression Analysis and Generalized Linear Models*. 3rd ed. SAGE Publications, Los Angeles, CA.

Galway, L.P., Allen, D.M., Parkes, M.W., Li, L. and Takaro, T.K., 2015. Hydroclimatic variables and acute gastro-intestinal illness in British Columbia, Canada: a time series analysis. *Water Resources Research* 512: 885–895.

Garvey, P., Carroll, A., McNamara, E., Charlett, A., Danis, K. and McKeown, P.J., 2016a. Serogroup-specific seasonality of verotoxigenic *Escherichia coli*, Ireland. *Emerging Infectious Diseases* 22(4): 742.

Garvey, P., Carroll, A., McNamara, E. and McKeown, P.J., 2016b. Verotoxigenic *Escherichia coli* transmission in Ireland: a review of notified outbreaks, 2004–2012. *Epidemiology & Infection* 1445: 917–926.

Gleason, J.A. and Fagliano, J.A., 2017. Effect of drinking water source on associations between gastrointestinal illness and heavy rainfall in New Jersey. *PloS One* 12(3): e0173794.

Gertler, M., Dürr, M., Renner, P., Poppert, S., Askar, M., Breidenbach, J., *et al*., 2015. Outbreak of Cryptosporidium hominis following river flooding in the city of Halle (Saale), Germany, August 2013. *BMC Infectious Diseases* 15: 1–10.

Greene, S.K., Peterson, E.R., Kapell, D., Fine, A.D. and Kulldorff, M., 2016. Daily reportable disease spatiotemporal cluster detection, New York City, New York, USA, 2014–2015. *Emerging Infectious Diseases* 22(10): 1808.

Greenwood, K.P. and Reid, S.A., 2020. Clustering of cryptosporidiosis in Queensland, Australia, is not defined temporally or by spatial diversity. *International Journal for Parasitology* 50(3): 209–216.

Guo, C., Du, Y., Shen, S.Q., Lao, X.Q., Qian, J. and Ou, C.Q., 2017. Spatiotemporal analysis of tuberculosis incidence and its associated factors in mainland China. *Epidemiology & Infection* 145(12): 2510–2519.

Hajat, S., Ebi, K.L., Kovats, S., Menne, B., Edwards, S. and Haines, A. 2003. The human health consequences of flooding in Europe and the implications for public health: a review of the evidence. *Applied Environmental Science and Public Health* 11: 13–21.

Hamilton, K.A., Waso, M., Reyneke, B., Saeidi, N., Levine, A., Lalancette, C., Besner, M.C., Khan, W. and Ahmed, W., 2018. *Cryptosporidium* and *Giardia* in wastewater and surface water environments. *Journal of Environmental Quality* 47(5): 1006–1023.

Hoang, T., Coletti, P., Melegaro, A., Wallinga, J., Grijalva, C.G., Edmunds, J.W., Beutels, P. and Hens, N., 2019. A systematic review of social contact surveys to inform transmission models of close-contact infections. *Epidemiology (Cambridge*, *Mass.)* 30(5): 723.

HPSC (Health Protection Surveillance Centre), 2019a. *Cryptosporidiosis in Ireland*, *2018*. HPSC, Health Service Executive, Dublin.

HPSC (Health Protection Surveillance Centre), 2019b. *VTEC Infection in Ireland*, *2017*. HSPC, Health Service Executive, Dublin.

HSE (Health Service Executive), 2017. *Epidemiology of Cryptosporidiosis in Ireland*, *2016*. Available online: https://www.hpsc.ie/a-z/gastroenteric/cryptosporidiosis/epidemiologicaldata/epidemiologyofcryptosporidiosisinirelandannualreports/Cryptosporidiosis.pdf

Hunter, P.R. and Thompson, R.A., 2005. The zoonotic transmission of *Giardia* and *Cryptosporidium*. *International Journal for Parasitology* 3511–3512: 1181–1190.

Hynds, P.D., Misstear, B.D. and Gill, L.W., 2012. Development of a microbial contamination susceptibility model for private domestic groundwater sources. *Water Resources Research* 48(12).

Hynds, P.D., Misstear, B.D. and Gill, L.W., 2013. Unregulated private wells in the Republic of Ireland: consumer awareness, source susceptibility and protective actions. *Journal of Environmental Management* 127: 278–288.

Hynds, P.D., Gill, L.W. and Misstear, B.D., 2014a. A quantitative risk assessment of verotoxigenic *E. coli* VTEC in private groundwater sources in the Republic of Ireland. *Human and Ecological Risk Assessment: An International Journal* 206: 1446–1468.

Hynds, P.D., Thomas, M.K. and Pintar, K.D.M., 2014b. Contamination of groundwater systems in the US and Canada by enteric pathogens, 1990–2013: a review and pooled-analysis. *PloS One* 95: e93301.

Jagai J.S., Castronovo, D.A., Monchak, J. and Naumova, E.N., 2009. Seasonality of cryptosporidiosis: a meta-analysis approach. *Environmental Research* 109(4): 465–478.

Jonkman, S.N., Maaskant, B., Boyd, E. and Levitan, M., 2008. Loss of life caused by the flooding of New Orleans after hurricane Katrina: a preliminary analysis of the relationship between flood characteristics and mortality. *4th International Symposium on Flood Defence*, Toronto, Canada, 6–8 May, pp. 6–8.

Kaneko, M., 1998. Chlorination of pathogenic E coli O157. *Water Science and Technology* 3812: 141.

Karch, H., Tarr, P.I. and Bielaszewska, M., 2005. Enterohaemorrhagic Escherichia coli in human medicine. *International Journal of Medical Microbiology* 295(6–7): 405–418.

Karmali, M.A., Gannon, V. and Sargeant, J.M., 2010. Verocytotoxin-producing Escherichia coli (VTEC). *Veterinary Microbiology* 140(3–4): 360–370.

Karunaweera, N.D., Ginige, S., Senanayake, S., Silva, H., Manamperi, N., Samaranayake, N., Siriwardana, Y., Gamage, D., Senerath, U. and Zhou, G., 2020. Spatial epidemiologic trends and hotspots of leishmaniasis, Sri Lanka, 2001–2018. *Emerging Infectious Diseases* 26(1): 1.

Kenny, T., Cronin, M. and Sage, C., 2018. A retrospective public health analysis of the Republic of Ireland's Food Harvest 2020 strategy: absence, avoidance and business as usual. *Critical Public Health* 281: 94–105.

Khan, A., Shaik, J.S. and Grigg, M.E., 2018. Genomics and molecular epidemiology of Cryptosporidium species. *Acta Tropica* 184: 1–14.

Kulldorff, M., 1999. Spatial scan statistics: models, calculations, and applications. In Glaz, J., Balakrishnan, N. (eds), *Scan Statistics and Applications*. Birkhäuser, Boston, MA, pp. 303–322.

Kulldorff, M., Heffernan, R., Hartman, J., Assunçao, R. and Mostashari, F., 2005. A space–time permutation scan statistic for disease outbreak detection. *PLoS Medicine* 2(3): e59.

Kulldorff, M., 2021. *SaTScan User Guide for Version 9.7*. Available online: https://www.satscan.org/cgi-bin/satscan/register.pl/SaTScan_Users_Guide.pdf?todo=process_userguide_download (accessed 7 November 2023).

Lal, A., 2016. Spatial modelling tools to integrate public health and environmental science, illustrated with infectious cryptosporidiosis. *International Journal of Environmental Research and Public Health* 13(2): 186.

Lal, A., Hales, S., French, N. and Baker, M.G., 2012. Seasonality in human zoonotic enteric diseases: a systematic review. *PLoS One* 74: e31883.

Lal, A., Cornish, L.M., Fearnley, E., Glass, K. and Kirk, M., 2015. Cryptosporidiosis: a disease of tropical and remote areas in Australia. *PLoS Neglected Tropical Diseases* 9(9): e0004078.

Latchmore, T., Hynds, P., Brown, R.S., Schuster-Wallace, C., Dickson-Anderson, S., McDermott, K. and Majury, A., 2020. Analysis of a large spatiotemporal groundwater quality dataset, Ontario 2010–2017: informing human health risk assessment and testing guidance for private drinking water wells. *Science of the Total Environment* 738: 140382.

Lau, C.L., Sheridan, S., Ryan, S., Roineau, M., Andreosso, A., Fuimaono, S., Tufa, J. and Graves, P.M., 2017. Detecting and confirming residual hotspots of lymphatic filariasis transmission in American Samoa 8 years after stopping mass drug administration. *PLoS Neglected Tropical Diseases* 11(9): e0005914.

Levy, K., Woster, A.P., Goldstein, R.S. and Carlton, E.J., 2016. Untangling the impacts of climate change on waterborne diseases: a systematic review of relationships between diarrheal diseases and temperature, rainfall, flooding, and drought. *Environmental Science & Technology* 50(10): 4905–4922.

Linton, S.L., Jennings, J.M., Latkin, C.A., Gomez, M.B. and Mehta, S.H., 2014. Application of space–time scan statistics to describe geographic and temporal clustering of visible drug activity. *Journal of Urban Health* 91(5): 940–956.

Lothigius, Å., Sjöling, Å., Svennerholm, A.M. and Bölin, I., 2010. Survival and gene expression of enterotoxigenic Escherichia coli during long-term incubation in sea water and freshwater. *Journal of Applied Microbiology* 1084: 1441–1449.

Luffman, I. and Tran, L., 2014. Risk factors for E. coli O157 and cryptosporidiosis infection in individuals in the karst valleys of east Tennessee, USA. *Geosciences* 43: 202–218.

Mao, Y., Zhang, N., Zhu, B., Liu, J. and He, R., 2019. A descriptive analysis of the spatiotemporal distribution of intestinal infectious diseases in China. *BMC Infectious Diseases* 191: 766.

McCormack, T., Naughton, O., Bradford, R., Campanyà, J., Morrissey, P., Gill, L. and Lee, M., 2020. *GWFlood Project: Monitoring*, *Modelling and Mapping Karst Groundwater Flooding in Ireland*. Geological Survey Ireland, Dublin.

McDowell, C.P., Andrade, L., O'Neill, E., O'Malley, K., O'Dwyer, J. and Hynds, P.D., 2020. Gender-related differences in flood risk perception and behaviours among private groundwater users in the Republic of Ireland. *International Journal of Environmental Research and Public Health* 176: 2072.

Medema, G.J. and Schijven, J.F., 2001. Modelling the sewage discharge and dispersion of Cryptosporidium and Giardia in surface water. *Water Research* 3518: 4307–4316.

Money, P., Kelly, A.F., Gould, S.W.J., Denholm-Price, J., Threlfall, E.J., and Fielder, M.D., 2010. Cattle, weather and water: mapping Escherichia coli O157:H7 infections in humans in England and Scotland. *Environmental Microbiology* 1210: 2633–2644.

Mons, C., Dumètre, A., Gosselin, S., Galliot, C. and Moulin, L., 2009. Monitoring of *Cryptosporidium* and *Giardia* River contamination in Paris area. *Water Research* 431: 211–217.

Mooney, S., Lavallee, S., O'Dwyer, J. and Hynds, P.D., 2021. Private groundwater contamination and extreme weather events: the role of demographics, experience and cognitive factors on risk perceptions of Irish private well users. *Science of the Total Environment* 784: 147118.

Morasch, B., 2013. Occurrence and dynamics of micropollutants in a karst aquifer. *Environmental Pollution* 173: 133–137.

Muenchhoff, M. and Goulder, P.J., 2014. Sex differences in pediatric infectious diseases. *The Journal of Infectious Diseases* 209(3): S120–S126.

Murphy, H.M., Prioleau, M.D., Borchardt, M.A. and Hynds, P.D., 2017. Epidemiological evidence of groundwater contribution to global enteric disease, 1948–2015. *Hydrogeology Journal 25*4: 981–1001.

Nagels, J.W., Davies-Colley, R. J., Donnison, A. M. and Muirhead, R.W, 2002. Faecal contamination over flood events in a pastoral agricultural stream in New Zealand. *Water Science and Technology* 45(12): 45–52.

NDFEM (National Directorate for Fire and Emergency Management) and DHPCLG (Department of Housing, Planning, Community and Local Government), 2016. *Report on Flooding December 4 2015 – January 13 2016*. NDFEM and DHPCLG, Dublin.

Nicholson, O. and Gebre, F., 2016. OPW response to the winter 2015/2016 flooding in Ireland. *Proceedings of the Irish National Hydrology Conference 2016*, pp. 63–80.

Nime, F.A., Burek, J.D., Page, D.L., Holscher, M.A. and Yardley, J.H., 1976. Acute enterocolitis in a human being infected with the protozoan *Cryptosporidium*. *Gastroenterology* 704: 592–598.

O'Dwyer, J., Morris Downes, M. and Adley, C.C., 2016. The impact of meteorology on the occurrence of waterborne outbreaks of vero cytotoxin-producing *Escherichia coli* VTEC: a logistic regression approach. *Journal of Water and Health* 141: 39–46.

O'Dwyer, J., Hynds, P.D., Pot, M., Adley, C. and Ryan, M.P., 2017. An investigation of the presence and determinants of antibiotic and multi-antibiotic resistance from groundwater derived *E. coli* isolates in the Midwest of Ireland. *Hydrogeology Journal* 25(4): 939–951.

O'Dwyer, J., Hynds, P.D., Byrne, K.A., Ryan, M.P. and Adley, C.C., 2018. Development of a hierarchical model for predicting microbiological contamination of private groundwater supplies in a geologically heterogeneous region. *Environmental Pollution* 237, 329–338.

ÓhAiseadha, C., Hynds, P.D., Fallon, U.B. and O'Dwyer, J., 2017. A geostatistical investigation of agricultural and infrastructural risk factors associated with primary verotoxigenic *E. coli* VTEC infection in the Republic of Ireland, 2008–2013. *Epidemiology & Infection* 1451: 95–105.

O'Hara, R., Green, S. and McCarthy, T., 2019. The agricultural impact of the 2015–2016 floods in Ireland as mapped through Sentinel 1 satellite imagery. *Irish Journal of Agricultural and Food Research*.

O'Leary, J.K., Blake, L., Corcoran, G.D., Sleator, R.D., and Lucey, B., 2020. Increased diversity and novel subtypes among clinical Cryptosporidium parvum and Cryptosporidium hominis isolates in Southern Ireland. *Experimental Parasitology*, 218: 107967.

O'Sullivan, M.B., Garvey, P., O'Riordan, M., Coughlan, H., McKeown, P., Brennan, A. and McNamara, E., 2008. Increase in VTEC cases in the south of Ireland: link to private wells. *Eurosurveillance* 1339: 18991.

Painter, J.E., Gargano, J.W., Yoder, J.S., Collier, S.A. and Hlavsa, M.C., 2016. Evolving epidemiology of reported cryptosporidiosis cases in the United States, 1995–2012. *Epidemiology & Infection*, 144(8): 1792–1802.

Penning-Rowsell, E., Tapsell, S. and Wilson, T., 2005. Key policy implications of the health effects of floods. In *Extreme Weather Events and Public Health Responses*. Springer, Berlin/Heidelberg, pp. 207–223.

Pollock, K.G., Ternent, H.E., Mellor, D.J., Chalmers, R.M., Smith, H.V., Ramsay, C.N. and Innocent, G.T., 2010. Spatial and temporal epidemiology of sporadic human cryptosporidiosis in Scotland. *Zoonoses Public Health* 57(7–8): 487–492.

Portier, C.J., Tart, K.T., Carter, S.R., Dilworth, C.H., Grambsch, A.E., Gohlke, J. and Whung, P.Y., 2013. A human health perspective on climate change: a report outlining the research needs on the human health effects of climate change. *Journal of Current Issues in Globalization* 64: 621.

Prema V. and Uma Rao, K., 2015. Time series decomposition model for accurate wind speed forecast. *Renewables: Wind*, *Water*, *and Solar* 2: 18.

Putignani, L. and Menichella, D., 2010. Global distribution, public health and clinical impact of the protozoan pathogen *Cryptosporidium*. *Interdisciplinary Perspectives on Infectious Diseases* 753512.

Rechel, B., Mahgoub, H., Pritchard, G.C., Willshaw, G., Williams, C., Rodrigues, B., Lewin, M. and Nair, P., 2011. Investigation of a spatiotemporal cluster of verotoxin-producing *Escherichia coli* O157 infections in eastern England in 2007. *Eurosurveillance* 16: 19916.

Robertson, C., Nelson, T.A., MacNab, Y.C. and Lawson, A.B., 2010. Review of methods for space–time disease surveillance. *Spatial and Spatio-temporal Epidemiology* 1: 105–16.

Semenza, J.C., 2020. Cascading risks of waterborne diseases from climate change. *Nature Immunology* 215: 484–487.

Schwartz, B.S., Harris, J.B., Khan, A.I., Larocque, R.C., Sack, D.A., Malek, M.A., *et al*., 2006. Diarrheal epidemics in Dhaka, Bangladesh, during three consecutive floods: 1988, 1998, and 2004. *American Journal of Tropical Medicine and Hygiene* 74(6): 1067.

Smith, K., Woodward, A., Campbell-Lendrum, D., Chadee, D., Honda, Y., Liu, Q., Olwoch, J.M., Revich, B. and Sauerborn, R., 2014. Human health: impacts, adaptation, and co-benefits. In *Climate Change 2014: Impacts*, *Adaptation*, *and Vulnerability. Part A: Global and Sectoral Aspects*. Contribution of Working Group II to the Fifth Assessment Report of the Intergovernmental Panel on Climate Change. Cambridge University Press, UK, pp. 709–754.

Stavenhagen, M., Buurman, J. and Tortajada, C., 2018. Saving water in cities: assessing policies for residential water demand management in four cities in Europe. *Cities* 79: 187–195.

Stensvold, C.R., Ethelberg, S., Hansen, L., Sahar, S., Voldstedlund, M., Kemp, M., Hartmeyer, G.N., Otte, E., Engsbro, A.L., Nielsen, H.V. and Mølbak, K., 2015. Cryptosporidium infections in Denmark, 2010–2014. *Danish Medical Journal* 62(5): A5086.

Tam, C.C., O'Brien, S.J., Tompkins, D.S., Bolton, F.J., Berry, L., Dodds, J., Choudhury, D., Halstead, F., Iturriza-Gómara, M., Mather, K., Rait, G. Ridge, A., Rodrigues, L.C., Wain, J. Wood, B., Gray, J.J and IID2 Study Executive Committee, 2012. Changes in causes of acute gastroenteritis in the United Kingdom over 15 years: microbiologic findings from 2 prospective, population-based studies of infectious intestinal disease. *Clinical Infectious Diseases* 54: 1275–1286.

Tango, T., Takahashi, K. and Kohriyama, K., 2011. A space–time scan statistic for detecting emerging outbreaks. *Biometrics* 67(1): 106–115.

Thompson, R.A., Koh, W.H. and Clode, P.L., 2016. *Cryptosporidium* – what is it? *Food and Waterborne Parasitology* 4: 54–61.

Toledo, R.D.S., Martins, F.D.C., Ferreira, F.P., de Almeida, J.C., Ogawa, L., dos Santos, H.L.E.P.L and Freire, R.L., 2017. *Cryptosporidium* spp. and *Giardia* spp. in feces and water and the associated exposure factors on dairy farms. *PLoS One* 124: e0175311.

Tornevi, A., Bergstedt, O. and Forsberg, B., 2014. Precipitation effects on microbial pollution in a river: lag structures and seasonal effect modification. *PloS One* 95: e98546.

Varga, C., Pearl, D.L., McEwen, S.A., Sargeant, J.M., Pollari, F. and Guerin, M.T., 2015. Area-level global and local clustering of human Salmonella Enteritidis infection rates in the city of Toronto, Canada, 2007–2009. *BMC Infectious Diseases* 151: 1–13.

Walsh, S., 2016. The rainfall of winter 2015/16 in Ireland. Paper presented at the National Hydrology Conference, Athlone, Co. Roscommon, Ireland. Available online: https://hydrologyireland.ie/wp-content/uploads/2016/11/06-Seamus-W-Rainfall-of-winter-2015_2016-Final.pdf (accessed 11 March 2024).

Wang, H. and Horton, R., 2015. Tackling climate change: the greatest opportunity for global health. *The Lancet* 38610006: 1798–1799.

Woodcock, N.H. and Strachan, R.A., 2009. *Geological History of Britain and Ireland*. John Wiley & Sons, New York, NY.

Wu, X., Lu, Y., Zhou, S., Chen, L. and Xu, B., 2016. Impact of climate change on human infectious diseases: empirical evidence and human adaptation. *Environment International* 86: 14–23.

Xiao, X., van Hoek, A.J., Kenward, M.G., Melegaro, A. and Jit, M., 2016. Clustering of contacts relevant to the spread of infectious disease. *Epidemics* 17: 1–9.

Zintl, A., Proctor, A.F., Read, C., Dewaal, T., Shanaghy, N., Fanning, S. and Mulcahy, G., 2009. The prevalence of *Cryptosporidium* species and subtypes in human faecal samples in Ireland. *Epidemiology & Infection* 1372: 270–277.

# Abbreviations

| | |
|---|---|
| **CI** | Confidence interval |
| **CIDR** | Computerised Infectious Disease Reporting |
| **CIR** | Crude incidence rate |
| **CSO** | Central Statistics Office |
| **ED** | Electoral division |
| **GLM** | Generalised linear modelling |
| **HSE** | Health Service Executive |
| **HUS** | Haemolytic–uraemic syndrome |
| **LOESS** | Locally estimated scatterplot smoothing |
| **OR** | Odds ratio |
| **OSWTS** | On-site domestic wastewater treatment system |
| **PAR** | Population at risk |
| **RR** | Relative risk |
| **SA** | Small area |
| **STL** | Seasonal and trend decomposition via the locally estimated scatterplot smoothing |
| **WWTP** | Wastewater treatment plant |

# An Ghníomhaireacht Um Chaomhnú Comhshaoil

Tá an GCC freagrach as an gcomhshaol a chosaint agus a fheabhsú, mar shócmhainn luachmhar do mhuintir na hÉireann. Táimid tiomanta do dhaoine agus don chomhshaol a chosaint ar thionchar díobhálach na radaíochta agus an truaillithe.

## Is féidir obair na Gníomhaireachta a roinnt ina trí phríomhréimse:

**Rialáil:** Rialáil agus córais chomhlíonta comhshaoil éifeachtacha a chur i bhfeidhm, chun dea-thorthaí comhshaoil a bhaint amach agus díriú orthu siúd nach mbíonn ag cloí leo.

**Eolas:** Sonraí, eolas agus measúnú ardchaighdeáin, spriocdhírithe agus tráthúil a chur ar fáil i leith an chomhshaoil chun bonn eolais a chur faoin gcinnteoireacht.

**Abhcóideacht:** Ag obair le daoine eile ar son timpeallachta glaine, táirgiúla agus dea-chosanta agus ar son cleachtas inbhuanaithe i dtaobh an chomhshaoil.

## I measc ár gcuid freagrachtaí tá:

### Ceadúnú

- Gníomhaíochtaí tionscail, dramhaíola agus stórála peitril ar scála mór;
- Sceitheadh fuíolluisce uirbigh;
- Úsáid shrianta agus scaoileadh rialaithe Orgánach Géinmhodhnaithe;
- Foinsí radaíochta ianúcháin;
- Astaíochtaí gás ceaptha teasa ó thionscal agus ón eitlíocht trí Scéim an AE um Thrádáil Astaíochtaí.

### Forfheidhmiú Náisiúnta i leith Cúrsaí Comhshaoil

- Iniúchadh agus cigireacht ar shaoráidí a bhfuil ceadúnas acu ón GCC;
- Cur i bhfeidhm an dea-chleachtais a stiúradh i ngníomhaíochtaí agus i saoráidí rialáilte;
- Maoirseacht a dhéanamh ar fhreagrachtaí an údaráis áitiúil as cosaint an chomhshaoil;
- Caighdeán an uisce óil phoiblí a rialáil agus údaruithe um sceitheadh fuíolluisce uirbigh a fhorfheidhmiú
- Caighdeán an uisce óil phoiblí agus phríobháidigh a mheasúnú agus tuairisciú air;
- Comhordú a dhéanamh ar líonra d'eagraíochtaí seirbhíse poiblí chun tacú le gníomhú i gcoinne coireachta comhshaoil;
- An dlí a chur orthu siúd a bhriseann dlí an chomhshaoil agus a dhéanann dochar don chomhshaol.

### Bainistíocht Dramhaíola agus Ceimiceáin sa Chomhshaol

- Rialacháin dramhaíola a chur i bhfeidhm agus a fhorfheidhmiú lena n-áirítear saincheisteanna forfheidhmithe náisiúnta;
- Staitisticí dramhaíola náisiúnta a ullmhú agus a fhoilsiú chomh maith leis an bPlean Náisiúnta um Bainistíocht Dramhaíola Guaisí;
- An Clár Náisiúnta um Chosc Dramhaíola a fhorbairt agus a chur i bhfeidhm;
- Reachtaíocht ar rialú ceimiceán sa timpeallacht a chur i bhfeidhm agus tuairisciú ar an reachtaíocht sin.

### Bainistíocht Uisce

- Plé le struchtúir náisiúnta agus réigiúnacha rialachais agus oibriúcháin chun an Chreat-treoir Uisce a chur i bhfeidhm;
- Monatóireacht, measúnú agus tuairisciú a dhéanamh ar chaighdeán aibhneacha, lochanna, uiscí idirchreasa agus cósta, uiscí snámha agus screamhuisce chomh maith le tomhas ar leibhéil uisce agus sreabhadh abhann.

### Eolaíocht Aeráide & Athrú Aeráide

- Fardail agus réamh-mheastacháin a fhoilsiú um astaíochtaí gás ceaptha teasa na hÉireann;
- Rúnaíocht a chur ar fáil don Chomhairle Chomhairleach ar Athrú Aeráide agus tacaíocht a thabhairt don Idirphlé Náisiúnta ar Ghníomhú ar son na hAeráide;
- Tacú le gníomhaíochtaí forbartha Náisiúnta, AE agus NA um Eolaíocht agus Beartas Aeráide.

### Monatóireacht & Measúnú ar an gComhshaol

- Córais náisiúnta um monatóireacht an chomhshaoil a cheapadh agus a chur i bhfeidhm: teicneolaíocht, bainistíocht sonraí, anailís agus réamhaisnéisiú;
- Tuairiscí ar Staid Thimpeallacht na hÉireann agus ar Tháscairí a chur ar fáil;
- Monatóireacht a dhéanamh ar chaighdeán an aeir agus Treoir an AE i leith Aeir Ghlain don Eoraip a chur i bhfeidhm chomh maith leis an gCoinbhinsiún ar Aerthruailliú Fadraoin Trasteorann, agus an Treoir i leith na Teorann Náisiúnta Astaíochtaí;
- Maoirseacht a dhéanamh ar chur i bhfeidhm na Treorach i leith Torainn Timpeallachta;
- Measúnú a dhéanamh ar thionchar pleananna agus clár beartaithe ar chomhshaol na hÉireann.

### Taighde agus Forbairt Comhshaoil

- Comhordú a dhéanamh ar ghníomhaíochtaí taighde comhshaoil agus iad a mhaoiniú chun brú a aithint, bonn eolais a chur faoin mbeartas agus réitigh a chur ar fáil;
- Comhoibriú le gníomhaíocht náisiúnta agus AE um thaighde comhshaoil.

### Cosaint Raideolaíoch

- Monatóireacht a dhéanamh ar leibhéil radaíochta agus nochtadh an phobail do radaíocht ianúcháin agus do réimsí leictreamaighnéadacha a mheas;
- Cabhrú le pleananna náisiúnta a fhorbairt le haghaidh éigeandálaí ag eascairt as taismí núicléacha;
- Monatóireacht a dhéanamh ar fhorbairtí thar lear a bhaineann le saoráidí núicléacha agus leis an tsábháilteacht raideolaíochta;
- Sainseirbhísí um chosaint ar an radaíocht a sholáthar, nó maoirsiú a dhéanamh ar sholáthar na seirbhísí sin.

### Treoir, Ardú Feasachta agus Faisnéis Inrochtana

- Tuairisciú, comhairle agus treoir neamhspleách, fianaise-bhunaithe a chur ar fáil don Rialtas, don tionscal agus don phobal ar ábhair maidir le cosaint comhshaoil agus raideolaíoch;
- An nasc idir sláinte agus folláine, an geilleagar agus timpeallacht ghlan a chur chun cinn;
- Feasacht comhshaoil a chur chun cinn lena n-áirítear tacú le hiompraíocht um éifeachtúlacht acmhainní agus aistriú aeráide;
- Tástáil radóin a chur chun cinn i dtithe agus in ionaid oibre agus feabhsúchán a mholadh áit is gá.

### Comhpháirtíocht agus Líonrú

- Oibriú le gníomhaireachtaí idirnáisiúnta agus náisiúnta, údaráis réigiúnacha agus áitiúla, eagraíochtaí neamhrialtais, comhlachtaí ionadaíocha agus ranna rialtais chun cosaint chomhshaoil agus raideolaíoch a chur ar fáil, chomh maith le taighde, comhordú agus cinnteoireacht bunaithe ar an eolaíocht.

## Bainistíocht agus struchtúr na Gníomhaireachta um Chaomhnú Comhshaoil

Tá an GCC á bainistiú ag Bord lánaimseartha, ar a bhfuil Ard-Stiúrthóir agus cúigear Stiúrthóir. Déantar an obair ar fud cúig cinn d'Oifigí:

1. An Oifig um Inbhunaitheacht i leith Cúrsaí Comhshaoil
2. An Oifig Forfheidhmithe i leith Cúrsaí Comhshaoil
3. An Oifig um Fhianaise agus Measúnú
4. An Oifig um Chosaint ar Radaíocht agus Monatóireacht Comhshaoil
5. An Oifig Cumarsáide agus Seirbhísí Corparáideacha

Tugann coistí comhairleacha cabhair don Ghníomhaireacht agus tagann siad le chéile go rialta le plé a dhéanamh ar ábhair imní agus le comhairle a chur ar an mBord.

**EPA Research**

**Webpages:** www.epa.ie/our-services/research/
**LinkedIn:** www.linkedin.com/showcase/eparesearch/
**Twitter:** @EPAResearchNews
**Email:** research@epa.ie